Advanced Technologies in Water Efficiency

homepage:https://atwe.razi.ac.ir

Online ISSN:2783-4964

# An experimental investigation of the influence of zigzag walls in the stilling basin on the hydraulic jump's properties

**Humam Amer Hadi** [1], **Ali Akbar Akhtari** [2✉], and **Atheer Zaki Al-Qaisi** [3]

1. Department of Civil Engineering, Faculty of Engineering, Razi University, Kermanshah, Iran. E-mail: humamamer2@gmail.com
2. Corresponding author, Department of Civil Engineering, Faculty of Engineering, Razi University, Kermanshah, Iran. E-mail: akhtari@razi.ac.ir
3. Department of Water Resources Management Engineering, College of Engineering, AL-Qasim Green University, Babylon, Iraq. E-mail: dr.atheermohsin@wrec.uoqasim.edu.iq

## Article Info

**Article type:**
Research Article

**Article history:**
Received 16 March 2025
Received in revised form 25 June 2025
Accepted 16 August 2025
Available online 22 December 2025

***Keywords***:
energy dissipater,
free surface profile,
hydraulic jump,
spillway,
stilling basin

## ABSTRACT

**Objective:** The objective of this study is to assess how stilling basin wall geometry (smooth vs. zigzag) affects hydraulic jump behavior and energy dissipation.It also investigates whether zigzag walls improve supercritical-to-subcritical flow conversion, reduce downstream scour, and support shorter, more efficient basin designs.

**Method**: The study used two stilling basin models in a hydraulic flume at the University of Babylon: Case 1 with smooth walls and blocks, and Case 2 with zigzag walls and the same blocks. Twenty-two runs (11 per case) were tested with discharges of 10–20 L/s, maintaining supercritical inlet Froude numbers of 4.30–5.70, and energy dissipation and downstream Froude numbers were measured for comparison.

**Results**: The results indicate that the average relative energy dissipation reached 61.1% in Case 1 and 64.9% in Case 2, demonstrating a 3.8% increase attributed to zigzag wall geometry. Additionally, energy dissipation in the smooth-wall basin exhibited high sensitivity to changes in $Fr_1$, with a 28.1% variation across the tested Froude range, whereas the zigzag configuration showed much more stable performance, with only 5.1% variation. Case 2 also generated lower downstream Froude numbers ($Fr_2$ between 0.46 and 1.20), reflecting better subcritical flow conditions. The free surface profile differed notably between cases, with Case 2 showing lower water depths in the center than near the side walls, while Case 1 maintained nearly uniform depths across the width.

**Conclusions**: The study concludes that zigzag side walls significantly enhance and stabilize hydraulic energy dissipation, leading to more favorable downstream flow regimes and reduced scour potential, which directly benefits dam safety. The lower $Fr_2$ values observed in Case 2 confirm improved compatibility with natural river flow conditions. The higher dissipation efficiency also suggests that zigzag geometry can help reduce the required length of stilling basins, offering a design advantage in both performance and economy. Although the zigzag walls create a non-uniform free surface profile, this behavior contributes positively to increased energy losses. Overall, the findings support the adoption of zigzag walls with middle blocks as an effective option for optimizing stilling basin performance and reducing structural dimensions.

**Cite this article:** Hadi, H. A., Akhtari, A. A., & Al-Qaisi, A. Z. (2025). An experimental investigation of the influence of zigzag walls in the stilling basin on the hydraulic jump's properties. *Advanced Technologies in Water Efficiency, 5* (4), 1-14. https://doi.org/ 10.22126/atwe.2025.12036.1162


Publisher: Razi University.
https://doi.org/10.22126/atwe.2025.12036.1162

## Introduction

The hydraulic jump and its stability inside the stilling basin represent some of the difficulties that occur after the installation of dam weirs and diversion dams. Large dams and diversion dams that the flood flow passes through are typically damaged by phenomena like scour holes, erosion of the river bed after the stilling basin, and transfer of hydraulic jump to the downstream. Stilling basins are external energy dissipators that are positioned adjacent to a culvert or chute's exit. According to Chow (1998), they can dissipate energy in hydraulic structures, lowering the net uplift pressure beneath them, avoiding scour downstream, and increasing the water level on the structures' downstream side. The hydraulic jump can be controlled in a number of ways. These methods ensure that jumps form inside the stilling basin and control their placement under any operating conditions. One strategy to stabilize the hydraulic jump and reduce the flow's energy when it enters the river is to place building blocks in the supercritical flow area. Tests on a downstream gate in a rectangular channel with hydraulic jump characteristics and energy dissipation revealed a relationship between the energy dissipation of hydraulic jumps and a function of gate opening, Froude, and Weber Numbers. Bhowmik (1991) conducted studies in the lab to illustrate the ability to enhance energy loss and lower the length of basins needed to a particular range for a Froude Number of 2.5 to 4.5. The hydraulic jump has been thoroughly studied using physical models. Ead and Rajaratnam (2002) investigated a series of hydraulic jump tests carried out on corrugated beds in a laboratory. The Froude numbers that were tested ranged from 4 to 10. Three values of relative roughness were investigated. The tailwater depth required to make a jump was shown to be much lower than that of the same jumps on smooth beds. Izadjoo and Shafai (2007) investigated how the flow characteristics of the hydraulic jump were affected by a corrugated bed with a trapezoidal shape. When comparing a trapezoidal-shaped corrugated bed with the same features to a smooth bed, the corresponding conjugate depth and hydraulic jump length show a 20% and 50% decrease, respectively. Abbaspour et. al (2009) conducted an experimental investigation of hydraulic jump characteristics across six corrugated beds with varying wave steepness levels. The corrugation and Froude numbers of the beds varied from 3.8 to 8.6 and 0.286 to 0.625, respectively. According to the data, the tailwater depth and jump length on corrugated beds are smaller than those of the identical jump on a smooth bed. Hayawi and Mohammed (2011) evaluated a hydraulic jump characteristics and energy dissipation positioned in the rectangular channel's downstream gate. They found that the dissipation of hydraulic jump energy was related to Weber Numbers, Froude, and gate opening. Ashraf and Zhi-lin (2012) carried out laboratory investigation with respect to the features of hydraulic jumps associated to a bed which has been artificially roughened that include baffle blocks in the shape of wedges. New experimental formulas that account for the relative bed roughness and the inflow Froude number were used to determine the hydraulic jump length and the subsequent depth ratio. Gandhi and Singh (2016) investigated the hydraulic jump characteristics, sequential depth ratio, jump efficiency, and relative jump length empirically in a trapezoidal channel with and without appurtenances. It is possible to make exact predictions for greater Froude number values by closely fitting empirical models with appurtenances under different dimensions and baffle block placements. Ibrahim (2017) conducted experiments to examine how block shapes affect the flow pattern behind radial gates. Although a level floor without baffle blocks was included in the test program to evaluate the effect of using the blocks, four different baffle block modes were considered. A chute spillway using baffle blocks was created by Christopher and Raphael (2019) The designer is given a range of baffle heights, useful configurations, and baffle spacing through the empirical design process.

Nassrin et al (2020) examined the performance of the new seven baffle block design in terms of reducing the size of stilling basins in irrigation systems. The study's findings demonstrate that the modified baffle block performs better in terms of jump length and hydraulic energy dissipation. Rasoul et al (2020) studied how an ogee spillway's bed-block roughness affects energy dissipation, and evaluated the length of jet. Applying an ogee spillway with block roughness that is set up on the bed at different takeoff angles and with and without a flip bucket. Alireza and Ebrahim (2021) did an experimental analysis to evaluate how the configuration of rectangular zigzag blocks influences the hydraulic jump characteristics in a trapezoidal channel. The results show a decline in the proportion of smooth beds to consecutive hydraulic jump depths with rectangular blocks. Alfiansyah et al (2022) investigated the fluctuations in the energy dissipater and examined the impact on the hydraulic jump and energy dissipation. A physical model was made of the USBR Type IV spillway system. Research has demonstrated that the combination and adjustment of dissipation features, such as riprap lengthening, end threshold, and floor elevation, may effectively dissipate energy downstream effects. A model was investigated by Pillai and Kansal (2022) to determine how new baffle blocks may be used to evolve stilling basins. The results show that in a hydraulic jump stilling basin, wedge-shaped baffle blocks with a vertex angle of 120° dissipate more high-velocity flow energy than rectangular baffle blocks.

The present research conducts experimental analysis on utilizing of zigzag walls and middle blocks in the stilling basin and their effects on the characteristics of the hydraulic jump taking into consideration the water's dynamic energy dissipation and the free surface profile of hydraulic jumps in stilling basins. Physical models were used for experiments in an ogee spillway (USBR alternative Type IV) with and without zigzag walls at a varying range of Froude numbers.

## Method

Due to the complicated flow patterns across the USBR stilling basin caused by the interaction of trapped air and turbulent flow. Our understanding of these interactions is incomplete (Wang & Chanson, 2013) The technique for predicting the stilling basin's hydraulic characteristics is physical modeling. Therefore, physical modeling was used for this study, and laboratory work was done to examine the effects of putting zigzag walls in the stilling basin on the hydraulic jump's properties.

## Flume and Instruments

Testing was done in a looping flume using the fluid lab at Babylon University's Engineering College, as seen in Fig. 1. The flume's dimensions are 10 m in length, 30 cm in width, and 45 cm in height for the side walls. The maximum discharge capacity of the pump in this flume is 20 l/s. To reduce turbulence in the entry area, a screen plate was placed at the flume's intake. Furthermore, in order to maintain a constant flow, the spillway models were positioned 2.5 m downstream of the entrance tank, where flow entered the laboratory flume gradually. A flow meter is installed on the pipeline and calibrated to measure the discharge of the incoming flow. On a brass rail, three water level sensors with a one-millimeter accuracy were mounted to the top of the flume sides.

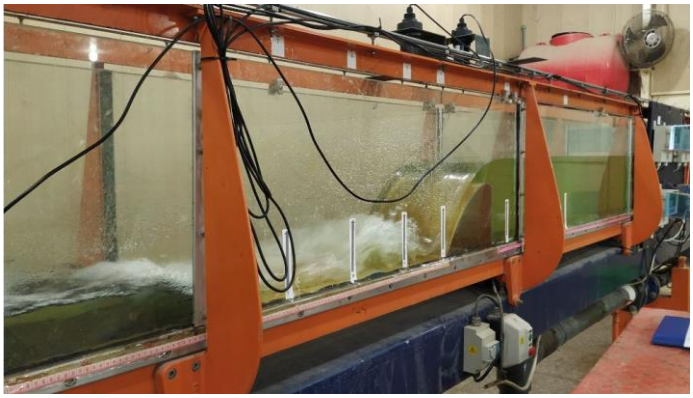

**Figure 1. The used flume**

## Design equations

The design model's limitations include a width of 30 cm and discharge rates ranging from 10 to 20 l/s. A spillway was created for those discharge rates based on the flume's dimensions in the lab to achieve a hydraulic jump. The discharge over an ogee crest is given by the following formula (USBR ,1987):

$$Q = C_d \, L \, h_e^{1.5} \quad (1)$$

where: Q is a discharge in m3/s, Cd is a discharge coefficient equal to 2.183 corresponding to the highest discharge in tests, L is a crest's effective length equal to 0.30 m , and he is an actual head under consideration on the crest in m.

## Description of laboratory models

Modified models for the stilling basin alternative type IV are created in the lab using the measurements of this kind. In this research, two laboratory models were made to represent two cases in the test procedure; namely case1 (spillway and stilling basin with smooth walls) and case2 (spillway and stilling basin with zigzag walls) as shown in Fig. 2. These models were constructed from wood and treated with epoxy and varnish to increase their smoothness and stop the wood from expanding from water. These models will not be constructed with the same parts as the prototype; instead, they will be changed. If the flowing surfaces of the water have a comparable form and nearly match the scale in terms of roughness (the model should typically be smoother than the prototype). The model will typically meet your need (USBR ,1987). Thus, in the two lab models, an ogee spillway has the following dimensions: 30 cm in width, 20 cm in height, and 26.9 cm in length. All details of laboratory models elements are presented in Fig. 3.

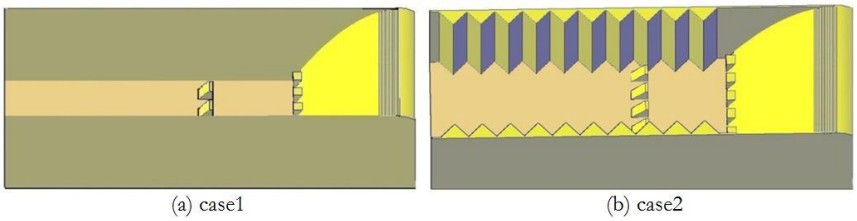


**Figure 2. Laboratory models cases**

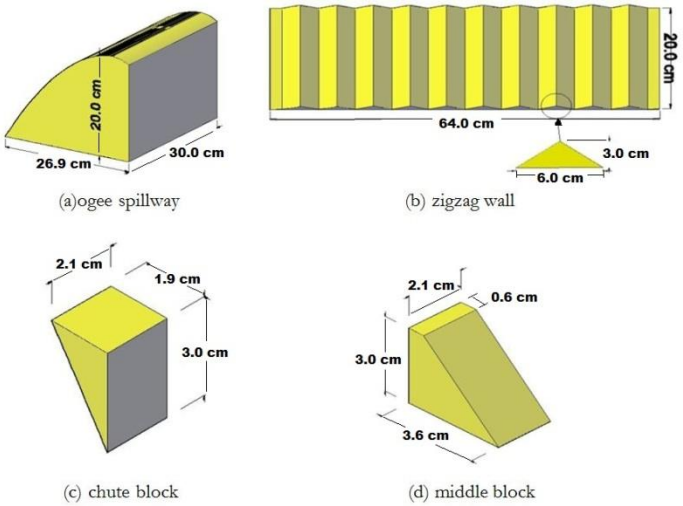


**Figure 3. Details of all elements of laboratory models**

## Dimensional analysis

Numerical analysis is the study, development, and use of approximation computer techniques to address continuous versus discrete mathematics problems that are unsolvable using exact and analytical techniques. The term "direct problem-solving methods" refers to a variety of continuous mathematics problems that are exactly resolved by an algorithm. On the contrary, there are numerous situations for which there is no direct solution, necessitating the employment of other techniques like an iterative method or the presentation of physical models. It appears that 11 parameters, which are detailed below, should be taken into account in this laboratory model.

($y_1$= depth of flow at the beginning of the stilling basin, $y_2$= depth of flow after the stilling basin, $b_1$= channel width before stilling basin, $b_2$= channel width after stilling basin, L= length of the stilling basin, $b_s$= the base of the zigzag triangle on the wall of the stilling basin, $d_s$= the height of the zigzag triangle on the wall of the stilling basin, $V_1$= flow velocity at the beginning of the stilling basin, g= gravity acceleration, ΔE= amount of energy loss along the stilling basin, $E_1$= Energy before the spillway, which is considered equal to the energy at the beginning of the basin)

$$\pi_1=y_1^{\alpha_1}.V_1^{\beta_1}.b_1 = L^{\alpha_1}.L^{\beta_1}.T^{-\beta_1}.L^1 = L^0.T^0 \quad \rightarrow \quad \pi_1=b_1/y_1 \ , \ \text{in same methods}$$

$$\pi_2=b_2/y_1 \ , \ \pi_3=y_2/y_1 \ , \ \pi_4=L/y_1 \ , \ \pi_5=ds/y_1 \ , \ \pi_6=bs/y_1 \ , \ \pi_6^{-}=\frac{\pi_5}{\pi_6}=\frac{ds/y_1}{bs/y_1}=\frac{ds}{bs}$$

$$\pi_7=Fr \ , \ \pi_8=\Delta E/y_1 \ , \ \pi_9=E_1/y_1 \ , \ \pi_9^{-}=\frac{\pi_8}{\pi_9}=\frac{\Delta E/y_1}{E_1/y_1}=\frac{\Delta E}{E_1}$$

$$f.\left(\frac{b_1}{y_1},\frac{b_2}{y_1},\frac{y_2}{y_1},\frac{L}{y_1},\frac{ds}{y_1},\frac{bs}{y_1},\frac{bs}{ds},Fr,\frac{\Delta E}{y_1},\frac{\Delta E}{E_1}\right)$$

Now, from the above dimensional analysis, the parameter Fr and the factor ΔE/E1 which have been considered in all article and references have been considered as the most important factors. Also, considering the experimental limitation, b2/b1=1 has been considered and large roughness numbers with a constant ratio bs/ds have been considered. The number of zigzags on the wall is constant because of the length of the stilling basin constant therefore, it cannot be an effective parameter.

## Test procedure

The tests conducted on the two cases in this part are based on the data from the laboratory model and the design. Three water level sensor readings were collected for each test. As shown in Fig. 4., the third sensor reads downstream at a distance of 120 cm from the spillway toe, while the other two sensors read upstream at a distance of 10 and 60 cm from the spillway beginning.

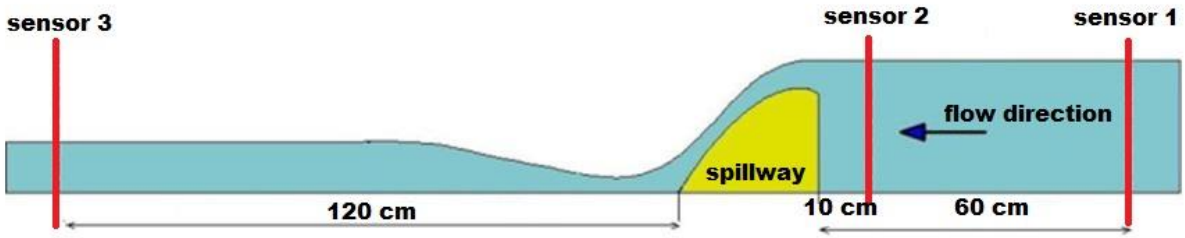


**Figure 4. Schematic representation of the sensors measurement sections**

The same laboratory test procedure was followed in the two cases. The following is a summary of this test:

- Turning on the flume pump.
- Modifying the flowmeter's reads to get the proper flow rate.
- Measuring the (us) and (ds) water depth from the sensors 1 and 3 respectively in order to calculate the energy losses in these sections.
- Measuring the water depth inside stilling basin in four sections as shown in Fig. 8 by using additional sensors and rulers.
- Eleven tests are carried out for each case, varying the flow rates from 10 l/s to 20 l/s.

## Energy Dissipation Calculations

Generally, the difference between the total energy upstream and downstream describes energy dissipation. Therefore, energy dissipation at dams and weirs is closely linked to spillway design, particularly when considering the difference between upstream and downstream water levels.

The Bernoulli Equation below is used in hydraulics to measure the total energy at the channel section for channels with a small slope (Chow ,1959):

$$E = z + d + \alpha \frac{V^2}{2g} \quad (2)$$

where, E is the total energy of flow in m, z is the elevation of a datum in m that is represented by flume zero slope bed, d is the depth below the water surface in m measured along the channel section, V is the flow velocity in m/s, g is the gravitational acceleration in m/s2 and α is Coriolis coefficient. The Coriolis coefficient in ogee weir is one (USBR ,1987). The ratio of energy loss to total energy upstream is known as the relative energy dissipation [19]. In order to determine the energy relative loss along the spillway system, the following formula was utilized:

$$\Delta E_r = \frac{\Delta E}{E_u} = \left(\frac{E_u - E_d}{E_u}\right) \quad (3)$$

in which the relative energy dissipation $\Delta E_{(r)}$ is represented by the left side of the equation. $E_u$ is the total flow energy at the upstream of the spillway in m. $E_d$ is the total flow energy at the downstream of the spillway in m. $\Delta E$ is the energy differential upstream and downstream of the spillway in m.

## Results

### Results of relative energy dissipation

The effects of zigzag walls on the relative energy dissipation in stilling basins were investigated in twenty-two laboratory tests (eleven tests for each cases 1 and 2). Table 1 shows the relative values of energy dissipation and Froude numbers of these two cases.

**Table 1. Relative energy –dissipation $\Delta E_r$ for the two cases**

| | case1 | | | case2 | |
|---|---|---|---|---|---|
| Q ($m^3/s$) | $Fr_1$ | $\Delta E_r$ | $Fr_2$ | $\Delta E_r$ | $Fr_2$ |
| 0.010 | 5.70 | 0.703 | 0.60 | 0.671 | 0.46 |
| 0.011 | 5.48 | 0.692 | 0.61 | 0.669 | 0.49 |
| 0.012 | 5.28 | 0.682 | 0.64 | 0.663 | 0.53 |
| 0.013 | 5.11 | 0.672 | 0.67 | 0.655 | 0.55 |
| 0.014 | 4.96 | 0.666 | 0.71 | 0.650 | 0.59 |
| 0.015 | 4.83 | 0.660 | 0.74 | 0.647 | 0.63 |
| 0.016 | 4.69 | 0.648 | 1.32 | 0.645 | 0.68 |
| 0.017 | 4.59 | 0.574 | 1.89 | 0.643 | 0.75 |
| 0.018 | 4.49 | 0.524 | 2.14 | 0.643 | 1.12 |
| 0.019 | 4.39 | 0.479 | 2.34 | 0.633 | 1.16 |
| 0.020 | 4.30 | 0.422 | 2.56 | 0.620 | 1.20 |
| **Av. $\Delta E_r$ %** | | 61.1% | | 64.9% | |

The water stream behavior in the stilling basin for the cases 1 and 2 is depicted in Fig. 5. Fig. 6 shows the effect of the Froude number ($Fr_1$) that calculated at the beginning of the stilling basin on the amount of relative energy dissipation ($\Delta E_r$). Fig. 7 represents the relationship between Froude number ($Fr_1$) and the Froude number measured at the tail water by sensor 3 ($Fr_2$) for cases 1 and 2.

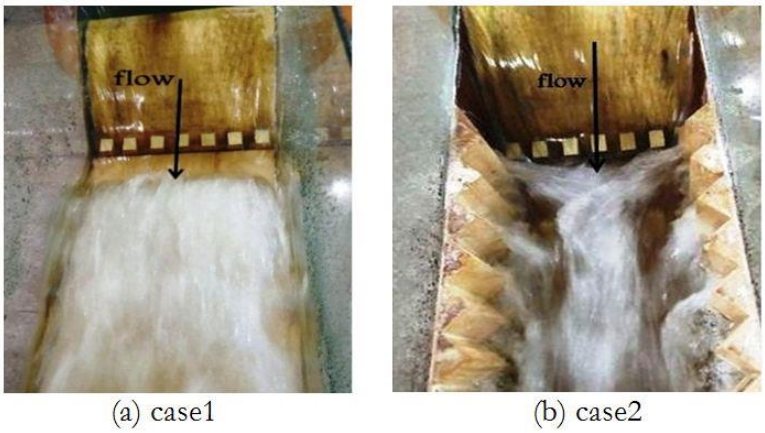


(a) case1 (b) case2

**Figure 5. Water stream behavior in the stilling basin for cases 1 and 2**

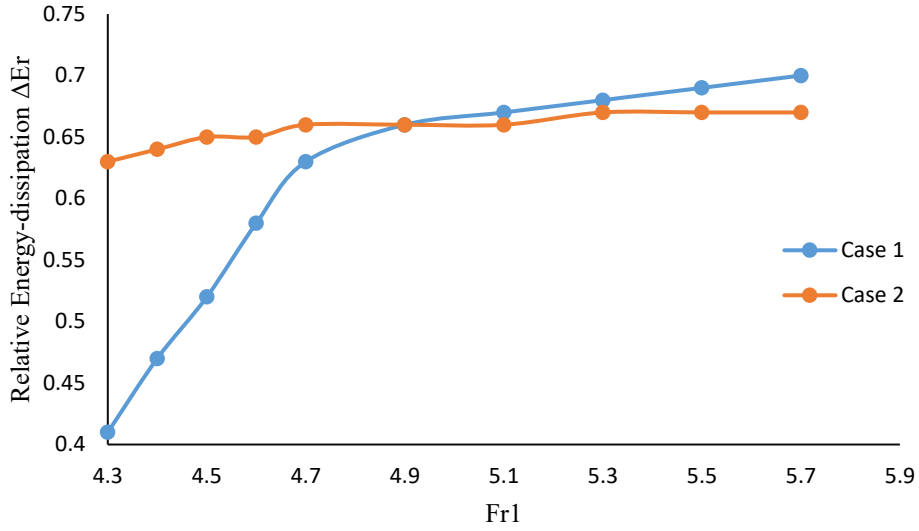


**Figure 6. Difference in relative energy dissipation versus $Fr_1$ for cases 1 and 2**

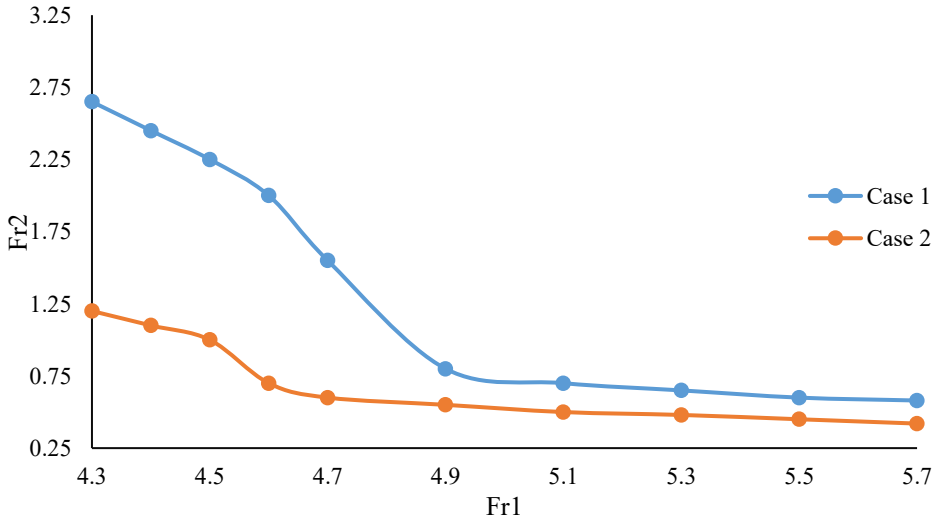


**Figure7. Difference in $Fr_1$ versus $Fr_2$ for cases 1 and 2**

According to Fig.6, it can be noted that case 1 indicates a 5.5% difference in dissipation energy due to a little drop in the rate of energy dissipation with an increase in Froude number 4.69 to 5.70. On the other hand, with a decrease in Froude number to 4.30, the rate of energy dissipation rapidly decrease, resulting in a 22.6% difference in dispersion energy. At Froude number lower than 4.69, the inability to dissipate the energy with the necessary efficiency arises due to the increasing water velocity and fewer energy dissipater blocks. Case2 indicates a little decrease in the dispersion energy difference of 5.1% with increase Froude number. Fig. 7 show that cases 2 is considered the best case because of achieving a small Froude number in the tail water ($Fr_2$).

## Free-surface profiles of water

Although the fact that the jump toe fluctuations and high degree of turbulence cause the free surface profile of hydraulic jumps to be extremely unstable in both horizontal and vertical direction movements. In order to know the behavior and free-surface profiles of water in the stilling basin considering the water depths along the hydraulic jump, which are important for stilling basin wall design, the stilling basin was divided into four sections (A, B, C, and D) as shown in Fig. 8. In each section, middle depth of water (dm) and edge depth of water (de) reads were recorded for the two cases. The depth of the water in the stilling basin is measured using precise sensors, through which the change in water height readings due to flow turbulence and water level fluctuations can be monitored, and the average readings can be taken and recorded. Tables 2 , and Table 3 show the values of dm and de reads in cases 1 and 2 respectively with a discharges from 0.10 m3/s to 0.20 m3/s. Fig. 9, and Fig. 10 show comparison of dm and de free-surface profiles of water for the cases 1 and 2 respectively, with a discharge of 0.20 $m^3/s$.

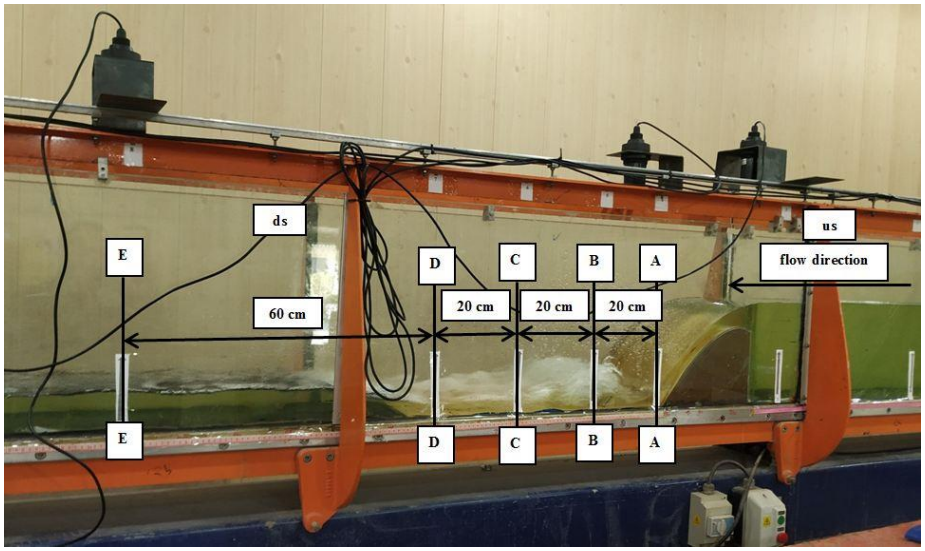


**Figure 8. Stilling basin divided sections**

**Table 2. $d_m$ and $d_e$ reads in the straight stilling basin for case 1**

| Q ($m^3/s$) | Fr1 | Section No. | | | | | | | |
|---|---|---|---|---|---|---|---|---|---|
| | | A | | B | | C | | D | |
| | | dm (m) | de (m) | dm (m) | de (m) | dm (m) | de (m) | dm (m) | de (m) |
| 0.010 | 5.70 | 0.014 | 0.015 | 0.091 | 0.080 | 0.012 | 0.010 | 0.015 | 0.013 |
| 0.011 | 5.48 | 0.016 | 0.017 | 0.104 | 0.093 | 0.015 | 0.012 | 0.022 | 0.019 |
| 0.012 | 5.28 | 0.017 | 0.018 | 0.111 | 0.101 | 0.019 | 0.016 | 0.015 | 0.013 |
| 0.013 | 5.11 | 0.020 | 0.021 | 0.115 | 0.104 | 0.019 | 0.016 | 0.020 | 0.018 |
| 0.014 | 4.96 | 0.022 | 0.023 | 0.120 | 0.109 | 0.027 | 0.024 | 0.024 | 0.021 |
| 0.015 | 4.83 | 0.023 | 0.024 | 0.122 | 0.111 | 0.032 | 0.027 | 0.025 | 0.022 |
| 0.016 | 4.69 | 0.025 | 0.026 | 0.138 | 0.129 | 0.034 | 0.029 | 0.027 | 0.024 |
| 0.017 | 4.59 | 0.027 | 0.028 | 0.141 | 0.130 | 0.058 | 0.053 | 0.024 | 0.021 |
| 0.018 | 4.49 | 0.029 | 0.030 | 0.145 | 0.134 | 0.054 | 0.049 | 0.020 | 0.018 |
| 0.019 | 4.39 | 0.030 | 0.031 | 0.151 | 0.140 | 0.046 | 0.040 | 0.019 | 0.017 |
| 0.020 | 4.30 | 0.031 | 0.032 | 0.152 | 0.141 | 0.032 | 0.027 | 0.019 | 0.017 |

**Table 3. $d_m$ and $d_e$ reads in the straight stilling basin for case 2**

| Q ($m^3/s$) | Fr1 | Section No. | | | | | | | |
|---|---|---|---|---|---|---|---|---|---|
| | | A | | B | | C | | D | |
| | | dm (m) | de (m) | dm (m) | de (m) | dm (m) | de (m) | dm (m) | de (m) |
| 0.010 | 5.70 | 0.026 | 0.077 | 0.067 | 0.078 | 0.034 | 0.059 | 0.028 | 0.049 |
| 0.011 | 5.48 | 0.031 | 0.080 | 0.072 | 0.081 | 0.035 | 0.064 | 0.032 | 0.051 |
| 0.012 | 5.28 | 0.034 | 0.085 | 0.086 | 0.083 | 0.040 | 0.072 | 0.032 | 0.056 |
| 0.013 | 5.11 | 0.037 | 0.087 | 0.091 | 0.085 | 0.044 | 0.082 | 0.034 | 0.058 |
| 0.014 | 4.96 | 0.039 | 0.089 | 0.102 | 0.087 | 0.046 | 0.092 | 0.040 | 0.064 |
| 0.015 | 4.83 | 0.040 | 0.093 | 0.118 | 0.088 | 0.052 | 0.099 | 0.044 | 0.069 |
| 0.016 | 4.69 | 0.041 | 0.095 | 0.124 | 0.089 | 0.071 | 0.106 | 0.042 | 0.074 |
| 0.017 | 4.59 | 0.043 | 0.099 | 0.132 | 0.089 | 0.077 | 0.109 | 0.042 | 0.082 |
| 0.018 | 4.49 | 0.046 | 0.105 | 0.139 | 0.090 | 0.085 | 0.112 | 0.039 | 0.087 |
| 0.019 | 4.39 | 0.048 | 0.113 | 0.140 | 0.093 | 0.089 | 0.114 | 0.043 | 0.091 |
| 0.020 | 4.30 | 0.052 | 0.119 | 0.141 | 0.096 | 0.092 | 0.117 | 0.045 | 0.093 |

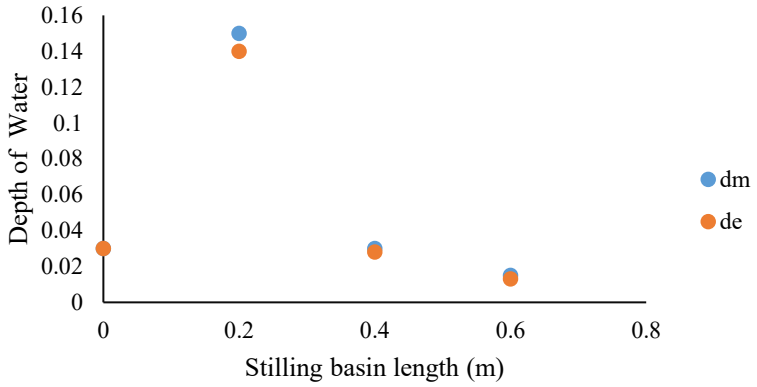


**Figure 9. Comparison of dm and de free surface profiles of water case 1; Q= 0.020 $m^3/s$**

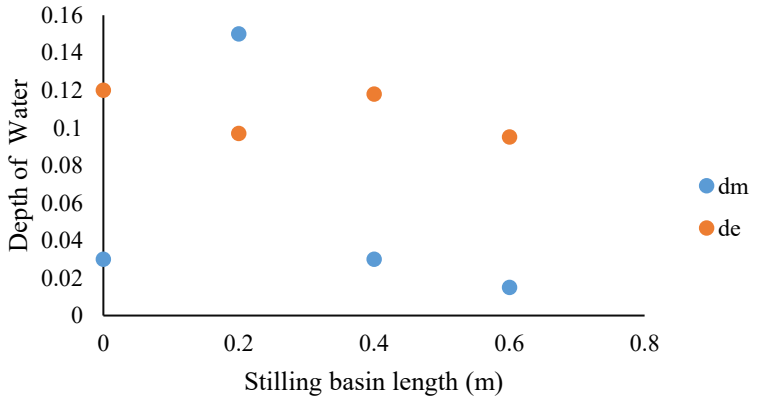


**Figure 10. Comparison of dm and de free surface profiles of water case 2; Q= 0.020 m3/s**

## Conclusions

This research focused on using zigzag walls in stilling basin. The research presented here advances the basic comprehension of these dispersing structures. Two distinct cases were examined experimentally in order to achieve that objective. In fact, as the using of zigzag walls in stilling basin, more upward flow caused more dispersion in the air, which in fact led to higher energy dissipation. By raising the discharge in two cases, as a result of lower flow resistance, relative energy dissipation was also decreased. When dissipating energy for high-velocity flows is necessary, blocks are utilized. However, investigating the cavitation between blocks in the stilling basins remains a problem, and the effect of a block on erosion at a spillway downstream, created by arranging and positioning of blocks on the stilling basin base, in addition to jet flow and a range of block forms. In this research, the effect of employing zigzag walls in a stilling basin on the quantity of kinetic energy dissipation was examined by experimental methods. Subsequently, a laboratory test was used to examine the impact of several independent parameter adjustments on the quantity of kinetic-energy dissipation. Moreover, the average amount of energy dissipation in stilling basin with zigzag walls of stilling basin ( case2) is (64.9%) compared to that in a smooth walls in stilling basin which is (61.1%) increased by (3.8%) for discharges of water range from (0.010 m3/s to 0.020 m3/s) for the eleven tests in the two cases. The use of blocks in the stilling basins gives a higher dissipation energy than the use of smooth stilling basins because these blocks are in the flow's direction and because the volume occupied by appurtenances contributes to the creation of a backwater problem (Peterka,1978).

It can be noted that case1 indicates a 5.5% difference in dissipation energy due to a little drop in the rate of energy dissipation with an increase in Froude number 4.69 to 5.70. On the other hand, with a decrease in Froude number to 4.30, the rate of energy dissipation rapidly decrease, resulting in a 22.6% difference in dispersion energy. At Froude number lower than 4.69, the inability to dissipate the energy with the necessary efficiency arises due to the increasing water velocity and fewer energy dissipater blocks. But in this case, the energy dissipation blocks are enough and able to effectively disperse the energy at Froude number ranging from 4.69 to 5.7. Case2 shows comparable behavior, with the exception of a little decrease in the dispersion energy difference of 5.1% with increase Froude number from 4.30 to 5.70. In general, using the second case gave stability in the amount of energy dissipation for all Froude numbers used .
From observing Fig. 10 for case2, it is found that the water heights in the middle of the stilling basin are generally lower than the water heights at the edge, while in Fig. 9 for case1, it is found that the height values are almost equal, in addition to the instability of the water levels along the length of the stilling basin.
From the previous results, it is conclude that the use of zigzag walls in the stilling basin leads to an increase in relative energy losses and the lowest Froude number (Fr2 between 0.46 to 1.20) at the downstream of stilling basin and also leads to reducing the length of the hydraulic jump at the downstream, thus reducing the length of the stilling basin. This reflects positively on reducing the cost and time of construction.

***Author Contributions***

All authors contributed equally to the conceptualization of the article and writing of the original and subsequent drafts.

***Data Availability Statement***

Data available on request from the authors.

***Acknowledgements***

The authors would like to thank all participants in the present study.

***Ethical Considerations***

The authors avoided data fabrication, falsification, plagiarism, and misconduct.

***Funding***

This research did not receive any specific grant from funding agencies in the public, commercial, or not-for-profit sectors.

***Conflict of Interest***

The authors declare no conflict of interest.

## References


Abbaspour, A., Hosseinzadeh Dalir, A., Farshadizadeh, D., & Sadraddini, A.A. (2009). Effect of sinusoidal corrugated bed on hydraulic jump characteristics. Journal of Hydro-environment Research, 3(2), 109-117. https://doi.org/10.1016/j.jher.2009.05.003

Alfiansyah, Y., Azmeri, A., Faris, Z., Ziana, Z., & Muslem, M. (2022). An experiment of energy dissipation on USBR IV stilling basin - Alternative in modification. *Journal of Water and Land Development*,53(IV–VI), 68-72. https://doi.org/10.24425/jwld.2022.140781

Alireza J., & Ebrahim, A.(2021). Experimental Study on the Effects of Rectangular Zigzag Blocks Geometry on Hydraulic Jump Characteristics in Trapezoidal Channel. *Journal of Hydraulics*, 16 (2), 31-42. https://doi.org/10.30482/jhyd.2021.261274.1496

Ashraf F., & Zhi-lin, S. (2012). Hydraulic jump basins with wedge-shaped baffles. *Journal of Zhejiang Univ-Sci A (Appl Phys & Eng)*, 13(7), 519-525. https://doi.org/10.1631/jzus.A1200037

Bhowmik, N. G., (1971). Hydraulic Jump Stilling Basin for Froude Number 2.5 to 4.5. *Illinois State Water Survey Publications*, Urbana, USA. https://books.google.com/books/about/Hydraulic_Jump_Type_Stilling_Basins_for.html?id=KUd2GQAACAAJ

Chow, V. T. (1959). Open-Channel Hydraulics. *McGraw-Hill Publications*, New York, USA. https://www.accessengineeringlibrary.com/binary/mheaeworks/

Chow, V. T. (1988). Open channel hydraulics. *McGraw-Hill Book Publications* Columbus, Ohio, U.S. https://www.accessengineeringlibrary.com/binary/mheaeworks

Christopher, B., & Raphael, C. (2019). United States Bureau of Reclamation Type IX Baffled Chute Spillways: A New Examination of Accepted Design Methodology Using CFD and Monte Carlo Simulations, Part I. *Water, mdpi journal*, 7 (1), 13. https://doi.org/10.3390/ECWS-3-05805

Ead, S.A., & Rajaratnam, N. (2002). Hydraulic jump on corrugated bed. *Journal of Hydraulic Engineering, ASCE*, 128(7), 656-663. https://doi.org/10.1061/(ASCE)0733-9429(2002)128:7(656)

Gandhi, S., & Singh, R.P. (2016). Empirical Formulation of Flow Characteristics in Trapezoidal Channels. *Journal of The Institution of Engineers*, (India), 97(3), 247-253. https://doi.org/10.1007/s40030-016-0153-3

Hayawi, H. A., & Mohammed A., Y. (2011). Properties of Hydraulic Jump Down Stream Sluice Gate. *Research Journal of Applied Sciences, Engineering and Technology*, 3(2), 81-83. https://www.researchgate.net/publication/215647334

Ibrahim M. M. (2017). Improve the Efficiency of Stilling Basin Using Different Types of Blocks. *American Journal of Engineering Research (AJER)*, 6(8), 295-304. https://www.researchgate.net/publication/359195975

Izadjoo, F., & Shafai Bejestan, M. (2007). Corrugated bed hydraulic jump stilling basin. *Journal of Applied Sciences*, 7(8), 1164-1169. https://doi.org/10.3923/jas.2007.1164.1169

Nassrin, J., Thair J., Khalid S., & Laith S. (2020). The Effects of Different Shaped Baffle Blocks on the Energy Dissipation. *Civil Engineering Journal*, 6(5), 961-973. http://dx.doi.org/10.28991/cej-2020-03091521

Novak, P., Moffat, A. I. B., Nalluri, C., & Narayanan, R. (2007). Hydraulic Structures. *Taylor and Frances Publications*, New York, USA. https://www.taylorfrancis.com/books/mono/10.1201/9781315274898/hydraulic-structures-novak-moffat-nalluri-narayanan

Peterka, A.J. (1978). Hydraulic Design of Stilling Basins and Energy Dissipators. *United States Department of Interior—Bureau of Reclamation Publications*, Denver, Colorado, USA. https://www.usbr.gov/tsc/techreferences/hydraulics_lab/pubs/EM/EM25.pdf

Pillai, N.N., Kansal, M.L.(2022). Stilling Basins Using Wedge-Shaped Baffle Blocks. *9th International Symposium on Hydraulic Structures Publications*, Roorkee, India. https://doi.org/10.26077/1d83-f83b

Rasoul D., Amir G., Ali A., & Silvia F. (2020). On the Effect of Block Roughness in Ogee Spillways with Flip Buckets. *Water, mdpi journal*, 5 (4), 182. https://www.researchgate.net/publication/344689815

USBR. (1987). Design of Small Dams. *United States Department of Interior- Bureau of Reclamation Publications*, Washington, DC, USA. https://www.usbr.gov/tsc/techreferences/mands/mands-pdfs/SmallDams.pdf

Wang, H., & Chanson, H. (2013). Free-Surface Deformation and Two-Phase Flow Measurements in Hydraulic Jumps. Research Report No. CH91/13, *School of Civil Engineering*, the University of Queensland, Brisbane, Australia. https://www.academia.edu/115367311/Free_Surface_Deformation_and_Two_Phase_Flow_Measurements_in_Hydraulic_Jumps

Advanced Technologies in Water Efficiency
homepage:https://atwe.razi.ac.ir
Online ISSN:2783-4964
Razi University

# Conceptualizing water bankruptcy in forbidden plains of Iran (Case study: Mahidasht plains)

**Lida Sharafi**[1], and **Kiumars Zarafshani**[2]✉

1. Agriculture-Jahad Organization, Kermanshah, Iran., & Department of Agricultural Extension & Education, Faculty of Agricultural, Razi University, Kermanshah, Iran. E-mail: lida.sharafi@yahoo.com
2. Corresponding author, Department of Agricultural Extension & Education, Faculty of Agricultural, Razi University, Kermanshah, Iran. E-mail: Zarafshani2000@yahoo.com

## Article Info

**Article type:**
Research Article

**Article history:**
Received 20 May 2025
Received in revised form 18 August 2025
Accepted 28 September 2025
Available online 22 December 2025

***Keywords***:
Mahidasht Plain,
thematic analysis,
water crisis,
water bankruptcy.

## ABSTRACT

**Objective:** The purpose of this case study was to conceptualize WB as perceived by irrigated farmers and agricultural experts in Mahidasht township.

**Method**: In recent years, climate change has caused a significant decrease in rainfall compared to the long-term average in Iran. In addition, mismanagement of water resources in the agriculture sector has caused the reduction of renewable water, destruction of the ecosystem, and local and regional water disputes. In such a way that there is a reservoir deficit of 350 BCM in Iran's underground water resources, which is about a quarter of the total reserves of underground water resources. According to the statistics of the country's water resources balance, the total amount of water harvest is equal to 96.37 billion $m^3$, of which 85.6 billion $m^3$ is related to the agricultural sector. As a consequence, water management experts have called for the state of "water bankruptcy" in the plains of the country, including the Mahidasht Plain in western part of Iran. However, any measures taken by water management experts need to conceptualize water bankruptcy (WB) as perceived by experts and farmers. Because environmental crises, including water bankruptcy, are rooted in human behavior. Since the correct perception of a problem is a prerequisite for behavior; therefore, conceptualizing "water bankruptcy" perceived by stakeholders can reveal the root causes of this phenomenon in the region. Thus, it should also be considered as the first step in solving the conflicts caused by this issue. This study used exploratory qualitative method using case study approach. This research, purposeful sampling through "critical case method" was used as a sampling frame of the study. The population of this study comprised 25 participants, including Experts in Agricultural Organization, Regional Water Company, faculty members in College of Agriculture, and farmers in Mahidasht Plain in Kermanshah Province. Individual interviews and group discussion sessions were used to collect data. Qualitative field notes were collected and coded using thematic analysis.

**Results**: The results of thematic analysis process revealed that the main concepts of WB are: excess water harvesting (EWH), reduced surface water (RSW), reduced ground water (RGW), condensation and change of aquifer (CCA), negative water balance (NWB), over harvesting of renewable water (ORW) and engaging in non-agricultural activities (ENA).

**Conclusions**: Policymakers and researchers can benefit from the results of this research in providing dynamic models of water allocation in common basins.

**Cite this article:** Sharafi, L. & Zarafshani, K. (2025). Conceptualizing water bankruptcy in forbidden plains of Iran (The case of Mahidasht plain). *Advanced Technologies in Water Efficiency, 5* (4), 15-45. https://doi.org/ 10.22126/atwe.2025.12466.1178


https://doi.org/ 10.22126/atwe.2025.12466.1178
Publisher: Razi University.

## Introduction

Water management has become a fundamental problem and its dimensions and complexities are increasing. According to the United Nations report, by 2030, only 60% of the world's population will have access to safe water. FAO has also forecasted that water withdrawal from reservoir will be 1.7 times faster than population growth. It is also estimated that by 2050, agricultural water demand will increase by 60% compared to 2006 and 2007 (Amiri et al., 2020).

The water crisis has become an important issue for people and policymakers for several decades, causing water conflict among stakeholders (Islami & Rahimi, 2019). In addition to climate change, inappropriate water management has exacerbated the water crisis. This problem is especially evident in the agricultural sector, which is closely related to water resources. Iran, which is located in an arid and semi-arid sector, is known as the most water-scarce country in the region, and its water reserves are running out. In addition, out of 609 water plains in Iran, 404 plains are in a prohibited or critical condition, and the total volume deficit of Iran's plains reservoir is estimated at 4867.8 MCM (Ministry of Energy Protection and Operation Deputy, 2019). Among these plains, Mahidasht, located in the western part of Iran, has been announced as a forbidden plain introduced as a Plain since 2007. The average yearly rainfall for 2022-4 was 144.9 mm in the Mahidasht Plain. This amount was reduced by 31% compared to the long-term average (Ghamarnia, 2023). In addition, continuous droughts and over-harvesting of water by farmers have reduced the reservoir volume in Mahidasht Plain by 260.20 MCM (Ghamarnia, 2023). Other researchers have clearly shown the critical situation of the plain in terms of aquifer depletion and water poverty (Veisi et al., 2021; Zarafshani & Sadvandi, 2017).

Thus, water resource experts have made an alarming sound and declared “water bankruptcy” as a post-crisis stage for water situation in Iran. They believe, the country is facing WB because the "liabilities" (water withdrawals) exceed the "reasonable value of assets held" (rates of aquifer recharge and recharge by surface water) (Collins, 2017). Water bankruptcy seems to place Iran in the most unprecedented historical challenges. A challenge that can make significant parts of the ancient geographical-political territory uninhabitable and be a prelude to political-social crises that endanger territorial integrity (Fattahi, 2018). Therefore, the increasing demand for water on the one hand and reduced access to water resources on the other hand has created conflict among users in the allocation of common water resources. Moreover, it has also attracted the attention of researchers and policymakers to adapt effective water management strategies (Sadat et al., 2018). Some researchers (e.g., Shahraki et al., 2024; Yazdian et al., 2022; Pournabi et al., 2022; Jalili Kamju & Khochiani, 2020; Jamalomidi & Moridi, 2020; Tayebzadeh Moghadam and Malekmohammadi, 2020; Abrahe et al., 2019; Sadat et al., 2018; Oftadeh et al., 2016) have used WB models to resolve water conflict, which in turn helps proper allocation of water among users. In addition, dispute resolution (bankruptcy) and game theory approaches have been used to resolve groundwater disputes (Abraha et al., 2019; Jamalomidi & Moridi, 2020). However, they failed to consider diverse concepts held by water users as well as water experts as to how they conceptualize (WB) before they consider a best model for water allocation. In other words, as pointed out by Wickramage (2019) Selection of the best allocation rule depends on how beneficiaries conceptualize the WB. Moreover, since there is no exact model or method to choose the best, it seems that the best model would be to utilize concepts held by beneficiaries. Therefore, this study attempts to fill this gap by providing concept of WB as perceived by water stakeholders.

Thus, a first step in effective water management is to conceptualize WB as perceived by end users as well as water policy experts in Iran. Conceptualization of WB has practical implication for water management policies in Iran in that any intervention made by policymakers starts with bottom up resulting in efficient use of water resources and thus resolves any water conflict among water end users. Therefore, this qualitative study sought to conceptualize WB as perceived by farmers and water management experts.

Access to safe water, sanitation and hygiene is the most basic human need for health and well-being. Billions of people will lack access to these basic services in 2030 unless progress quadruples. Demand for water is rising owing to rapid population growth, urbanization and increasing water needs from agriculture, industry, and energy sectors. In December 1992, the United Nations General Assembly adopted resolution in which 22 March of each year was declared World Day for Water with a focus the Sustainable development Goal 6 (Qanadi, 2023).

In Sustainable Development Goal 6 in 2023 declares the importance of achieving "clean water and sanitation for all". It is one of the 17 Sustainable Development Goals established by the United Nations General Assembly to succeed the former Millennium Development Goals (MDGs). According to the United Nations, the overall goal is to: "Ensure availability and sustainable management of water and sanitation for all" (UNDP, 2015). Some of these targets are: Substantially increase water-use efficiency across all sectors and supply of freshwater to address water scarcity and substantially reduce the number of people suffering from water scarcity; Protect and restore water-related ecosystems, including forests, wetlands, rivers, aquifers, and lakes; and Support and strengthen the participation of local communities in improving water management (Kufeoglu, 2022).

However, the reports and field surveys of the United Nations show that the world has still failed to achieve this goal and billions of people, businesses, health centers, farms and factories still do not have access to proper water services (Qanadi, 2023).

In the meantime, around 70 percent of global freshwater resources are used for agriculture (Ingrao et al., 2023). In developing countries such as Iran, water use in agriculture accounts for 90 percent of all water withdrawals (Doungmanee, 2016). Therefore, water shortage causes the greatest damage to the agricultural sector and farmers' livelihood.

In addition, Iran, which is located in arid and semi-arid regions, consecutive droughts have severely affected natural resource dependent sectors such as agriculture, causing huge economic losses (e.g., loss of food and feed production, increased livestock mortality, declining household farm incomes, and rising food prices) in this sector. It has also caused irreparable damage, including biodiversity loss, water security risk, reduced soil fertility, increased wind erosion, reduced plant fertility, increased disease incidence and pest invasion, increased fires, and lost canopies (Sharafi et al., 2020).

On the other hand, according to the report of the Water Research Institute of the Ministry of Energy in Iran, the amount of water harvesting from the total renewable water sources in normal periods is estimated to be 95%. Meanwhile, the normal percentage of harvesting renewable water sources is defined as 40-50% (Bazrafshan, 2021).

Therefore, all the evidence indicates that Iran is far from achieving sustainable development goal 6. Thus, water crises in recent years have caused the discussion of WB to be raised by some experts.

Water bankruptcy (WB) is raised when common and divisible property (E) is going to be divided between (i) the claimant and the amount of claim (Ci), so that the amount (E) is less than the total claim of the claimants (C). In bankruptcy, resources must be divided between a

group of claimants, while the amount of claim is not enough to satisfy all the claims (Herrero & Villar, 2001). Yet in another definition, WB is considered as a new approach to solve water conflicts among different stakeholders from shared water resources. Bankruptcy theory is a subset of game theory that examines the problem of redistribution of limited common resources between claimants in several ways. For example, this approach uses the common methods of Proportional bankruptcy (P), Adjusted Proportional (AP), Constrained Equal Loss (CEL), Constrained Equal Award (CEA), Piniles (PIN) and Talmud (TAL) (Abraha et al. al., 2019; Zare Farjoudi, et al., 2019; Jamalomidi & Moridi, 2020).

There are limited practical studies in the field of WB due to its novelty. These studies have mainly focused on technical aspects of WB such as economic and mathematical methods to better develop water allocation models in different national and international basins (Shahraki et al., 2024; Yazdian et al., 2022; Pournabi et al., 2022; Tian et al., 2021; Jalili Kamju and Khochiani, 2020; Jamalomidi and Moridi, 2020; Tayebzadeh Moghadam and Malekmohammadi, 2020; Abrahe et al., 2019; Nafarzadegan et al., 2019; Sadat et al., 2018; Oftadeh et al., 2016; Mulugeta Degefu and He, 2016; Madani et al., 2014; Zarezadeh et al., 2012; Herrero and Villar, 2001). However, limited attention has been paid to conceptualization of WB. While conceptualizing WB is as a first step in resolving water conflicts between the outsiders (policy makers) and the insiders (farmers).

It is worth mentioning that as far as the authors searched, no study has been done on the conceptualization of water bankruptcy, therefore, in the following, studies that develop water allocation models in the conditions of water bankruptcy have been done.

Using the theory of games and the MODFLOW model, Yazdian et al. (2022) in Iran, presented an optimal model for minimizing the reduction of groundwater level. The results revealed that farmers with clear foresight are in better position to avoid any cost endured by water mismanagement. Jamalomidi & Moridi (2020) conducted a study in Hormozgan province using bankruptcy models in order to manage groundwater resource conflicts. These researchers first simulated the groundwater flow model using MODFLOW software. Then, using the collaborative method (one of the bankruptcy methods), they calculated new aquifer withdrawal values and entered them into the simulation model and compared the results with the current situation. In their study, five bankruptcy methods were used in order to manage the extraction of production wells. The results showed that the aquifer's groundwater level increased which in turn resulted in improvement of aquifer.

Sadat et al. (2018) examined the optimal redistribution of water resource allocation in the Aras watershed (the common border of the four countries of Turkey, Armenia, Azerbaijan and Iran) using the combination of bankruptcy dispute resolution methods and Particle Swarm Optimization algorithm. Results revealed the superiority of the method bound to the same loss (CEL) over other bankruptcy methods. In other words, the average supply of water needs in the basin in 2020 scenario will increase by almost two billion cubic meters and in 2050 scenario by almost 1.5 billion cubic meters compared to other bankruptcy methods. Interestingly, the applicant with the lowest amount of demand (Turkey) is given the last priority given that Turkey is located in upstream of the basin. Thus, further application of this method requires consideration of alternative facilities and satisfaction of the stakeholders.

In another study, Mulugeta Degefu and He (2016) examined different scenarios for water scarcity in the Nile River Basin. In their study, they applied bankruptcy allocation rules to predict available water allocation of the river basin. Their study contributes to allocation of water scarcity in the Nile River basin and other border river basins in order to prevent water conflicts and ensure the sustainability of fresh water resources. In another study, Zarezadeh et al. (2012) investigated Qazluzan-Sefidroud river basin in Iran. This river basin is located

across eight provinces of the country which during the past a few years has suffered from social economic development projects leading to diverse water conflicts. They used four bankruptcy methods, i.e., relative, modified relative, equal profit bound, and equal loss bound in order to provide a fair allocation for different scenarios. The results showed that the plan based on the same profit constraint is the most acceptable allocation under all scenarios.

Madani et al. (2016) investigated the roots of WB by applying socio-economic perspective during drought in Iran. The authors found seventeen factors that influenced WB in Iran: rapid population growth, migration and expansion of urbanization, inadequate infrastructure for water distribution, deterioration of water quality, unsustainable agriculture, unrealistic self-sufficiency of food security, increasing water demand, cheap price for water and energy, indiscriminate dam construction, illegal deepening of wells, drought recurrent, occurrence of floods, climate change, bottom up development projects, economic sanctions and instability, inappropriate structure of water governance, and low level of environmental awareness. In another research, Moradian & Behvar (2018) found that the water crisis in Iran has multiple causes. For example, they showed that structural and physical view of development practitioners, the laws and regulations of water sector, and establishment of water activities affected water crisis in the region. They also identified inappropriate cultivation patterns, incorrect policies, invaluable perception of water price influenced water scarce in Iran. The study also highlighted several procedures to increase water use efficiency. For example, modernizing irrigation systems, correct timing of irrigation, and land leveling.

Overall, we can conclude that most WB researchers have used quantitative and technical approach to understand WB. However, more study is needed to take a qualitative non-technical approach to better understand the concept of WB. Moreover, quantitative researchers have neglected the emic views as pointed out by Chambers (1983). For example, conceptualizing WB as perceived by end users would help researchers in identifying dynamic models in their WB formulas when measuring this phenomenon.

## Method

This study employed an exploratory qualitative method using a case study approach. A case study is a detailed study of a specific subject, such as a phenomenon (In this study, the phenomenon is water bankruptcy). Also, this study utilized documentary research in order to achieve research goals and additional information. The documentary research method serves only as a supplement to the conventional social surveys. The use of documentary methods refers to the analysis of documents that contain information about the phenomenon we wish to study (Mogalakwe, 2006).

The population of this study comprised Experts in Agricultural Organization, Regional Water Company, faculty members in College of Agriculture, and farmers in Mahidasht Plain in Kermanshah Province located in western part of Iran. Compared to the quantitative research, purposive sampling is used in qualitative research, as it allows the researcher to focus on specific areas of interest and gather in-depth data on those topics. It is also commonly used in small-scale studies with limited sample size (Gall et al., 2003, Merriam, 2002). In this study, purposeful sampling through “critical case method” was used as a sampling frame of the study. Critical case sampling is a method in which samples are selected because of their extreme importance and are at the center of the subject. People or places that provide the most information are critical cases (Ranjbar et al., 2011). In this study, 15 experts and 10 key informant farmers were interviewed through semi-structured interview (a total of 25 people).

In qualitative studies, data saturation was used to determine the sample size (Francis et al., 2010). Saturation is among the most common guiding principle for assessing the adequacy of purposive samples in qualitative research (Morse, 2015). When the data begin to repeat, so that further data collection is redundant, signifying that an adequate sample size is reached (Francis et al., 2010). In other words, saturation refers to the point in data collection when no additional issues or insights are identified and data begin to repeat so that further data collection is redundant, signifying that an adequate sample size is reached. Saturation is an important indicator that a sample is adequate for the phenomenon studied and thereby demonstrates content validity (Francis et al., 2010). Reaching saturation has become a critical component of qualitative research that helps make data collection robust and valid (O'Reilly and Parker, 2013). Moreover, saturation is "the most frequently touted guarantee of qualitative rigor offered by authors to reviewers and readers" (Morse, 2015, p. 587). Hence, in this study, data saturation was achieved with 25 people; so the researchers stopped interviewing more people.

18 semi-structured individual interviews and 2 group discussion sessions were used to collect data. Data sources in this study include documentation, interviews, group discussions, participatory arrangements. The questions were related to issues discussed in the literature and designed to stimulate verbal reflection on the issue of water crisis in the region: Some questions were raised: Do you think the water situation in the region is in bankruptcy? What does water bankruptcy mean? How is the water situation in the region? Do farmers believe that the water situation in the region is in bankruptcy? Why has the Regional Water Company declared Mahidasht plain as a forbidden plain? What types of crops are grown in the area? How is the rainfall in the region in recent years? Is the farmer allowed to harvest as much water as he wants? What is the status of authorized and unauthorized wells in the region? How are agricultural water decisions taken in the region? Will farmers participate in the decision-making process for agricultural water management? And etc.

The researcher noted and recorded. The interviews lasted, between 20 until 110 minutes, for each person, depending on the time and willingness of the participants to continue the discussion. Interviews were continued until researcher reached saturation in that no new information emerged; then, sampling was stopped. In total, Interviews lasted for 843 minutes (14 hours and 5 minutes) and further documents related to Mahidasht Plain were collected. All interviews were conducted between April and May 2023.

Qualitative field notes were collected and coded using thematic analysis. Thematic analysis goes beyond the counting of obvious words and phrases and focuses on recognizing and explaining explicit and implicit ideas (Naeem et al., 2023). Braun and Clarke (2006) propose three steps for thematic analysis. 1) analyzing and describing the text, 2) describing and interpreting the text, and 3) combining and integrating the text. The first stage includes 3 steps (getting familiar with the text, creating initial codes and coding, searching and recognizing themes), the second stage includes 2 steps (drawing the network of themes, analyzing the network of themes) and the third stage includes 1 step (compilation of the report).

Themes were identified on two levels, semantic and latent. In the analysis of existing themes, the formation and development of themes is an interpretive work, and the analysis is not just a description but a form of theorizing.

In this study, in order to analyze the data, first, interviews text was implemented, word by word. Then, interviews notes and materials were reviewed several times and using open coding, key phrases were extracted. Then, by comparing these codes (phrases), similar codes were categorized and developed a theme (concept).

In relation to uncertainty analysis, it should be stated that this study was done using a qualitative paradigm (Fig. 1). Qualitative analysis is analysis that returns a classification rather than a numerical value. Therefore, in qualitative studies, validation and error is not done with software and statistics like in quantitative studies; instead, data and findings accuracy are checked using trustworthiness criteria (Enworo, 2023; Ahmed, 2024; Merriam, 2002). Trustworthiness of qualitative study is approved through credibility, transferability, dependability, and confirmability (Enworo, 2023; Ahmed, 2024; Merriam, 2002). Trustworthiness of this study was investigated through data sources triangulation and methods triangulation. In this way, the data was collected in several times and in different ways (available documents, individual interviews and group discussions). As a result, an effort was made to consider diversity in the selection of samples, and therefore, several people were interviewed (Thurmond, 2001). In addition, the results were studied and reviewed by the research team, and finally their opinions were applied to the obtained results, and this ensured the validity of the work (peer review) (Merriam, 2002). By implementing these techniques, researchers performed error and uncertainty analysis. The study process is summarized in Fig. 1.

## Study area

The study area is located in the Mahidasht sub-catchment area of the Karkheh River Basin in the middle of Kermanshah Province, Iran (Fig. 1) with a total area of 1,463 $Km^2$. The maximum and minimum elevations of the region are 2764 and 1310 m, respectively. In the Mahidasht plain, agriculture is the main source of the income of about 19,000 inhabitants. Shallow and deep (~1,500) wells exist in the area with an average annual water extraction of 105 MCM. The large number of wells is the main source of groundwater abstraction, which has increased pressure on the Mahidasht aquifer. The 30-year hydrograph shows a 15.3 m decline in water levels with an average annual reduction of 0.51 m (Fig. 2).
The first time Mahidasht Plain was announced as forbidden plain was in 2005/7/4 (Band-Ab Consulting Engineers Company, 2023).

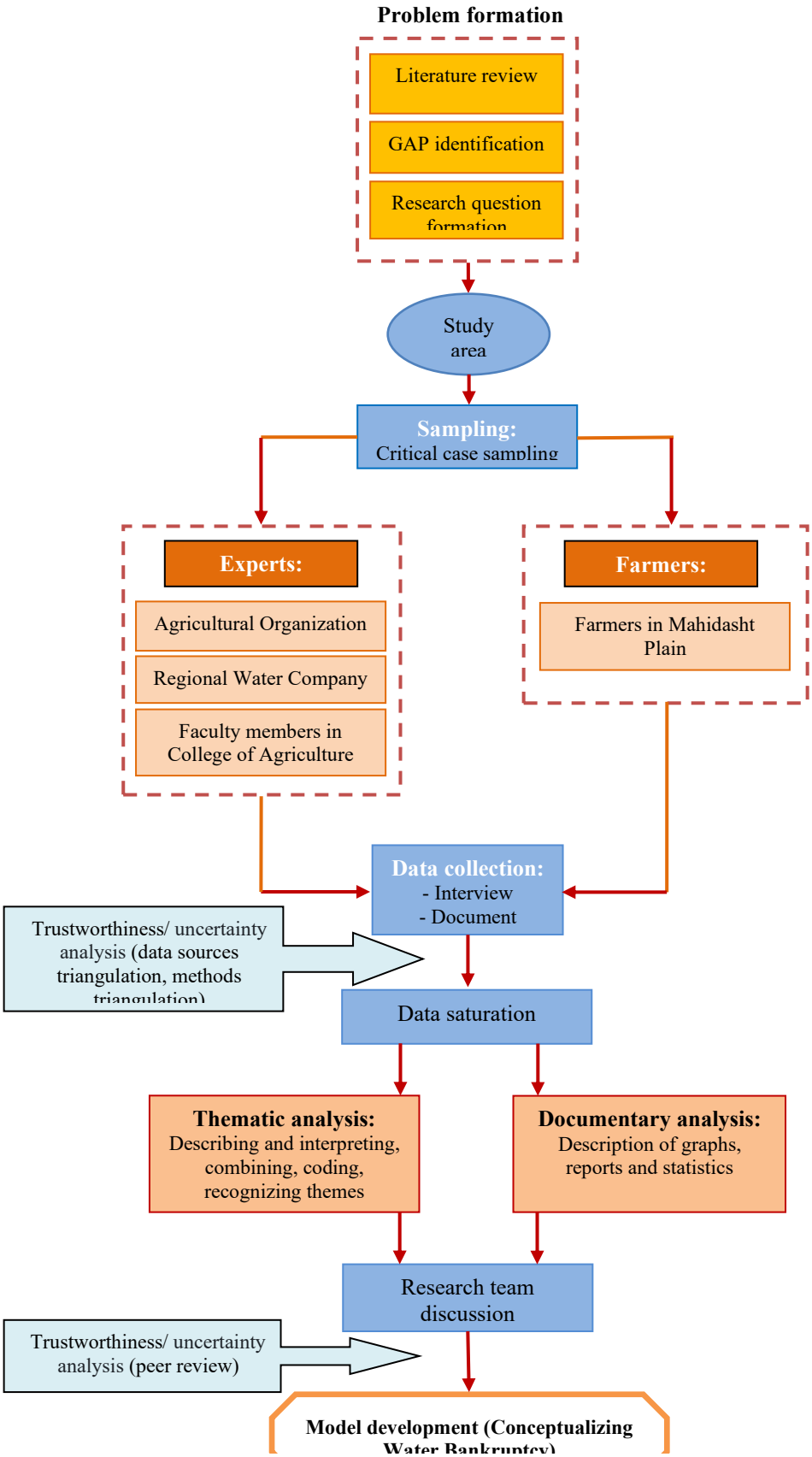


**Figure 1. Flow chart of the research process**

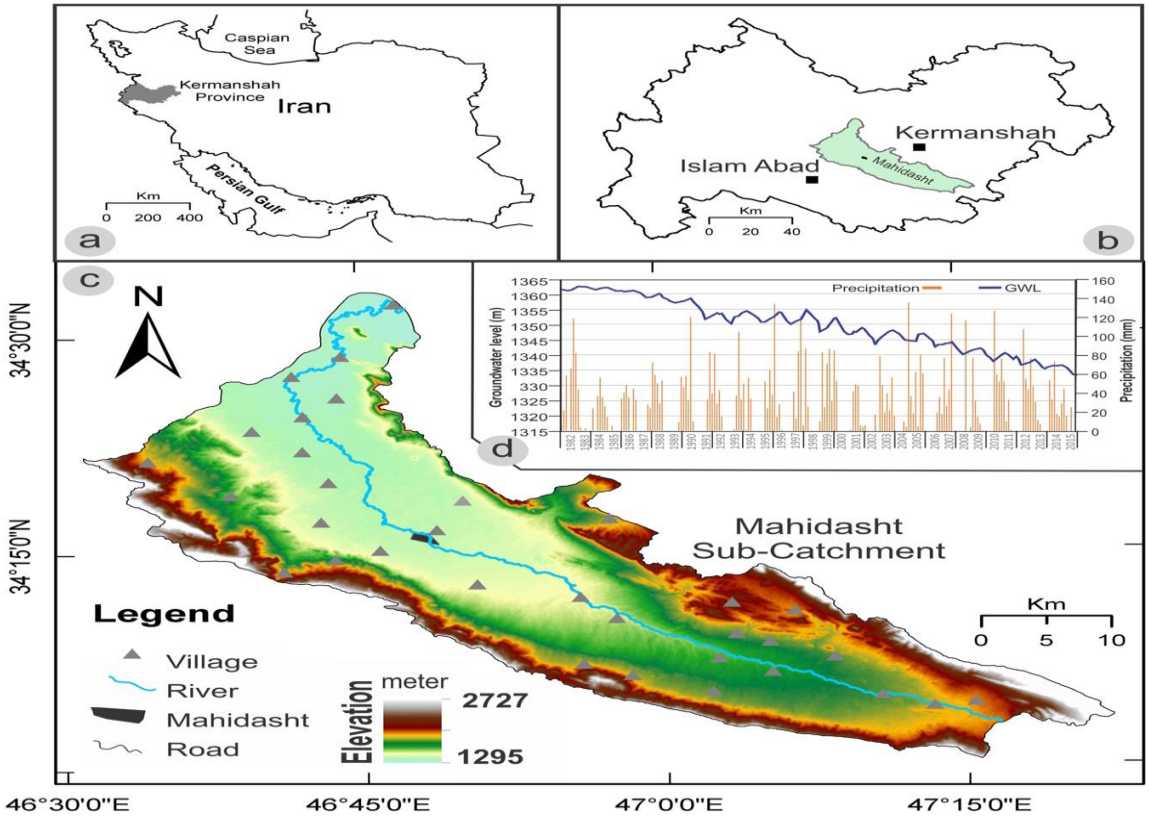


**Figure 2. Geographical location of study area: a) Iran; b) Kermanshah province; c) the elevation status of the region based on DEM status map, and d) unit hydrograph of Mahidasht aquifer (Majidipour et al., 2021)**

## Results

The analysis of water bankruptcy (WB), as perceived by participants, is highlighted in the following sections.

### Conceptualization of water bankruptcy as perceived by water experts

The results revealed 60 initial codes that further developed to twelve themes. As shown in table 1 and Fig. 2, excess water harvesting (EWH), reduced surface water (RSW), reduced ground water (RGW), condensation and change of aquifer (CCA), disruption of drinking water (DDW), negative water balance (NWB), over harvesting of renewable water (ORW), reached dead point with water (RDW), reduced water table (RWT), formation of hard pan (FHP), water forbidden (WF), engaging in non-agricultural activities (ENA).

**Table 1. Concepts of water bankruptcy as perceived by water experts**

| Quotes (open coding) | Type of thematic | Theme (axial coding) |
|---|---|---|
| Well exploitation permit is not based on real context. We announced certain amount of water harvest permit for normal years not dry years. We do not tell farmers that this amount is not for dry years! Farmers are in competition with one another and they are only concerned with harvesting water. They even irrigate their fields during rainfall season. | Latent | |
| Linear programing is dominant but not sufficient. Over-water permits to farmers have caused misconception as if there is ample of water to use. | Latent | |
| Over harvesting of water has to stop otherwise there will be no drinking water in the long run or stop cultivating spring cultivars. | Latent | |
| They only see short terms by deepening their wells and using irrigated method, they thought everything would be fine and continued over harvesting water without thinking about the future. If they think there is water for the next two years, they'll continue over using water. | Latent | |
| In general, at least 70% of the water consumed in Iran is used in agriculture. In our province, water consumption is more, because our economy is mostly agriculture. Also, average water consumption is high in Mahidasht Plain. | Latent | |
| We had 30 years of over harvesting. This is a terrible situation. Even four consecutive rains wouldn't do any good. | Semantic | Excess water harvesting |
| We can seal off the wells but it would conflict among us. There is no way out. | Latent | |
| Water resources are not good at all in Mahidasht Plain. Also, they do not have permission to utilize water. They may go towards illegal digging of wells. | Latent | |
| For example, a farmer has 10 hectares of land, he can make a living with 4 hectares, but he consumes more than he needs. | Latent | |
| During the past 3 years (from 1995 to 1999), the volume of water withdrawal from Mahidasht Plains has increased by more than 100%. | Latent | |
| Farmers are not satisfied with what they should withdraw from their wells. They vandalize water meters. | Semantic | |
| We installed water meters, but we do not have any restrictions on water withdrawals. Now the meters are rechargeable. | Semantic | |
| We at Regional Water Company do not allow over water harvesting, but farmers start to burglarize. | Semantic | |
| Water mismanagement without scientific background has caused many burdens on water resources. | Latent | |
| When demand for water is excessive, bankruptcy occurs. | Latent | |
| Water harvest is far more than the capacity. | Semantic | |

**Continue of table 1. Concepts of water bankruptcy as perceived by water experts**

| Quotes (open coding) | Type of thematic | Theme (axial coding) |
|---|---|---|
| There used to be other water resources such as river and rainfall. But now theses resources have depleted. The permits we issued are no longer useful and farmers continue to over use water from their wells. | Semantic | Reduced surface water |
| Current precipitation only compensates a certain amount of water shortage. In the wet season, water rises and in dry season water falls. The situation in Mahidasht is far more devastating to be compensated with current rainfall. | Latent | |
| Mahidasht Plains is a large area and there is no surface water to replenish so we are only dependent on groundwater. | Semantic | |
| It is true that during the past two years of drought, the capacity of water increased by about 300 mm, but two years later, a drought occurred and caused a further decrease water capacity. . | Latent | |
| Severe drought caused water shortage. On the other hand, we over harvested and this has caused shortage of water. | Latent | |
| In my opinion, Mahidasht Plain is 100% water bankrupt and with this amount of precipitation, the situation will never return. | Latent | |
| In general, Iran is water bankrupt because the average rainfall is 250 mm. | Latent | |
| Mahidasht Plains has no surface water. Only the Mereg River has dried up. | Semantic | |
| Farmers don't believe that there is no water. Also, with 10 mm of rain they think that the lack of water has been compensated. Although the have deepened their wells and created series of problems but they don't care at all. | Latent | Reduced groundwater |
| In Mahidasht Plain, during the past 30 years, we could reach less than 3-4 meters of water. We cultivated any type of crop we wanted but now the water table is way down with restrictions of digging wells. | Semantic | |
| In Mahidasht Plains, groundwater has reached way below and it takes time for water to reach below the surface. In the short term, this rainfall will not have much effect on discharge of the wells. | Semantic | |
| In Mahidasht Plains, we experienced water drop of 50-60 cm per year. Therefore, in the last 30 years, we had a water drop of 15 to 20 meters. Farmers clearly see what is going on. | Semantic | |
| Farmers know that there is no water due to dry wells. But they still deepen their wells due to their poor livelihood. | Latent | |
| We have been in crisis for many years now. The groundwater tables have reached salinity which in turn reduced yields. | Latent | |
| The water level has dropped between 20, 30, and 40-meters causing aquifer to reach the state of crisis. | Latent | |
| Believe it or not, we have wells that are 120 meters deep. | Latent | |

**Continue of table 1. Concepts of water bankruptcy as perceived by water experts**

| Quotes (open coding) | Type of thematic | Theme (axial coding) |
|---|---|---|
| Water holding capacity has decreased in the plain thus We cannot harvest the same amount of water as before. Soil pores were coarser before and the harvesting capacity has decreased. Special hydration has changed. | Semantic | Condensation and change of aquifer |
| The groundwater has reached way below and the soil structure is broken causing soil cracks and sinkholes. | Semantic | |
| In Mahidasht Plains, water holding capacity has decreased (for example, it has decreased by 20 cm). Topsoil has destroyed and cannot be regenerated. | Semantic | |
| Mahidasht Plains used to be fertile and wide with excessive rainfall and there was no need to dig a well. Now, water holding capacity has extensively reduced. | Latent | |
| Many years have passes by and this aquifer is no longer as effective as before due to changing characteristic of the aquifer. I don't think things will return as before. | Semantic | |
| If the aquifer is compressed with no point of return, water bankruptcy emerges. | Semantic | |
| Corn farmers admit that the wells are not sufficient and they have to irrigate with irrigation tapes even though is not enough. | Latent | Disruption of drinking water |
| We needed drinking water but we only had 12 liters. | Semantic | |
| We are also faced with health problems due to water shortage. Only if we reach famine, farmers would believe. | Semantic | |
| Mahidasht Plains has a serious problem with drinking water. The groundwater table is low and the hydrograph is strongly negative. | Semantic | |
| The groundwater level has decreased. In 2001 till now, the groundwater has reduced tremendously. | Semantic | |
| A large local company dug a well but reached zero water. | Latent | |
| The aquifer has decreased by 260 million $m^3$ (negative balance). The groundwater level has also decreased by year 1400. A local company asked me to find a place for him to dig a well but I refused. | Semantic | Negative water balance |
| Iran's water balance is bankrupt, especially in Mahidasht because of over crop harvesting. Rainfall in Mahidasht Plain is also limited, which is below Iran's annual average. The Plain has a large area with extensive crop cultivation with situation getting worse each year. | Semantic | |
| The water balance is negative and is getting worse year by year. It will never be compensated. With this amount of rains, the balance will never reach positive. | Semantic | |
| Every year, the balance between produced water to consumed water is negative. We have reached water bankrupt. | Semantic | |

**Continue of table 1. Concepts of water bankruptcy as perceived by water experts**

| Quotes (open coding) | Type of thematic | Theme (axial coding) |
|---|---|---|
| The aquifer has decreased by 260 million $m^3$ (negative balance). The groundwater level has also decreased by year 1400. A local company asked me to find a place for him to dig a well but I refused. | Semantic | Negative water balance |
| Iran's water balance is bankrupt, especially in Mahidasht because of over crop harvesting. Rainfall in Mahidasht Plain is also limited, which is below Iran's annual average. The Plain has a large area with extensive crop cultivation with situation getting worse each year. | Semantic | |
| The water balance is negative and is getting worse year by year. It will never be compensated. With this amount of rains, the balance will never reach positive. | Semantic | |
| Every year, the balance between produced water to consumed water is negative. We have reached water bankrupt. | Semantic | |
| Three indicators such as Falkenmark, Institute of Water Resources Management, and Institute's index are used to measure water status. The Falkenmark index is based on annual volume of renewable water resources per capita indicating individual water use. Deficiency index happens when an annual per capita volume of water is equivalent to 1000 cubic meters. Stress index occurs when an annual per capita volume of water is equivalent to 1700 cubic meters. Countries with annual per capita less than 1000 cubic meters are considered water scarce. However, countries with less than 500 cubic meters per capita per year are imposing pressure on people. | Latent | Over harvesting of renewable water |
| According to the United Nations, if we consume 40% or more of renewable resources, we are in the critical state. We now have 100 billion cubic meters of renewable water. According to the Ministry of Agriculture, about 62 billion $m^3$ is used in agriculture. However, Ministry of Energy states otherwise (80 billion $m^3$). A clear contradiction at policy level. We are better of importing some agricultural products (virtual water). | Latent | |
| We have no right to harvest renewable water needless to say we did. | Semantic | |
| For example, one year of wet season causes delay in groundwater drop. Nature helps by providing rain thus delays groundwater drops. All projects such as aquifer restoration, increased performance and efficiency of irrigation systems is word of mouth. We hardly survive. | Latent | Reached dead point with water |
| We have reached dead end (over water harvesting and huge number of wells). There might be a solution but not with this type of management. | Semantic | |
| We might be able to control the situation but we cannot save the Plain. | Latent | |
| There are about 1000 legal wells and 200-300 illegal wells in Mahidasht Plain. The water table of water has gone way below. | Semantic | Reduced water table |
| In sandy soil water is stored. If water table goes below 20 cm, the soil to settle. It would never be the same. | Latent | |
| The hard pan is formed in the surface horizons of the soil. How do you expect rainwater penetrates to the lower level and groundwater aquifers? | Semantic | Formation of hard pan |
| Excessive use of chemical fertilizers, especially urea, hardens the soil and creates hard pan. | Semantic | |

**Continue of table 1. Concepts of water bankruptcy as perceived by water experts**

| Quotes (open coding) | Type of thematic | Theme (axial coding) |
|---|---|---|
| Mahidasht Plain as one of our worse Plain is known as critical forbidden Plain so that it has been adjusted to certain measures. This helps to allocate minimum amount of access water to farmers. However, other Plains in the province has received improvement factor. Let us say water forbidden Plain. | Semantic | Water forbidden |
| Farmers are no longer cultivating because there is no water. | Semantic | Engaging in non-agricultural activities |

"Excess water harvesting" (EWH) has been proposed as the first concept of WB by experts. This concept consists of 16 representative phrases that express the expert's consensus regarding this concept. In other words, the emphatic statements about this concept all indicate that farmers in the region are extracting excessive water from the plain' capacity, with no legal restrictions on water harvesting. Therefore, EWH is considered as WB.

The second concept that the experts frequently raised regarding WB is "reduced surface water" (RSW) and "reduced ground water" (RGW) which each of these was characterized by 8 representative terms. From the experts' point of view, rainfall has decreased in recent decades, which leads to the decrease of surface water sources such as rivers. To the extent that the most important river in the region (Mereg River) has dried up. On the other hand, water harvesting continues to rise, which has caused the groundwater aquifers to drop sharply, with recent rains having no significant impact on water flow. Therefore, experts consider this issue as WB.

Other important concepts of WB in the studied area were "condensation and change of aquifer" (CCA) and "disruption in drinking water" each with 6 primary quotes. Water and soil experts believe that the significant decline in groundwater levels has condensed the soil structure, breaking down soil particle pores (creating micropores), thereby reducing water-holding capacity. This situation arises because, despite adequate rainfall, water cannot be stored due to the compression and condensation of the aquifer. Therefore, water and soil experts introduce WB as CCA.

Regarding the disruption in drinking water, some experts said that the water situation in the region is critical and the authorities are facing problems in providing drinking water and sanitation. Therefore, this situation shows that the plain is facing a severe water shortage and is bankrupt. Thus, experts consider the disruption in drinking water as an indicator of WB.

Another key concept that was raised by some water experts is "negative water balance" (NWB) with 4 emphatic codes. According to them, water harvesting is more than the water input to the plain, resulting in a negative water balance that cannot be offset by recent rainfall. In fact, experts consider WB to mean a NWB.

Concepts such as "over harvesting of renewable water" (ORW) and "reached dead point with water" (RDW) each include 3 primary quotes. Regarding ORW, the experts admitted that currently, over 40% of renewable water resources are utilized in Iran, reflecting the country's critical water situation. Therefore, experts interpreted the bankruptcy of Mahidasht Plain as an ORW.

Some experts also used the term RDW for WB. They believe that the excess water harvesting and the existence of several wells in the region have caused the water situation to reach a dead end, and nothing can be done.

Among the other concepts of WB that were mentioned by the experts, there were concepts such as "reduced water table" (RWT) and "formation of hard pan" (FHP), each of these topics is also mentioned with 2 initial terms.

Excess water harvesting (EWH) and the existence of several wells in the region have caused the reduce water table. As a result, this issue has made it more difficult to access groundwater. Hence, sometimes re-excavation is required to reach the groundwater tables. This issue leads to saltwater intrusion into groundwater aquifers. Therefore, some experts believe that RWT indicates the WB in the region.

Some soil experts consider the FHP on the soil surface as a reason for WB. They explained that overuse of chemical fertilizers (e.g., urea) hardens the soil, forming a surface crust. In this case, it is not possible for rain water to penetrate to the lower layers, and considering that the only water input in Mahidasht Plain is rain water, this problem causes a severe shortage of groundwater in the region, and WB occurs.

"Water forbidden" (WF) and "engaging in non-agricultural activities" (ENA) with 1 initial phrase are other concepts raised by experts in relation to WB in Mahidasht Plain. Water experts stated that the Mahidasht Plain is one of the critical forbidden plains that well-drilling permits should not be issued, and water-intensive crops should not be cultivated. They use the forbidden water concept for WB.

Some experts also believe that the severe lack of water in the region has caused many farmers to stop farming and engaging in non-agricultural jobs. These experts consider engaging in non-agricultural jobs as an indicator of the critical water situation and WB in the region.

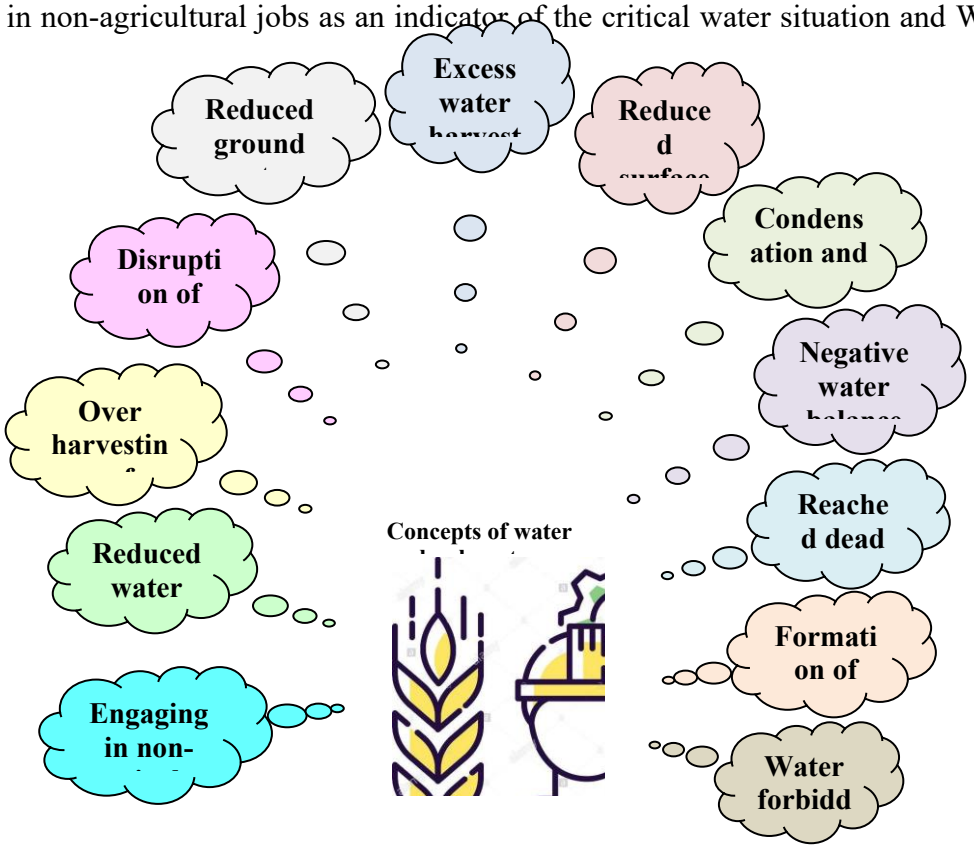


**Figure 2. Conceptualization of water bankruptcy as perceived by water experts**

## Conceptualization of water bankruptcy as perceived by water farmers

The results revealed 47 initial codes, which were consolidated into five themes. As shown in table 2 and Fig. 3, excess water harvesting (EWH), reduced surface water (RSW), agricultural bankruptcy (AB), reduced ground water (RGW), and water forbidden (WF).

**Table 2. Concepts of water bankruptcy as perceived by farmers**

| Quotes (open coding) | Type of thematic | Theme (axial coding) |
|---|---|---|
| We should use floating pump equal to size of our land and not more. Most think its their right to do so. | Semantic | Excess water harvesting |
| Mahidasht Plain has water problem. There is excessive exploitation among legal wells. Deep wells are also drying up. | Semantic | |
| Farmers dug their wells without restrictions and in close distance. An unknown middleman asked me to pay x for him to give me a permit to dig a new well. | Semantic | |
| Farmers use water as much as they can with this in mind that if he doesn't someone else would. | Semantic | |
| Smart meter is useless for farmers. I know someone who uses 8 sprinklers without anyone complaining. | Latent | |
| I know a x factory who is draining all the water with his two wells (250 meters) that is located in Sarab Niloufar Lake. | Latent | |
| All crops grown in the region are water-bearing crops. If water experts had informed us about impact of high-water bearing crops and even penalize us, we would have stop cultivating such crops. | Latent | |
| Unfortunately, farmers are not allowed to over collect water, but they do anyway. | Semantic | |
| I am allowed to use 2 liters of water per second, but I use 30 liters of water per second. I am willing to pay for the extra. | Semantic | |
| Even If farmer knows that there will be no more water in 5 years, he would still over collect water without thinking of next generation. | Latent | |
| Land tenants and some owners install strong floating pump and extract 20 inches of water per second. | Semantic | |
| There are 32 wells in our village and if placed on any dam, it will dry it up. | Latent | |
| A Factory X in my area consumes 50 liters of well water per second for 12 months. | Latent | |
| Farmer is allowed to harvest as much water as he wishes. Thus far no one has stopped it. | Semantic | |
| There are illegal wells in Mahidasht Plain and farmers over collect from them. | Semantic | |
| We wanted to plant corn, but we saw that the water was decreasing day by day. | Latent | |
| In Mahidasht Plain, there are plenty of wells. | Latent | |
| A Factory X in the Plains has several wells and they pump water day and night. | Latent | |
| We do multi cropping with all restriction on water harvest. | Latent | |
| Farmers recklessly harvest a large amount of water. | Semantic | |
| 550 square meters of land is located next to Mereg River. Mereg is one of the dead rivers which has water only autumn. I suggested that they put a dam on the river so that we can use it whenever there is a flood. The fields have become infertile due to lack of water. | Semantic | Reduced surface water |
| Water has decreased with concurrent drought for the past a few years. It's a mistake to think that this year was a wet season. In Kermanshah alone there was 120-130 mm. The land is dry. | Semantic | |
| During wet season, we cultivated variety of crops. But during dry season we only do rain fed farming. | Semantic | |
| Rainfall has reduced by 100%. This year we had 330 mm and last year we had 250 mm. Any rainfall below 700-800 mm is onset of drought. | Semantic | |
| When I was a kid we used to swim in Mereg River because it was full of water but it has dried due to drought for the past a few years. | Semantic | |
| Rainy season has disappeared and it is getting worse. If we have a good wet season, we can expect to have a good year in the next 10 to 12 years. | Latent | |
| Rainfall has decreased a lot and it is 100% due to water loss. | Semantic | |
| Droughts have also caused dehydration. | Latent | |
| The Mereg River has no water. | Semantic | |

**Continue of table 2. Concepts of water bankruptcy as perceived by farmers**

| Quotes (open coding) | Type of thematic | Theme (axial coding) |
|---|---|---|
| I had 10 hectares of irrigated farming. I have decided to let go of 5 hectares and plant spring or autumn peas so that I don't have to water a lot. | Semantic | **Agricultural bankruptcy** |
| We are now faced with the lowest water level in the last 20 years. In summer, the water reaches 1 inch. We did not cultivate half of the land due to lack of enough water. | Semantic | |
| I used to cultivate 10 hectares, but now I cultivated 4 hectares by sowing spring cultivars. I had no choice otherwise I had to let go of farming and find some other jobs. | Semantic | |
| We have limited water in the Plain and we are going bankrupt and have to leave farming. | Semantic | |
| I have sowed 4 hectares of sugar beet but before I had 11 hectares because I had access to more water. | Semantic | |
| Agriculture is not profitable and is on the verge of bankruptcy. While it is profitable in anywhere else. | Latent | |
| We have to cultivate less land. There is no water. | Semantic | |
| We do single cropping because we don't have access to sufficient water. | Semantic | |
| Tenants engage in multi cropping. They sow potatoes that need water every other day. They pump water from February to October. The tenants pay 60000 dollars and take advantage of owner's well. The result is empty groundwater resources. | Semantic | **Reduced groundwater** |
| The groundwater level has gone down or its very scarce. We have to go below 70 meters to see any water but before we saw water below 3 meters. I know a friend who dug a well below 201 meters but couldn't get 6 inches of water. | Semantic | |
| Water is running out and groundwater layers are disappearing. The layers are no longer able to store water and therefore we are facing environmental disaster. | Latent | |
| Many wells have been dug and groundwater sources have gone down. In the past we used to collect water from 3-4 meters deep but even now 40-50 meters deep doesn't give us any water. | Semantic | |
| Water has decreased a lot and compared to the previous years we had a 50-meter water drop (10-12 years ago). | Semantic | |
| One of the water Karstic resources is located under the Mahidasht plain, most of which is empty. | Semantic | |
| All this rain has come (last year and this year), but it has not penetrated enough and therefore the wells are dried. | Latent | |
| Although Mahidasht Plain is known as forbidden Plain, water experts still issue permission to harvest. | Semantic | **Water forbidden** |
| I know that the plain has been forbidden for the past 15-20 years and I also know that there is no water. | Semantic | |

The first key concept that farmers conjured from the term WB was "excess water harvesting" (EWH). This concept with 20 emphatic phrases expresses the farmers' emphasis on this concept. Farmers are also aware of the fact that water exploitation is done indiscriminately, so that deep wells are also drying up. Meanwhile, there is no serious lever to prevent EWH, and if the farmer uses too much, he is only required to pay a fine. Therefore, from the point of view of farmers, EWH means WB.

Among the other concepts that farmers raised after hearing the term WB, were "reduced surface water" (RSW) and "reduced ground water" (RGW), each of these concepts is specified with 9 representative expressions in Table 1. From the point of farmers, the amount of rainfall has decreased over recent years and this situation is getting worse year by year. The lack of rain has led to consecutive droughts, which has resulted in the drying up of the Merg River. On the other hand, due to the fact that the amount of water in the region depends on the amount of precipitation, the water level of the groundwater aquifers in the region has dropped

sharply, so that the wells are drying up and the farmers have increased the depth of their wells to access water. Therefore, farmers consider the RSW resources and the decreased groundwater as the WB in the region.

"Agricultural bankruptcy" (AB) with 9 primary codes is one of the influential concepts expressed by farmers regarding WB in Mahidasht Plain. They stated that due to the lack of water, they did not cultivate a part of their land and farming is not profitable for them. Some farmers also decided to abandon farming.

Some of the farmers were aware that Mahidasht Plain has been declared as "forbidden plain" (FP) and pointed out that the Regional Water Company should not permit excessive exploitation of water and drilling wells, because the region has a severe water shortage. Meanwhile, many lands in the region rented to farmers in other provinces and they have also cultivated water crops such as potatoes and corn. These farmers use the term water forbidden (WF) for WB.

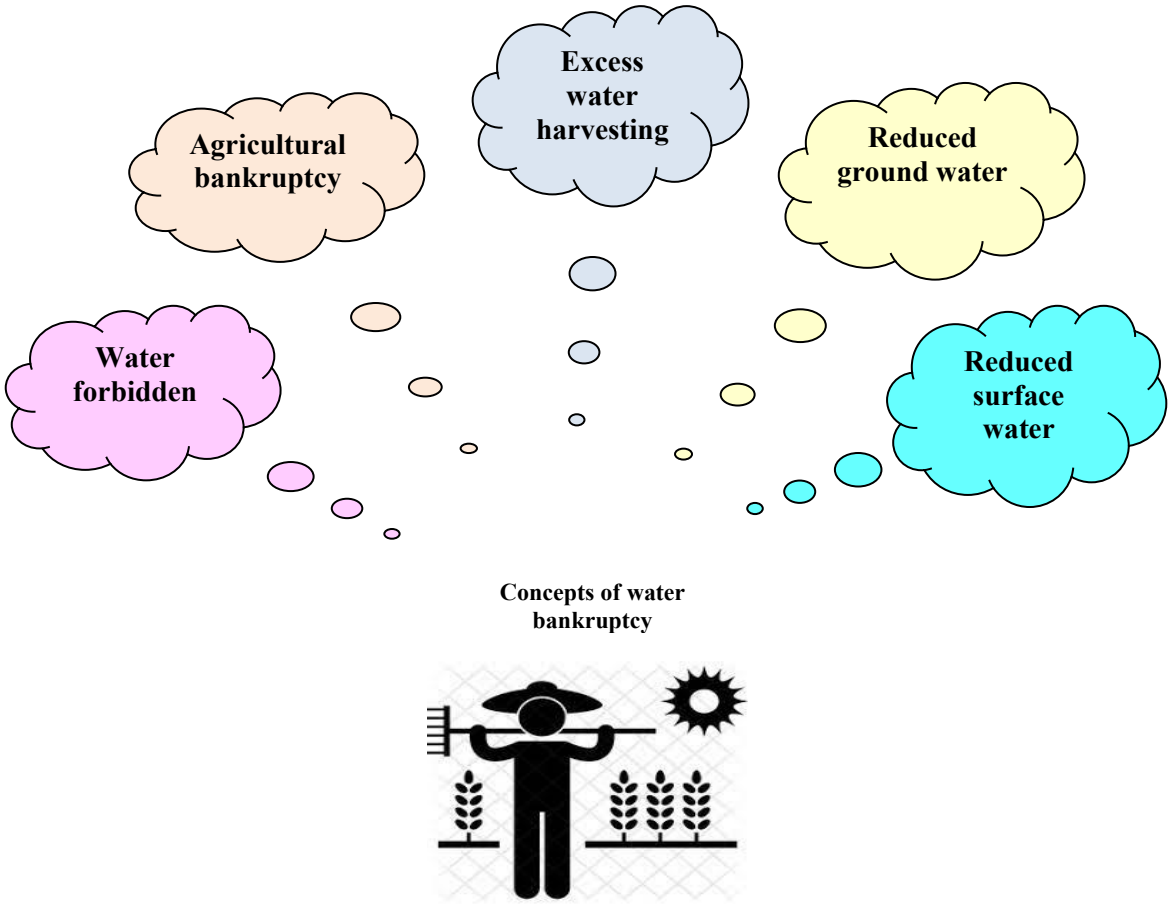


**Fig. 3. Conceptualization of water bankruptcy as perceived by farmers**

This qualitative study sought to investigate how Iranian farmers conceptualized WB in forbidden Plain of Mahidasht in western Iran. Moreover, this study uncovered water experts' perception of WB. Results revealed that water experts conceptualize WB as excess water harvesting (EWH), reduced surface water (RSW), reduced ground water (RGW), condensation and change of aquifer (CCA), disruption of drinking water (DDW), negative water balance (NWB), over harvesting of renewable water (ORW), reached dead point with water (RDW), reduced water table (RWT), formation of hard pan (FHP), water forbidden

(WF), engaging in non-agricultural activities (ENA). Moreover, farmers conceptualize WB as excess water harvesting (EWH), reduced surface water (RSW), agricultural bankruptcy (AB), reduced ground water (RGW), and water forbidden (WF). Interestingly, both groups shared similar concept in five themes but differed in other seven themes. This difference may be due to technical concepts shared by water experts. In the following paragraph we will discuss each and every theme in detail.

### Excess water harvesting (EWH)

As mentioned in result section, "excess water harvesting" (EWH) is the first concept of water bankruptcy as perceived by water experts. This concept was quoted 36 times in which 16 quotes belonged to water experts and the remaining belonged to farmers. This clearly indicates that water experts and farmers are fully aware of excess water harvest by farmers. The excess water harvesting may be due to unauthorized wells, the presence of water-bearing crops, economic and livelihood pressure, competition and collusion of farmers with each other. However, water experts had enforced legal issues concerning unauthorized harvesting but farmers had not paid attention to policies regarding untheorized. Because they are aware that dealing with farmers are one of the most significant factors affecting conflict in the region and have unfortunate consequences in the society. Several studies in water field (Tatar et al., 2019; sefidgar et al., 2023; Naderi et al., 2024) show that most of the conflicts between the local community and organizations are related to water issues. These conflicts cause that society security to be endangered and it leads to high economic consequences, such as reduction in production and employment at the community level, and the country needs to import foreign products in relation to strategic products. As stated by one of the experts:

> "Se*aling of unauthorized well may lead to unemployment, social insecurity and food security, and lowers production. Therefore, the government does not seek to seal the wells*."

On the other hand, the regional water company does not have enough manpower to monitor the actions of farmers and cannot directly monitor these issues (illegal well drilling and Excess water harvesting). In addition, licensing more water harvesting for farmers and charging their cards will provide a high source of income for the water organization, and in fact, selling more water makes more profit for the organization, and this is contrary to water scarcity situation in the region. This issue has caused experts not to follow up on the sealing illegal wells or the restriction of harvesting in legal wells. Therefore, the weakness in the implementation of institutional and legal frameworks for water distribution is clearly seen in the organization, which leads to excess water harvesting and water bankruptcy.

Another farmer protested to water organization management said:

> *Now that we are in water crisis, authorities should seal unauthorized wells rather than just imposing penalties. For example, the administration can penalize 1100 dollar for 10 hectares of water cultivation, which is a good source of income for the administration".*

According to the Ministry of Energy, 45% of all wells in the country are illegal. In Kermanshah province, 36% of wells are illegal (Ghamarnia, 2023). However, there is no information on Unauthorized wells since they are not registered; therefore, farmers take advantage and utilize water as much as they can from these unauthorized wells. Consequently, water harvest from these unauthorized wells is not considered in the balance of water resources. Therefore, some experts believe that issuing permits to unauthorized wells causes

water harvesting is calculated more realistically and more accurate statistics of the water condition in the region are obtained.

One of the water experts impatiently stated:

> "*Filling the well is costly. No matter how they fill the well, farmers will dig a well from another place because it's their job. Therefore, government does not interfere because they do not wish to cause social tension*".

A concept that emerged from the data among farmers was overuse of water that can be related to his perception in that if he doesn't take advantage they will be overrun by others. This is the reason why there are no restrictions on water harvesting by farmers. In this regard, the findings of the study by Amiri and Mirkzadeh (2022) showed that farmers in Mahidasht are not willing to install smart meters so that they can easily harvest water.

On the other hand, farmers who use this technology charge it after they reach the allowed amount of water. Therefore, it is worth considering that the experts have banned drilling and more water harvesting in the region, while it is possible to excess water harvesting by paying a fine! Hence, the farmer has agreed to pay fine for cultivation of water crops in the area, because it is very economical for the farmer.

According to one of the farmers in the region:

> *"... The Regional water charges our usage card and we pay for it no matter how much it is. There is a conflict of interest, the more water the administration delivers (sells), the better."*

As shown in Tables 1 and 2, most water-based crops such as potatoes, corn, beets, and tomatoes are cultivated in the region. This clearly indicates that although Mahidasht Plain has been introduced as a critical prohibited plain for many years, there is limited monitoring and restrictions the Agricultural Jihad Organization and the Water Affairs Department. This in turn has encouraged farmers to engage in over use of water. Moreover, the problem seems to be more complicated when a few lender farmers decided to lease their property to other farmers of the region. One of the farmers stated:

> *"The tenants do not care about their boundaries and restrictions. They cultivate without considering the amount of water they are allowed to use."*

For farmers who have rented land, water, environment and resource sustainability conservation are not important. For the farmers who have leased their land, the same thinking prevails and the concern of their subsistence life prevents them from makeing a right decision for future generation. In confirmation of this analysis, the findings of Majidipour et al. (2021) and Fattahi Chaghabaghi et al. (2023) regarding the groundwater sustainability of Mahidasht aquifer showed that most parts of the region are in an unstable state in terms of groundwater and the application of the management scenario of 30-40% reduction in groundwater extraction will not stabilize the central areas of the aquifer. In fact, on the one hand, the environmental awareness of farmers is low, and they are not fully aware about climate change, and they hope that the water situation will improve in the coming years; on the other hand, economic benefit is the first priority for them.

In line with concepts emerged, Ghamarnia (2023) showed that drought and over-harvesting caused the groundwater reservoirs in Kermanshah province to have a cumulative deficit of one billion and 34 MCM. In addition, 300 MCM are also overdrawn from all the aquifers in the province. In another study, Visi et al. (2021) estimated water poverty index in the plains of Kermanshah province. Results revealed that Mahidasht Plain is in a state of severe agricultural water poverty by using water poverty indicators in terms of aquifer stability (the total volume of discharge from the aquifer to the volume the whole supply to the aquifer). This result meant that Mahidasht Plain is in worse condition in compare to other

plains in Kermanshah Province. In a similar study, Zarafshani and Sadvandi (2017) also concluded that the Mahidasht Plain is in a state of severe agricultural water poverty by using water poverty indicators. Madani et al. (2016) also point to the lack of environmental information in Iran and they believe that awareness among the people is increasing as a result of the environmental trend that has been created in recent years; For example, in this study, some farmers mentioned climate changes and droughts and the reduction of surface water in the region.

It can be concluded that both farmers and experts are in accordance in terms of WB concept as well as in line with theoretical rendition of reality.

### Reduced surface water (RSW)

A second concept that emerged from the data by both groups was "reduction of surface water" (RSW). This concept was quoted 17 times by participants (8 phrases by experts and 9 phrases by farmers).

Both groups of participants stated that the amount of rainfall in Mahidasht region has decreased for several years and this has led to consecutive droughts. In other words, considering the amount of rainfall as well as the flow from Mereg River, we can conclude that Mahidasht Plain is faced with critical status. The amount of water entering Mahidasht Plain is negligible, while the amount of water extracted is significant causing unacceptable water feeding.

In this regard, the global statistics and evidence also show that the climate has changed. In terms of the average surface temperature of Earth, these indirect estimates show that 1989 to 2019 was very likely the warmest 30-year period in more than 800 years; the most recent decade, 2010-2019, is the warmest decade in the instrumental record so far (since 1850) (McNutt and Ramakrishnan, 2020)

Therefore, the evidence of climate change is compelling: sea levels are rising, glaciers are retreating, precipitation patterns are changing, and the world is getting warmer (Adedeji et al., 2014). Meanwhile, countries such as Iran, which are located in arid and semi-arid regions, are very sensitive to climate change (Silva et al., 2023).

The issue of climate change in Iran can be seen concretely, including the decrease in rainfall and successive droughts. In this regard, the head of the National Center for Climatology in Iran announced that over the next 40 years, the Middle East region, including Iran, will face severe drought for 30 years. This growing threat has started in recent years and in the next 90 years, the amount of rainfall will decrease, the temperature will increase and the groundwater table level will disappear (Sharafi et al., 2020). In various studies in the world and in Iran, the decrease in rainfall in recent decades has been confirmed (Sharafi et al., 2020; McNutt and Ramakrishnan, 2020; Mianabadi and Davary, 2023).

In this regard, Kermanshah province has also experienced drought with different intensities in several time periods.

In this regard, Ghamarnia (2023) evaluated changes of surface flows in Kermanshah province. He concluded that during drought period in 2017, the average annual runoff volume of Kermanshah province has decreased by more than 40%. Moreover, rainfall during wet season in 2022-3 was 21% lower than the long-term average rainfall. In a study conducted by Sharafi et al. (2020) for one-year meteorological drought changes (SPI) in the rain gauge stations of Kermanshah indicated that Mahidasht rain gauge station faced 17 years of meteorological drought in a 30-year period (1986 to 2014). This result shows a significant decrease of surface water in the region. Since rain is the only source of water entering the

plain, we can conclude that this phenomenon has had a significant impact on reduction of the water source of the plain and the drying up of the Merah River.

The debatable point is that if the decrease in rainfall continues for many years, due to the direct effect on water resources, it will cause agriculture crisis. The continuation of meteorological and hydrological droughts in the region has caused insecurity in the economy of rural household. For this reason, many farmers in the region have irrigated their lands (drilling wells and setting up irrigation systems) and start cultivating water crops. As a result, the extraction of water from the well has increased and this problem, as a serious challenge, aggravates the water shortage in the region.

Interestingly, many experts and farmers pointed out that although rainfall has been unsatisfactory for two consecutive years, the Plain has not been fed enough is not fed and there is still a shortage of water.

Therefore, it is evident that both groups of experts and farmers are fully aware of the reduction of rainfall and surface water in the region. Therefore, according to these alarming conditions, the participants understand water bankruptcy as the reduction of surface water. In fact, experts and farmers believe that one of the concepts of water bankruptcy is the reduction of surface water, which is consistent with the reality of society.

### Reduced ground water (RGW)

Another concept that was raised by both groups of farmers and water experts was "reduced ground water" (RGW). This concept was derived through 15 phrases (8 phrases by experts and 7 phrases by farmers). As previously mentioned, the existence of many authorized and unauthorized wells in the region has led to a large drop in groundwater. Farmers and water experts believed that depletion of groundwater resources is due to the reform that was passed in parliament stating that any wells that was dug illegally before 1385 in plains across Iran and was identified by Ministry of Energy and that followed legal distance from other wells in the region equipped with sprinkler irrigation is subject to exploitation license (Center Researches of the Islamic Council, 2010).

Moreover, reduction of rainfall and consecutive droughts are also the cause of reduced ground water resources. As stated by one of the farmers: "*It takes time for these rainfalls to penetrate to lower layers and thus has limited impact on the discharge of current wells*". According to data provided by Iran's water information Center (https://mrsi-g.ir), from 1959 to 2023, the groundwater of Mahidasht Plain has decreased by about 0.5 meters every year. This reduction of water resources is very clear and can be seen by farmers causing them to illegally deepen their wells. In this regard, Gorgani et al. (2017) predicted that in the upcoming year, the groundwater level will intensively continue to decrease in the future. In other words, the annual trend will continue in the future in such a way that the average water level of most piezometers will decrease until 2031 since general trend of these piezometers in the last 20 years confirms this phenomenon. Also, Hosseini et al. (2019) assessed the sustainability of groundwater resources in 30 aquifers in Iran using environmental indicators. Their results demonstrate that state of ground water quantity and quality is unsustainable. Moreover, Emaduddin et al. (2020) showed that groundwater level trend in Mahidasht Plain has a downward direction, which follows a gentle downward trend from 1981 to 1998 and a steep slope from 1998 to 2015. In addition, in 2015, the level of groundwater is at the lowest value during the studied period. The survey of Mahidasht Plain water level during the mentioned period shows a drop of about 23 meters in aquifers. Furthermore, Khalilpour et al. (2018) also indicated that water level of wells in Mahidasht Plain has dropped during a 16-year period (1998-2015). Overall, current evidence shows a significant decrease in

groundwater in the region showing consistency between farmer's conceptualization of WB and the realities of the studied region.

Majidipour et al. (2021) evaluated the stability of Mahidasht aquifer groundwater based on socio-economic and environmental indicators. The results of their study showed that in most areas are in the unstable category, so that 62% of the area has had a drop in water level of more than 10 meters.

According to experts in this filed, one of the reasons for the excess water harvesting from wells, which has led to the drop in groundwater, is that water is extremely cheap in Iran. Water is nearly free in rural areas and in the agricultural sector. Therefore, water cost is never a limiting factor for agricultural activities and only the physical unavailability of water can limit farming. Despite the recent increase in energy prices, energy has also been a relatively cheap resource in Iran. Although groundwater extraction requires considerable amounts of energy, the relatively cheap price of electricity or diesel does not make pumping costs prohibitive. The actions of the government to support farmers have resulted in substantial subsidization of water and energy. While groundwater water is becoming scarcer across the country, the government continues to pay significant subsidies, eliminating any conservation incentive agricultural water users (Madani et al., 2016).

### Condensation and change of the aquifer (CCA)

This theme emerged from experts with six basic phrases. They believed that lack of rainfall during the past a few years coupled with excessive harvesting and depletion of groundwater have caused a significant change in the aquifer. This has led to condensation and compression of voids making them less viable in water holding capacity. In other words, not only, the groundwater has been depleted but the aquifer has also been damaged. Some water management experts in Iran believe that Mahidasht Plain has been settled and that the characteristics of aquifer has changed and thus do not function as they used to function.

According to scientific studies, soil compaction can have a number of negative effects on soil quality, water conservation and crop production including the following:

- causes soil pore spaces to become smaller;
- reduces water infiltration rate into soil;
- decreases the rate that water will penetrate into the soil root zone and subsoil;
- increases the potential for surface water ponding, water runoff, surface soil waterlogging and soil erosion;
- reduces the ability of a soil to hold water and air, which are necessary for plant root growth and function;
- reduces crop emergence as a result of soil crusting;
- impedes root growth and limits the volume of soil explored by roots;
- limits soil exploration by roots and decreases the ability of crops to take up nutrients and water efficiently from soil;
- reduces crop yield potential (McKenzie, 2010).

In this regard, Ghamarnia (2023) estimated changes of Mahidasht aquifer as -260.02 million cubic meters indicating a sad situation in terms of water.

A large number of soil science scholars have indicated an ideal condition for any soil is to contain 50% of air and water. In case of excessive water extraction in the basement, the coarse pores of soil particles are broken down creating micro pores. These micro pores cause soil space to block and thus reducing water holding capacity. This in turn develops runoff and flood and consequently washing away soil surface that usually takes 300 years to form 1 cm of soil in dry and semi-arid areas.

It is interesting to note that, in many cases, the agricultural method creates such hard pan. Excessive use of fertilizers and pesticides, long-term use of tillage tools at a fixed depth, the prevalence of flood irrigation, the traffic of heavy vehicles such as tractors, combine harvesters, etc., cause hard soles, which can be solved with proper management.
Apparently, water experts presented an interesting concept of WB because as the water storage tank (aquifer) is destroyed, the Plain will not be able to maintain water.

### Agricultural bankruptcy (AB)

The last concept that was derived from interview with farmers and water experts was agriculture being lost or agricultural bankruptcy (AB). This concept was emerged through one phrase by experts and 9 phrases by farmers. Open interview by farmers revealed that many farmers have left part of their land uncultivated or in some cases turned into rain-fed farming with lower income. Therefore, this group of farmers lost their jobs. In this regard, Pournabi et al. (2022) investigated the allocation of water in the Karkhe River in Iran using bankruptcy models. The results showed that, because of climatic conditions and agricultural demands, full wetland restoration was out of reach and led to minimum satisfaction levels for agricultural beneficiaries. In addition, the percentage of the water supply was increased by applying the scenario of crop restriction in the conditions of the full restoration of the wetland; for example, in the Abbas Plain region, this increase was achieved by almost 10–15% in all methods. On the other hand, decreasing the area under cultivation shifted the allocation problem in the basin to a non-bankruptcy one.

A few farmers leased their farm land to other farmers from nearby provinces due to shortage of water. They believed that farming is no longer profitable. However, tenant farmers used soil and water in unsustainable manner.

Considering that there is no special industry such as factories in the region and farmers do not know any other skills (their main occupation is agriculture), they cannot earn the income that provide their livelihood and many family and social problems such as job insecurity, conflict among family members, unemployment, migration, conflict with other villagers, psychological problems, etc. have arisen for them.

As one of the farmers put it this way: "in the past our wells were semi deep but when farmers from other provinces came to lease our land for 2800-3000 dollar per hectare, we were motivated to deepen our wells."

Non-native farmers in the village have created many social and environmental problems in the region. Because the renters pay attention to their economic benefit and use excessive water resources as much as possible to produce more, and make maximum use of chemical fertilizers and poisons. So that according to some farmers, the smell of nitrates has filled the entire area. Also, migrant farmers, in order to produce a marketable product, add acid to the soil to turn the soil into a powder and produce more suitable potatoes in terms of shape. All the mentioned above makes cases for concern and regret.

Ghanbari et al. (2020) confirm that farmers' destructive behavior in Mahidasht Plain that has led to environmental and socio-cultural consequences due to leasing by tenant farmers. For example, soil structure and texture as well as quantity and quality of water resources were ruined by tenant farmers. The soil structure has turned into acidic characteristic due to the overuse of fertilizer and pesticide. Moreover, soil texture and chemical properties, including soil pH, have also been changed.

In his study in Kermanshah province, Ghamarnia (2023) concluded that the main cause of groundwater depletion and pollution is mismanagement and exploitation of groundwater by non-native farmers and immigrants from neighboring provinces. This unsustainable behavior

by non-native farmers in one hand and over exploitation of water resources in the other hand have made farmers in Mahidasht Plain to minimize their agricultural activities. Therefore, farmers use the concept of agricultural bankruptcy for WB.

## Conclusions

Iran is located in a dry and semi-arid climate (Sharafi et al., 2020). Therefore, drought has become a permanent feature of the country's climate, particularly in recent decades (Rezaei et al., 2024). Consequently, average rainfall in Iran is reported to be lower than the global average (yearly perception average in Iran is 260 mm compared to the world perception average 800 mm). Therefore, there is always critical situation in many plains of Iran. This problem when become more complicated that the management system in Iran follows the "crisis management" strategy. Crisis management is significantly non-productive, untimely, and not economically viable (Gerber and Mirzabaev, 2017; Zhao et al., 2017), because poor management system has caused a disaster (water shortage and water bankruptcy) and after causing huge damages, it seeks to solve problems. The status of 404 forbidden plains out of 610 plains in the country is proof of this claim (Ministry of Energy Protection and Operation Deputy, 2019).

According to this situation, in recent decades, the new concept “water bankruptcy” (WB) presented by some experts in order to water optimal management and conflict resolution. Water bankruptcy (WB) can be conceptualized as a relative concept and can occur at any level of supply or demand. Significantly, bankruptcy can be a social construct, meaning a product of expectations as well as customary behavior.

Water bankruptcy (WB) problems, which are currently observed in most plains of Iran, including Mahidasht plain in Kermanshah province (10 prohibited plains and 2 critical prohibited plains in Kermanshah province), have been formed over decades and cannot be solved immediately. Much of the damage to the country’s water and ecosystem are irreversible within a short period of time. Iran has many interrelated water challenges with complicated root causes. To solve these issues, it is necessary to adopt a comprehensive approach that involves implementing multiple concurrent strategies. The most effective solutions to Iran’s water problems are long term and they are economically and politically costly to implement. Therefore, unless there is a change in public opinion regarding pro-environment actions and policies, Iran’s water management will continue its inertia and will not pursue radical changes in its solutions and regulations (Madani et al., 2016). If the policymaking do not adopt basic strategies for optimal water management, they must pay a significant cost for its unsustainable water management in the near future. Thus, unless major efforts are directed at reduction of the country’s water demand, further deterioration of water resources should be expected.

One noteworthy point is that, various researchers have analyzed the WB based on technical aspects such as economic and mathematical methods to better develop water in different national and international basins. Although, technical indicator, are popular because it is easy to apply and understand but these do not help to explain the true nature of water scarcity. The more complex indicators are not widely applied because data are lacking to apply them and the definitions are not intuitive (Rijsberman, 2006).

Therefore, for examine any new problem, it is necessary to conceptualize problem and analyze understanding stakeholders towards phenomenon, because the correct understanding of the phenomenon reveals the roots of phenomenon and the causes of stakeholder’s behavior (experts and farmers). Hence, the concepts extracted in the present study can be used as the benchmark for social, economic and environmental indicators of WB. Meanwhile, this

important issue (conceptualization of WB) has been neglected by researchers and policy makers.

In such a way that the researchers of the present study could not find studies about the social dimensions especially the conceptualization of WB. This issue was raised as a limitation and research gap in this study. Thus, the results of this study can be considered as an important innovation in the development of literature in WB and the identification of variables for measuring this phenomenon; In this way, experts and researchers can consider these concepts in the measuring the WB in region to obtain realistic information. Hence, focusing on the social perspective of WB can lead to practical strategies.

In the end, the following recommendations are suggested:

- Before dealing with the technical issues of phenomenon (water bankruptcy), the social dimensions of the phenomenon should be examined; in such a way that the accurate conceptualization from the point of view of the stakeholders in relation to phenomenon takes place;
- The identified concepts (15 concepts in this research) should be used in the water allocation models so that more complete dynamic models can be provided for the allocation of common water basins.
- Traditional and semi-mechanized agriculture wastes water. By modernizing agriculture, part of this problem can be solved.
- Modifying the cultivation pattern towards the development of less water crops in the region is one of the basic strategies to optimize agricultural water consumption.
- One of the reasons for excessive water consumption is the low price of energy (water, electricity, etc.) in Iran. If the real price of water is calculated, its excessive consumption can be reduced.
- The environmental awareness of farmers is low, so increasing their environmental awareness and education can lead to optimal water use.

***Declaration of competing interest***

The authors declare that they have no known competing financial interests or personal relationships that could have appeared to influence the work reported in this paper.

***Author Contributions***

All authors contributed equally to the conceptualization of the article and writing of the original and subsequent drafts.

***Acknowledgements***

The authors wish to thank Dr. Houshang Ghamarnia for providing the necessary information and resources about region. Special thanks to Dr. Hossein Azadi for language editing of the article. His extraordinary contributions have greatly improved the quality of this paper.

## References


Abrahe, A., Ahmadi, M. h., Kazmininejad, S. A., & Rajabpour, R. (2019). Investigating the Theory of Water Bankruptcy and Management in Sharing Water Resources of Fahlian River. *The 3rd Iran Water and Wastewater Engineering and Science Congress*, Shiraz University, Shiraz, Iran. https://civilica.com/doc/1184371/

Ahmed, SK. (2024). The pillars of trustworthiness in qualitative research. *Journal of Medicine, Surgery, and Public Health*. 2, 100051. https://doi.org/10.1016/j.glmedi.2024.100051

Amiri., A., Shaneche, M., & Golshani, A. (2020). The Effect of Public Policy Process on Water Crisis in the Islamic Republic of Iran. *Research letter of Political Science*, 15 (4), 45-72. https://doi.org/10.22034/ipsa.2020.417

Amiri, S. & Mirakzadeh A. A. (2022). Investigation of Factors Affecting the Acceptance of Smart Water Gauge among Farmers in Mahidasht Plain, *Advanced Technologies in Water Efficiency*, 2 (3), 36-53. https://doi.org/10.22126/atwe.2022.7873.1020

Bazrafshan, J., Khalili, A., Zand-Parsa, Sh., Sepaskhah, A., Alizadeh, A., & Farhoodi, J. (2021). Documentary Study of the Situation of Agricultural Water Resources and Uses in Iran: Analysis of the Current Situation, Pathology and Solutions to the Challenges. *Strategic Research Journal of Agricultural Sciences and Natural Resources*, 6 (1), 35-50. https://doi.org/10.22047/srjasnr.2021.128740

Braun, V., & Clarke, V. (2006). Using thematic analysis in psychology. *Qualitative research in psychology,* 3 (2), 77–101. https//:doi.org/10.1191/1478088706qp063oa

Chambers, R. (1983). Rural Development, Putting the last first. London, *Longman Publications*, London, England. http://ndl.ethernet.edu.et/bitstream/123456789/54506/1/198.pdf

Collins, G. (2017). Iran's Looming Water Bankruptcy. *The James A. Baker III Institute for Public Policy of Rice University Publications*, Center for energy studies, Texas, United States. https://www.bakerinstitute.org/sites/default/files/2017-04/import/CES-pub-IranWater-040317.pdf

Doungmanee, P. (2016). The Nexus of Agricultural Water Use and Economic Development Level. *Kasetsart Journal of Social Sciences*, 37 (1), 38-45. https://doi.org/10.1016/j.kjss.2016.01.008

Emadodin, S., Shadiee Majd, N., & Arekhi, S. (2020). Analysis of the Impact of Land Use Change on Groundwater Level Drop) Case Study: Mahidasht, Kermanshah province). *Journal of Natural Environmental Hazards*, 09 (25), 123-140. https://doi.org/10.22111/jneh.2020.31698.1565

Enworo, O.C. (2023). Application of Guba and Lincoln's parallel criteria to assess trustworthiness of qualitative research on indigenous social protection systems, *Qualitative Research Journal*, 23 (4), 372-384. https://doi.org/doi.org/10.1108/QRJ-08-2022-0116

Fattahi, S. (2018). National Water Report and Complexity based policy. *Strategic Studies of Public Policy*, 8 (27), 321-328. https://sspp.iranjournals.ir/article_31143_a7d72361e2bb1183df75a532bc897c41.pdf

Fattahi Chaghabagi, A., Akhund Ali, A.M., & Azari, A. (2023). Assessment of the sustainability indicators of groundwater resources (case study of Mahidasht aquifer). *Advanced Technologies in Water Efficiency*, 3 (2), 1-14. https://doi.org/10.22126/atwe.2023.9082.1050

Francis, J., Johnson, M., Robertson, C., Glidewell, L., Entwistle, V., Eccles, M., & Grimshaw, J. (2010). What is an adequate sample size? Operational sing data saturation for theory-based interview studies. *Psychol. Health*, 25, 1229-1245. https://doi.org/ 10.1080/08870440903194015

Gall, M. d., Borg, W. r., & Gall, J. P. (2003). Educational Research: An Introduction. Allyn and Bacon, Publications, Boston, Massachusetts. https://books.google.com/books/about/Educational_Research.html?id=_rRhQgAACAAJ

Gerber, N., & Mirzabaev, A. (2017). Benefits of Action and Costs of Inaction: Drought Mitigation and Preparedness – a Literature Review. World Meteorological Organization (WMO) and Global Water Partnership (GWP) WMO, Geneva, Switzerland and GWP, Stockholm, Sweden. https://www.gwp.org/globalassets/global/about-gwp/publications/integrated-drought-management-programme/drought_a-literature-review.pdf/

Qamarnia, H. (1401). A brief overview of the potentials of Kermanshah Province. *The Third National Conference on Deficit Irrigation and the Use of Non-Conventional Waters in Agriculture in Dry Areas. Razi University of Kermanshah*, Kermanshah, Iran. https://civilica.com/l/100580/pgn-2/

Ghanbari, M., Rostami, F., & Geravandi, Sh. (2020). Consequences of Cash-rent Farming in Kermanshah's Mahidasht: Marshallian versus Cheungian Perspectives. *Journal of Rural Research*, 11 (2), 384-395. https://doi.org/10.22059/jrur.2019.257829.1255

Gharb Water Consulting Engineers. (2022). Design of Quantitative and Qualitative Monitoring Network of Underground Water Resources: Mahidasht-Sarfirouzabad Study Area, Selected Agricultural Wells. Kermanshah Regional Water Company, *Water Resources Basic Studies Office*, Groundwater Department. 1-44. https://doi.org/10.22034/hydro.2024.57118.1298

Gorgani, Sh., Bafkar, A., & Fatemi, SE. (2017). Prediction of Groundwater Pollution Potential Using the DRASTIC Index and Annual Time Series Analysis (Case Study: Plain Mahidasht Kermanshah). Iran. *J. Health & Environ*, 10 (3), 317-328. http://ijhe.tums.ac.ir/article-1-5962-en.html

Herrero C., & Villar A. (2001). The Three Musketeers: Four Classical Solutions to Bankruptcy Problems. *Mathematical Social Sciences*, 42 (3), 307–328. https://doi.org/10.1016/S0165-4896(01)00075-0

Hosseini, S. M., Parizi, E., Ataie-Ashtiani, B., & Simmons, C. T. (2019). Assessment of sustainable groundwater resources management using integrated environmental index: Case studies across Iran. *Science of the Total Environment*, 676, 792–810. https://doi.org/10.1016/j.scitotenv.2019.04.257

Ingrao, C., Strippoli, R., Lagioia, G., & Huisingh, D. (2023). Water scarcity in agriculture: An overview of causes, impacts and approaches for reducing the risks. *Heliyon*, 9 (8), e18507. https://doi.org/10.1016/j.heliyon.2023.e18507

Islami, R., & Rahimi, A. (2019). Policymaking and Water Crisis in Iran. *Journal of the Macro and Strategic Policies*, 7 (27), 410-434. https://doi.org/10.32598/JMSP.7.3.5

Islamic Council Research Center. (2010). The Law on Assignment of Water Wells without Exploitation License. 8 (31501), *Council Resolutions*, Notification No. 392/28251. https://rc.majlis.ir/fa/law/show/782294

Jalili Kamju, S. P., & Khochiani, R. (2020). Application of the Bankruptcy Theory and Conflicting Claims on Water Resources Allocation of Zayanderud. *The Journal of Economic Modeling Research*, 39, 45-80. https://doi.org/10.29252/jemr.10.39.45

Jamalomidi, M., & Moridi, A. (2020). Bankruptcy Method in Reducing Groundwater Resources Conflicts and Aquifer Balancing (Case Study: Haji Abad Aquifer). *Iran-Water Resources Research*, 16 (4), 1-14. https://doi.org /20.1001.1.17352347.1399.16.4.1.1

Ketabchy, M. (2021). Investigating the Impacts of the Political System Components in Iran on the Existing Water Bankruptcy. *Sustainability*, 13 (13657), 1-22. https://doi.org 10.3390/su132413657

Khalilpoor, S., Asghari, S., Ghorbani, A., & Naji doomirani, S. (2018). Analysis of Underground Water Level Changes Kermanshah Plain Mahidasht. *The 13th National*

*Conference on Watershed Science and Engineering of Iran and the 3rd National Conference on Natural Resources and Environment*, Mohaghegh Ardabili University, Ardabil, Iran. https://civilica.com/doc/827182/

Kufeoglu, S. (2022). SDG-6 Clean Water and Sanitation. In book: Emerging Technologies, Value Creation for Sustainable Development, Springer Publications, New York City, United States. https://doi.org/ 10.1007/978-3-031-07127-0_8.

Madani, K., AghaKouchak, A., & Mirchi, A. (2016). Iran's Socio-economic Drought: Challenges of a Water-Bankrupt Nation. *Iranian Studies*, 49(6), 997-1016. https://doi.org/10.1080/00210862.2016.1259286

Majidipour, F., Bagher Najafi, S. M., Taheri, K., Fathollahi, J., & Missimer, T. M. (2021). Index-based Groundwater Sustainability Assessment in the Socio-Economic Context: A Case Study in the Western Iran. *Environmental Management*, 67, 648–666. https://doi.org/10.1007/s00267-021-01424-7

Mazaheri, M., & Abdul Manafi, N. (2016). Investigating the Water Crisis and Its Consequences in the Country. *Islamic Council Research Center*, serial number 15608. https://rc.majlis.ir/fa/report/show/1040201

McKenzie, R. H. (2010). Agricultural Soil Compaction: Causes and management. Agriculture and Rural Development Publications, Lethbridge, Alberta. https://www1.agric.gov.ab.ca/$department/deptdocs.nsf/all/agdex13331/$file/510-1.pdf

Merriam, Sh. B. (2002). Qualitative Research in Practice: Examples for Discussion and Analysis, Jossey-Bass Publications, San Francisco. California. https://pocketbook.de/de_de/downloadable/download/sample/sample_id/4281232/?srsltid=AfmBOoojUGM4fYiIvOVowcPRU_lznochEA3JRzlSejifjPWhj2lzRPdl

Mianabadi, A., & Davary, K. (2023). Investigation of Changes in the Amount and Distribution of Precipitation and Temperature in Iran and Their Effects on Extreme Events. *Development Sustainable and Water of J*, 10 (2), 13-26. https://doi.org/10.22067/jwsd.v10i2.2301-1203

Mogalakwe, M. (2006). The Use of Documentary Research Methods in Social Research. *African Sociological Review*, 10 (1), 221-230. https://www.researchgate.net/publication/267994948_The_Use_of_Documentary_Research_Methods_in_Social_Research

Moradian, F., & Behvar, Sh. (2018). Blue Bankruptcy is an Obstacle to Economic Development. Kermanshah Province Sustainable *Development National Conference: Opportunities, Challenges and Prospects, Razi university*, Kermanshah, Iran. https://civilica.com/doc/901442/

Morse, J. M. (2015). Data were saturated. *Qual Health Res*, 25 (5), 587-8. https://doi.org/10.1177/1049732315576699

Mulugeta Degefu, D., & He, W. (2016). Allocating Water under Bankruptcy Scenario. *Water Resources Management*, 30, 3949–3964. https://doi.org/10.1007/s11269-016-1403-x

Naderi, L., Karamidehkordi, E., Badsar, M., & Moghadas, M. (2024). Impact of Climate Change on Water Crisis and Conflicts: Farmers' Perceptions at the ZayandehRud Basin in Iran. *Journal of Hydrology: Regional Studies*, 54, 101878. https://doi.org/10.1016/j.ejrh.2024.101878

Naeem, M., Ozuem, W., Howell, K., & Ranfagni, S. (2023). A Step-by-Step Process of Thematic Analysis to Develop a Conceptual Model in Qualitative Research. *International Journal of Qualitative Methods*, 22, 1–18. https://doi.org/10.1177/16094069231205789

Nafarzadegan, A. R., Vagharfard, H., Nikoo, M. R., & Nohegar, A. (2019). Developing a Multi-Objective Linear Model for an Optimal Water Allocation Based on Four Bankruptcy Rules and Solve it Through the Fuzzy Compromise Approach. *Watershed Management Research*, 23 (3), 95-110.

https://doi.org/10.22092/wmej.2019.125834.1205

Oftadeh, E., Shourian, M., & Saghafian, B. (2016). Evaluation of the Bankruptcy Approach for Water Resources Allocation Conflict Resolution Basin Scale, Iran's Lake Urmia Experience. *Water Resources Management*, 30, 3519–3533. https://doi.org/_10.1007/s11269-016-1368-9

O'Reilly, M., & Parker, N. (2013). Unsatisfactory Saturation: A critical exploration of the notion of saturated sample sizes in qualitative research. *Qualitative Research*, 13 (2), 190–197. https://doi.org/10.1177/1468794112446106

Pournabi, N., Janatrostami, S., Ashrafzadeh, A., & Mohammadi, K. (2022). Comparison of Bankruptcy Methods in the Operation Management of the Karkheh River Basin to Allocate more Water to the Hawr-Al-Azim Wetland. *AQUA-Water Infrastructure, Ecosystems and Society*, 71(11)1263-1277. https://doi.org/: 10.2166/aqua.2022.126

Qanadi, M. (2023). Acceleration in Changes to Solve Water and Sewage Crises (Editor-in-Chief Lecture). *Journal of Water and Wastewater Science and Engineering*, 8 (2), 1-2. https://doi.org/10.22112/jwwse.2023.404160.1367

Ranjbar, H., Haghdoost, E. A., Salsali, M., Khoshdel, E., Salisani, M. E., & Bahrami, N. (2011). Sampling in Qualitative Research: A Guide for Beginning. *J Army Univ Med Sci*, 10 (3), 238-250. https://sid.ir/paper/96654/fa

Rezaei, S., Masoompoor Samakoosh, J., Miri, M. (2024). Analysis of drought characteristics (severity, duration, magnitude) in Iran based on multivariate standardized drought index. *Advanced Technologies in Water Efficiency*, 4 (1), 82-98. https://doi.org/doi:10.22126/ATWE.2024.10319.1114

Rijsberman, F. R. (2006). Water scarcity: Fact or fiction?. *Agricultural Water Management*, 80 (1–3), 5-22. https://doi.org/10.1016/j.agwat.2005.07.001

Sadat, M., Shourian, M., & Moridi, A. (2018). Reallocation of Water Resources in Transboundary River Basins Using the Bankruptcy Approach. *Iranian Journal of Soil and Water Research*, 50 (5), 1141-1151. https://doi.org/10.22059/ijswr.2018.260256.667948

Sefidgar, S., Rostami, F., & Tatar, M. (2023). A Schematic Representation of the Water Conflict from Activists' Perspective in the Villages of the Gavshan Dam Basin. *Journal of Rural Research*, 14 (1), 136-151. https://doi.org/10.22059/jrur.2023.352928.1803

Shahraki, A. S., Singh, V. P., & Bazrafshan, O. (2024). Developing a Bankruptcy Theory to Resolve Stakeholders' Conflict over Optimal Water Allocation: The Case of Hirmand Catchment. *Water*, 16 (9), 1303. https://doi.org/10.3390/w16091303

Sharafi, L., Zarafshani, K., Keshavarz, M., Azadi, H., & Van Passel, S. (2020). Drought Risk Assessment: Towards Drought Early Warning System and Sustainable Environment in Western Iran. *Ecological Indicators*, 114, 1-12. https://doi.org/doi.org/10.1016/j.ecolind.2020.106276

Silva, LAP., Silva, CR., Souza, CMP., Bolfe, EL., Sena Souza, JP., & Leite, ML. (2023). Mapping of Aridity and its Connections with Climate Classes and Climate Desertification in Future Scenarios– Brazilian Semi-Arid Region. *Sociedade and Natureza*, 35, e67666, 1-12. https://doi.org/10.14393/SN-v35-2023-67666x

Tatar, M., Papzan, A., & Ahmadvand, M. (2019). Explaining the Good Governance of Agricultural Surface Water Resources in the Gawshan Watershed Basin, Kermanshah, Iran. *J. Agr. Sci. Tech*., 21 (6), 1379-1393. https://doi.org/20.1001.1.16807073.2019.21.6.11.0

Tayebzadeh moghadam, N., & Malekmohammadi, B. (2020). Using Bankruptcy Theory Methods for Fair Allocation of Water Resources in order to Reduce Environmental Conflicts (Case Study: Lake Urmia Basin). *Water Resources Engineering*, 13 (44), 95-105. https://doi.org/20.1001.1.20086377.1399.13.44.8.9

Thurmond, V. A. (2001). The Point of Triangulation. *Journal of Nursing Scholarship*, Third quarter 2001, Pp. 253-258. https://doi.org/ 10.1111/j.1547-5069.2001.00253.x

Tian, J., Yu, Y., Li, T., Zhou, Y., Li, J., Wang, X., & Han, Y. (2021). A cooperative game model with bankruptcy theory for Water Allocation: A case study in China Tarim River Basin. *Environmental Science and Pollution Research*, 29, 2353-2364. https://doi.org/10.21203/rs.3.rs-439945/v1

UNDP. (2015). Goal 6: Clean water and sanitation. *United Nations Development Programme*, New York, United States. https://www.undp.org/sustainable-development-goals/clean-water-and-sanitation

Veisi, A., Kalantari, Kh., & Motiee, N. (2021). Zoning Plains of Karkheh Catchment in Kermanshah Province Based on the Enhanced Agricultural. *Iranian Journal of Soil and Water Research*, 52 (12), 3125-3138. https://doi.org/10.22059/ijswr.2021.328820.669054

Wickramage, H. A. M. (2019). Bankruptcy Model Application to Missouri River Water Allocation. *In Partial Fulfillment of the Requirements for the Degree of Master of Science*, Agribusiness and Applied Economics, Fargo, North Dakota. https://doi.org/ 10.13140/RG.2.2.33573.00483

Yazdian, M., Rakhshandehroo, Gh., Nikoo, M. R., & TalebBidokhti, N. (2022). Developing a Model Based on Games Theory for Optimal Allocation of Water to Stakeholders in Shared Water Resources under Water Bankruptcy Conditions: Application of Chicken Game. *Water Resources Engineering Journal*, 15 (52), 1-14. https://doi.org/ 10.30495/wej.2021.26673.2284

Zarafshani, K., & Saadvandi, M. (2017). Determining Agricultural Water Poverty Index in Kermanshah Province: The Case of Mahidasht Basin, Iran. *J. Agr. Sci. Tech*., 19, 541-552. https://doi.org/_20.1001.1.16807073.2017.19.3.19.8

Zare Farjoudi, S. Moridi, A., & Mousavi Nadoushani, S.S. (2019). Application of Bankruptcy Method in Point and Non-Point Source Pollution Allocation in the Rivers. *Iran-Water Resources Research*, 15 (2), 88-97. https://doi.org/_20.1001.1.17352347.1398.15.2.7.6

Zarezadeh, M., Madani, K., & Morid, S. (2012). Resolving Transboundary Water Conflicts: Lessons Learned from the Qezelozan-Sefidrood River Bankruptcy Problem. *World Environmental and Water Resources Congress 2012*: Crossing Boundaries,New Mexico, United States. https://doi.org/10.1061/9780784412312.243

Zhao, H., Xu, Z., Zhao, J., & Huang, W. (2017). A drought rarity and evapotranspiration-based index as a suitable agricultural drought indicator. *Ecol. Indic*., 82, 530–538. https://doi.org/10.1016/j.ecolind.2017.07.024

Advanced Technologies in Water Efficiency

homepage:https://atwe.razi.ac.ir

Online ISSN:2783-4964

# Three-Dimensional porous media as a novel approach for stilling basin optimization: An experimental comparison with solid elements

**Seyed Amin Asghari Pari** [1]✉, **Sirus Saeedi** [2], and **Mahmood Shafai Bajestan** [3]

1. Corresponding author, Department of Civil Engineering, Faculty of Engineering, Behbahan Khatam Alanbia University of Technology, Behbahan, Iran. E-mail: asghari_amin@bkatu.ac.ir
2. Department of Civil Engineering, Faculty of Engineering, Behbahan Khatam Alanbia University of Technology, Behbahan, Iran. E-mail: sirus.saeedi@gmail.com
3. Department of Water Structures, Faculty of Water and Environmental Engineering, Shahid Chamran University of Ahvaz, Ahvaz, Iran. E-mail: m_shafai@yahoo.com

## Article Info

**Article type:**
Research Article

**Article history:**
Received 11 June 2025
Received in revised form 20 September 2025
Accepted 22 November 2025
Available online 25 March 2024

***Keywords***:
hydraulic jump,
stilling basin,
energy dissipation,
porous media,
Ogee spillway.

## ABSTRACT

**Objective:** The purpose of this research is to experimentally investigate and compare the effects of solid and porous baffle blocks and roughness elements on hydraulic jump characteristics downstream of an ogee spillway, aiming to optimize stilling basin design for reduced length and enhanced energy dissipation.

**Method:** Experiments were conducted in a 10 m horizontal flume with an ogee spillway, testing various arrangements of solid (impermeable) and porous (permeable, $\Phi$=0.25) cubic blocks (2.1 cm) as baffle blocks and bed roughness. Five discharges (5–17 L/s) corresponding to Froude numbers ($Fr_1$=4.58–5.75) were used, measuring sequent depths ($y_1$, $y_2$) and jump length ($L_j$) with a point gauge and visual grid. A total of 157 runs compared configurations against a smooth-bed control. Baffle Block Configurations: Single-Row (full-width bar, double-block with central gap, triple-block with two gaps); Double-Row (two rows spaced 2.1 cm apart); Stepped Co-Flow (downstream row twice the height of upstream); Stepped Opposing-Flow (upstream row twice the height of downstream). Bed Roughness Configurations: Row-wise (transverse rows spaced 2.1 cm or 6 cm); Staggered (checkerboard/offset pattern); Zigzag (dense interlocking pattern); Combined Roughness (alternating rows of solid and porous cubes).

**Results:** All configurations reduced sequent depth ratio ($y_2/y_1$) and jump length ($L_j$) compared to the classical jump. Porous elements outperformed solid ones: porous baffle blocks achieved 16–43% $L_j$ reduction (vs. 12–29% for solid), and porous roughness 7–47% (vs. 5–35% for solid). Optimal setups included double-row porous baffles, zigzag porous roughness, and row-wise (6 cm spacing) porous/combined roughness. Porous media enhanced energy dissipation via internal shear, jet interactions, and turbulence, leading to up to 36% shorter relative jump length ($L_j/y_2$) than USBR standards.

**Conclusions:** Porous appurtenances provide a superior, novel approach for stilling basin optimization, enabling more compact, cost-effective designs through volumetric energy dissipation mechanisms beyond form drag.

**Cite this article:** Asghari Pari, S.A., Saeedi, S., & Shafai Bajestan, M. (2025). Three-Dimensional porous media as a novel approach for stilling basin optimization: An experimental comparison with solid elements. *Advanced Technologies in Water Efficiency, 5* (4), 46-67. https://doi.org/ 10.22126/atwe.2025.12466.1178


https://doi.org/10.22126/atwe.2025.12466.1178

Publisher: Razi University.

## Introduction

The longevity and structural integrity of major hydraulic structures such as dams, spillways, and barrages are critically dependent on the effective management and dissipation of the immense kinetic energy of downstream flows. Failure to control this energy can lead to severe engineering challenges, including catastrophic bed scour, tailwater degradation, and compromised structural stability. A stark real-world example is the Taunsa Barrage, where, soon after its 1958 operation, a cascade of problems emerged, including the uprooting of impact baffle blocks, damage to the basin floor, and significant bed retrogression. Despite numerous repair efforts and expert committees, these issues persisted, highlighting the profound limitations of traditional design approaches (Zulfiqar & Kaleem, 2015).

To mitigate such risks, the hydraulic jump serves as the primary energy dissipation mechanism. This phenomenon, characterized by the abrupt transition of a high-velocity supercritical flow to a low-velocity subcritical flow, is fundamental to protecting the channel bed from erosion (Bélanger, 1841). The performance and safety of a hydraulic structure are thus intrinsically linked to the design of its stilling basin, which is engineered to contain the highly turbulent jump and dissipate residual energy within a protected, often concrete-lined, area (Peterka, 1984). The complex nature of the hydraulic jump, with its wall jet-like velocity profiles and high turbulence intensities, has been the subject of extensive investigation, focusing on free surface fluctuations and internal bubbly flow structures across a wide range of Froude numbers (Chachereau & Chanson, 2011; Wang & Chanson, 2015; Murzyn & Chanson, 2009).

To enhance dissipation efficiency and forcibly shorten the required basin length, stilling basins are almost universally equipped with appurtenances. The engineering community has explored a vast array of solid, impermeable elements to optimize this process. These include standard baffle blocks (Habibzadeh et al., 2012), friction blocks (Chaudary & Sarwar, 2014), and various forms of terminal sills (Mansour et al., 2004; Alikhani et al., 2010). Research has pushed the boundaries of geometric innovation, examining splitter blocks (Verma & Goel, 2003), curved blocks (Eloubaidy et al., 1999), T-shaped and triangular blocks (Tiwari & Goel, 2016), and the effect of negative steps on the basin floor, which have been shown to increase energy dissipation by up to 11% (Sayyadi et al., 2022). Among these, Wedge-Shaped Baffle Blocks (WSBBs) have received considerable attention, with studies demonstrating their ability to reduce basin length by 15–25% by creating more extensive wake regions and promoting efficient lateral flow spreading compared to traditional impact blocks (Pillai et al., 1989; Goel, 2008). In parallel, the influence of bed roughness has been identified as a key factor, with studies developing semi-empirical methods to correlate jump characteristics with roughness parameters (Maleki & Fiorotto, 2021) and employing numerical models to show how roughness height and spacing affect jump length (Nikmehr & Aminpour, 2020).

Despite these advancements, conventional solid elements primarily rely on form drag for energy loss and are not without their own challenges. As observed at the Taunsa Barrage, vertical-faced blocks are susceptible to uprooting under intense, fluctuating hydrodynamic pressures. Furthermore, traditional impact blocks can suffer from flow reattachment on their sides, a phenomenon that diminishes their effective drag force and overall efficiency (Frizell & Svoboda, 2012). While modern numerical tools like FLOW-3D have proven invaluable for investigating and optimizing these traditional designs with high accuracy (Macián-Pérez et al., 2020b; Zaffar & Hassan, 2023b), the fundamental dissipation mechanism remains surface-based. A promising but less explored paradigm is the use of porous media for energy

dissipation. Unlike their solid counterparts, porous elements introduce additional, highly effective energy dissipation mechanisms. As flow penetrates the porous structure, energy is dissipated not only by form drag but also through a volumetric process involving internal shear stresses, complex jet interactions, and intense turbulence generation within the interconnected pore network. This process can be theoretically described using Darcy's law for low-velocity flows, which relates flow rate to permeability and pressure gradient, and the Forchheimer equation for high-velocity, non-Darcy flows where inertial effects dominate: $\Delta P/L = (\mu/k)\, v + \rho\, \beta\, v^2$, where k is permeability, β is the Forchheimer coefficient, v is velocity, μ is viscosity, and ρ is density. These theories highlight how porous media enhance dissipation via quadratic inertial terms, suggesting higher efficiency in turbulent hydraulic jumps (e.g., Sajjadi et al., 2025; Tahmasbipour et al., 2024; Ahadiyan et al., 2024). Dimensionless parameters such as permeability ($k/y_1^2$) and tortuosity (path complexity) further justify their use by quantifying internal flow resistance (Salahi et al., 2024; Ahadiyan et al., 2024a). This suggests that porous elements could achieve a higher rate of energy dissipation within a more compact volume, leading to significant reductions in stilling basin length and associated construction costs.

Although recent numerical investigations have begun to explore the potential of porous baffles (Zaffar & Hassan, 2023a), a critical research gap remains. There is a lack of systematic, direct experimental comparison of 3D porous versus solid elements of identical geometry, particularly when applied as both baffle blocks and bed roughness elements downstream of an ogee spillway. Therefore, the present study aims to provide a comprehensive experimental investigation to address this gap. Through detailed physical modeling, this research seeks to: (1) systematically quantify the reduction in sequent depth and jump length for various arrangements of solid and porous elements compared to the classical jump; (2) identify the most effective configuration in terms of energy dissipation and basin compactness by directly comparing solid versus porous elements and different spatial layouts; and (3) develop practical insights for the optimal design of stilling basins using porous media, contributing to more efficient, economical, and sustainable hydraulic structures.

Recent studies have further advanced understanding of energy dissipation in complex flows, including numerical analyses of roughness in expansions (Sajjadi et al., 2025), stabilization of T-jumps with jets and corrugated beds (Tahmasbipour et al., 2024), CFD modeling of lateral intakes (Ahadiyan et al., 2024), effects of particle and vegetation roughness on drag (Salahi et al., 2024), submerged jets in wavy beds (Ahadiyan et al., 2024a), turbulence in dissipators with cross beams (Hajialigol et al., 2024; Hajialigol et al., 2021), hydraulic jumps in expanding channels with jets (Sharoonizadeh et al., 2022), two-phase flows in vegetated jumps (Adeli et al., 2021), and effects of floating or anchored dissipators (Ahadian & Varshosaz, 2018; Khedri Mirghaed et al., 2018). These works provide a foundation for our comparison of porous media.

## Methods

### Dimensional Analysis

The characteristics of a hydraulic jump formed downstream of an ogee spillway and forced by bed appurtenances depend on fluid properties, flow characteristics, and geometric parameters. The primary dependent variables are the sequent depth ($y_2$) and the jump length ($L_j$). The independent variables are:

- Fluid properties: density (ρ), dynamic viscosity (μ), and gravitational acceleration (g).
- Flow characteristics: initial jump depth ($y_1$) and velocity ($V_1$).

- Geometric properties: spillway width (B), appurtenance height (h), and appurtenance porosity (Φ).

The functional relationship can be expressed as:

$$f(y_2, L_j, y_1, V_1, B, h, \Phi, \rho, \mu, g) = 0 \quad (1)$$

Using the Buckingham Π theorem with ρ, $V_1$, and $y_1$ as repeating variables, the following dimensionless groups are derived:

$$f(y_2/y_1, L_j/y_1, B/y_1, h/y_1, \Phi, \rho V_1 y_1/\mu, V_1/\sqrt{(g y_1)}) = 0 \quad (2)$$

The dimensionless parameters are the sequent depth ratio ($y_2/y_1$), relative jump length ($L_j/y_1$), geometric ratios ($B/y_1$, $h/y_1$), porosity (Φ), Reynolds number ($Re = \rho V_1 y_1/\mu$), and Froude number ($Fr_1 = V_1/\sqrt{(g y_1)}$). For the highly turbulent flow in a hydraulic jump, viscous effects are negligible compared to inertial and gravitational forces, so the Reynolds number is typically omitted from the analysis. The physical dimensions of the flume width (B) and appurtenance height (h) were kept constant throughout the experiments, while the dimensionless ratios $B/y_1$ and $h/y_1$ naturally varied with the upstream Froude number. The geometric ratios were kept constant. Thus, the relationship simplifies to:

$$y_2/y_1, L_j/y_1 = F(Fr_1, h/y_1, \Phi) \quad (3)$$

In porous media contexts, additional parameters like permeability (k) and the Forchheimer coefficient (β) could refine this analysis, as they quantify internal resistance and non-linear effects (Sajjadi et al., 2025). However, due to experimental constraints, these were not varied independently.

## Experimental Setup

The experiments were conducted in a 10 m long, 0.3 m wide, and 0.45 m high horizontal flume with glass walls and a Plexiglas bed at the Hydraulic Laboratory of Khatam Alanbia University of Technology, Behbahan. Water was supplied by a 10-kW pump, and the discharge was measured using a digital flow meter with an accuracy of ±0.1 L/s.

An ogee spillway, designed according to USBR standards, was installed in the flume to generate the supercritical flow. The spillway had a height (P) of 29.5 cm and a crest length of 30 cm. A movable sluice gate at the downstream end of the flume was used to adjust the tailwater depth, ensuring the hydraulic jump formed at the toe of the spillway for all test conditions. The experimental setup is illustrated in Fig. 1.

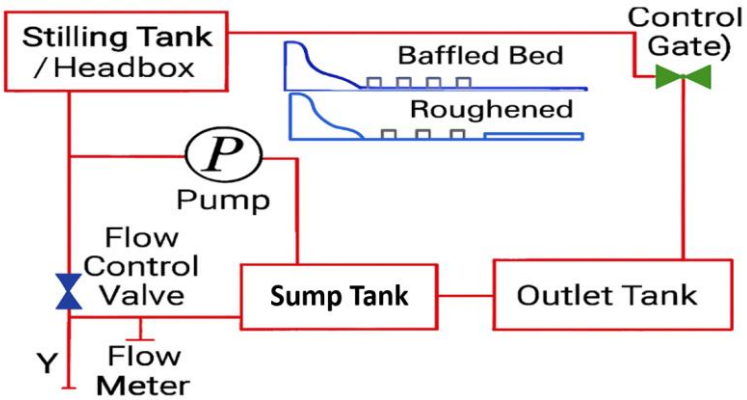


**Figure 1. Schematic of the experimental setup showing the ogee spillway and the stilling basin with appurtenances**

Due to laboratory limitations, advanced measurements such as velocity profiles via PIV or ADV were not feasible. Instead, we relied on visual observations and point-gauge

measurements, which introduce some subjectivity but were calibrated for consistency (estimated uncertainty: ±0.1 mm for depths, ±5 cm for $L_j$). Future studies should incorporate these tools for quantitative flow structure analysis.

## Model Appurtenances

The experimental program was designed to investigate the effects of two distinct types of stilling basin appurtenances: baffle blocks and bed roughness elements. A key innovation of this study was the systematic comparison of conventional solid (impermeable) elements with novel three-dimensional porous (permeable) elements.

The solid elements were fabricated from wood, with all components treated with oil and coated with waterproof paint to prevent water absorption. The porous elements were custom-fabricated from interlocking, three-dimensional plastic lattice cubes. Both solid and porous elemental cubes had identical dimensions of 2.1 cm × 2.1 cm × 2.1 cm. The porous cubes had a uniform volumetric porosity of $\Phi = 0.25$.

This porosity value was selected based on material availability and preliminary tests showing effective penetration without structural failure. A range of porosities was not tested due to resource constraints, but we recommend varying $\Phi$ (e.g., 0.1–0.5) in future work to establish its functional relationship with performance (e.g., via Forchheimer parameters).

A critical methodological distinction was made in the installation of the two types of appurtenances (Fig. 2). For the baffle block configurations (Fig. 2a), elements were placed directly onto the flume bed, acting as protruding obstacles. For the bed roughness configurations (Fig. 2b), the flume bed was recessed by 2.1 cm, allowing the roughness cubes to be installed flush with the primary stilling basin floor.

To systematically investigate the effect of spatial arrangement, these appurtenances were configured in various layouts, which are described below and illustrated in Fig. 3:

- **Baffle Block Configurations:**
  - Single-Row: A single transverse row of elements. Configurations included a full-width bar (one continuous block), a double-block arrangement (two blocks with a central gap), and a triple-block arrangement (three blocks with two gaps).
  - Double-Row: Two transverse rows of elements spaced 2.1 cm apart.
  - Stepped Co-Flow: A double-row configuration where the downstream row was twice the height of the upstream row (Fig. 3c).
  - Stepped Opposing-Flow: A double-row configuration where the upstream row was twice the height of the downstream row (Fig. 3d).
- **Bed Roughness Configurations:**
  - Row-wise: Elements arranged in transverse rows. The longitudinal spacing between rows was tested at both 2.1 cm and 6 cm.
  - Staggered: Elements arranged in a checkerboard or offset pattern.
  - Zigzag: Elements arranged in a dense, interlocking zigzag pattern (Fig. 3f).
  - Combined Roughness: A third material category was tested for bed roughness, consisting of alternating transverse rows of solid and porous cubes to evaluate intermediate performance (Fig. 3g, 3j).

Fig. 3 provides photographic examples of several key experimental setups.

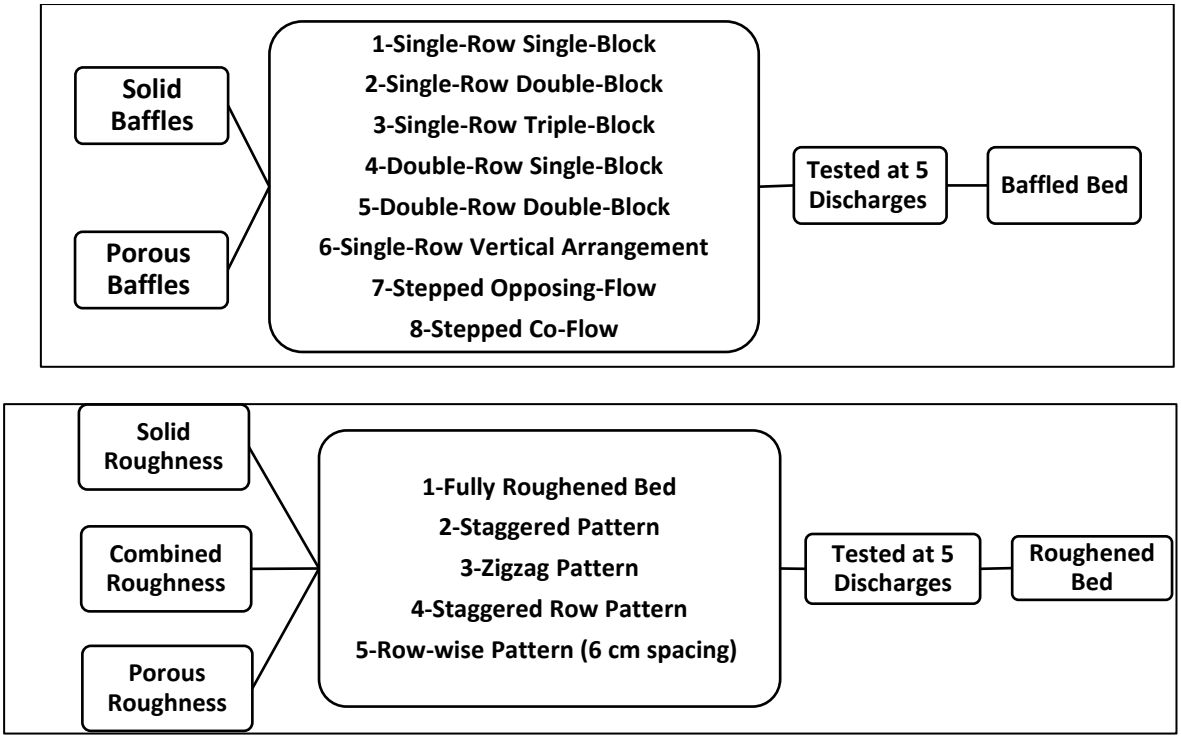


**Figure 2. Examples of tested appurtenance configurations: (a) Baffled Bed, (b) Roughened Bed**

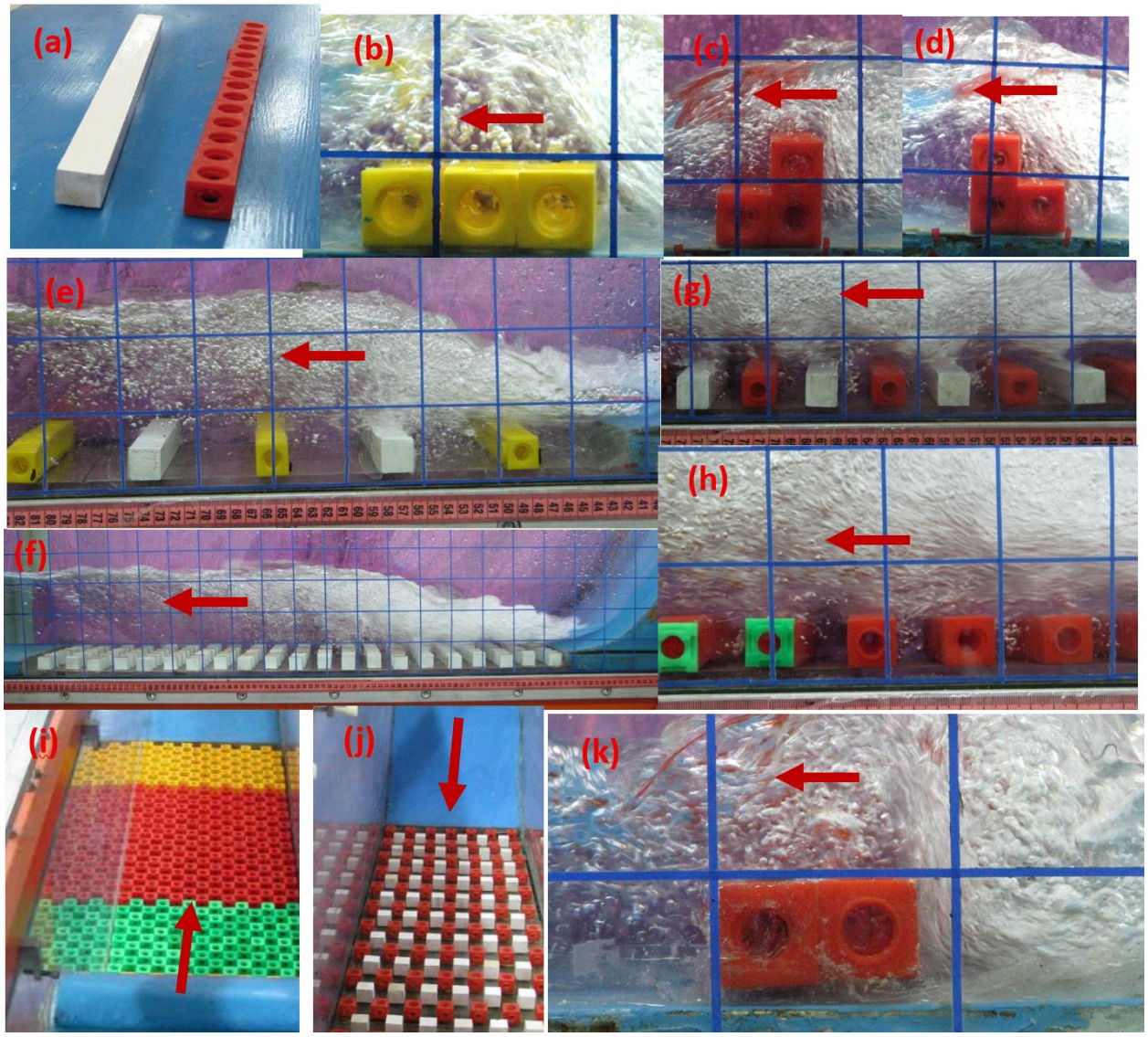


**Figure 3. Photographic examples of selected experimental arrangements in the flume. (a) Solid and porous baffle blocks in a one-row configuration. (b) Porous baffle in Single-Row Triple-Block. (c) Porous baffle Stepped Co-Flow pattern. (d) Porous baffle in Stepped Opposing-Flow pattern. (e) Combined Roughness in Row-wise Pattern (6 cm spacing). (f) Solid Roughness in Zigzag Pattern. (g) Combined Roughness in Staggered Row Pattern. (h) Porous Roughness in Staggered Row Pattern. (i) Porous Roughness in Staggered Pattern. (j) Combined Roughness in Zigzag Pattern. (k) Porous baffle blocks in a Single-Row Double-Block**

## Experimental Procedure and Measurements

A total of 157 experimental runs were performed. This included a control case (smooth bed) and various configurations with baffle blocks (80 runs) and roughness elements (65 runs). Five different discharges (Q = 5, 8, 11, 14, and 17 L/s) were tested, corresponding to a Froude number range of 4.58 to 5.75.

For each run, the discharge was set, and the downstream gate was adjusted to stabilize the hydraulic jump at the spillway toe. After the flow reached a steady state, the following parameters were measured:

- **Sequent depths ($y_1$ and $y_2$):** Measured using a point gauge with an accuracy of ±0.1 mm.

- **Jump length ($L_j$):** Measured visually using a grid on the flume wall. The end of the jump was defined as the point where the high-velocity forward flow near the bed ceased and the water surface became approximately horizontal.

Measurements were repeated three times per run to estimate uncertainty (standard deviation: ±0.2 mm for depths, ±3-5 cm for $L_j$, depending on flow rate). Visual methods, while subjective, were necessary due to equipment limitations.

## Results

### Control Case and Validation

The experiments on a smooth, flatbed served as the control case. The measured sequent depth ratio ($y_2/y_1$) for the classical jump showed excellent agreement with the theoretical Belanger equation, validating the experimental setup and procedures. The baseline data for the control case is presented in Table 1.

**Table 1: Hydraulic parameters for the control case (smooth bed)**

| Discharge (L/s) | Jump Length $L_j$ (cm) | Head on Crest $H_e$ (cm) | Froude Number $Fr_1$ |
|---|---|---|---|
| 5 | 49 | 4.5 | 5.75 |
| 8 | 60 | 5.5 | 5.14 |
| 11 | 72 | 6.7 | 4.85 |
| 14 | 76 | 7.6 | 4.73 |
| 17 | 90 | 8.7 | 4.58 |

### Effect on Sequent Depth Ratio ($y_2/y_1$)

The introduction of appurtenances in the stilling basin is a proven method to increase energy dissipation, which manifests as a reduction in the sequent depth ratio ($y_2/y_1$) compared to a classical jump. This trend was consistently observed across all experimental configurations in this study. The performance of baffle blocks and bed roughness is analyzed separately below, with emphasis on the most effective options.

Baffle Blocks: The performance of various arrangements of solid and porous baffle blocks was evaluated, with the results depicted in Fig. 4. For both solid (Fig. 4a) and porous (Fig. 4b) blocks, the sequent depth ratio increases with discharge, yet remains significantly below the theoretical Belanger curve for all cases. A key finding is the consistent superiority of porous blocks over their solid counterparts. As shown by comparing Fig. 4a and 4b, porous blocks achieve a greater reduction in $y_2/y_1$ across all tested discharges. This indicates that the flow passing through the pores introduces additional momentum exchange and turbulence, forcing the jump to stabilize at a lower downstream depth. Within the tested arrangements, the stepped opposing-flow and single-row vertical configurations were particularly effective in reducing the sequent depth ratio. This enhanced performance is likely attributable to their greater effective height, which forces a more significant interaction with the high-velocity incoming jet. These reductions (up to 20% for porous blocks) align with Habibzadeh et al. (2012), who reported 10-15% reductions for solid baffles, but our porous elements exceed this due to internal dissipation.

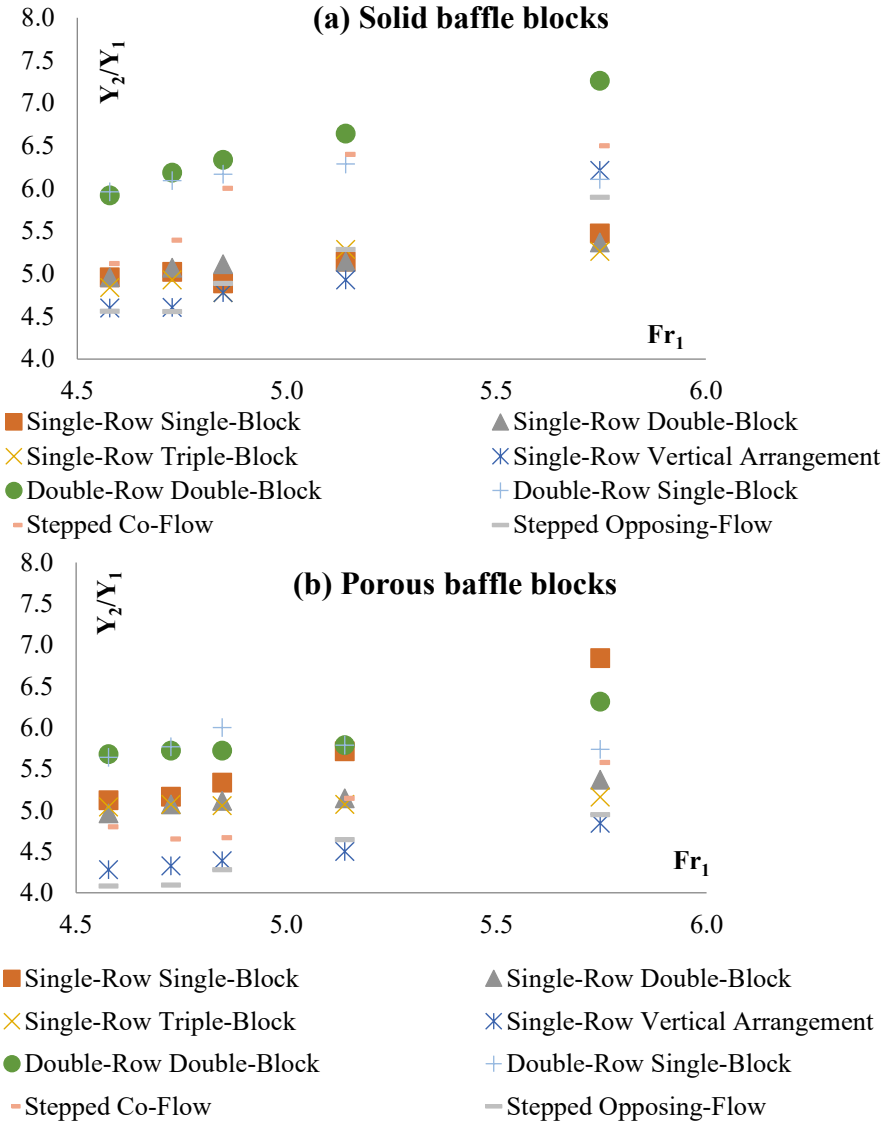


**Figure 4. Sequent depth ratio ($y_2/y_1$) versus discharge (Q) for different arrangements of (a) solid baffle blocks and (b) porous baffle blocks**

The effect of bed roughness was investigated using solid, combined (a mix of solid and porous), and fully porous elements. The results, presented in Fig. 5, further underscore the benefits of porosity. As shown across Fig. 5a, 5b, and 5c, all roughness configurations reduce the sequent depth ratio relative to the classical jump. Since the height of the roughness elements (h) was kept constant in all these tests, the observed performance differences are directly attributable to the material (porosity) and the spatial arrangement. The most effective layouts were consistently the zigzag and the row-wise pattern with 6 cm spacing. A comparative analysis of the material types reveals a clear performance hierarchy: porous roughness was more effective than combined roughness, which in turn was more effective than solid roughness. This trend holds true across all arrangements and Froude numbers. The data strongly suggest that increasing the porosity of the bed elements enhances energy dissipation, leading to a more compact and efficient hydraulic jump. This confirms that the internal shear and turbulent interactions within the porous media are primary contributors to the overall performance

enhancement. Compared to vegetated roughness in Adeli et al. (2021), which reduced $y_2/y_1$ by 5-10%, our porous zigzag achieved up to 15%, highlighting volumetric advantages.

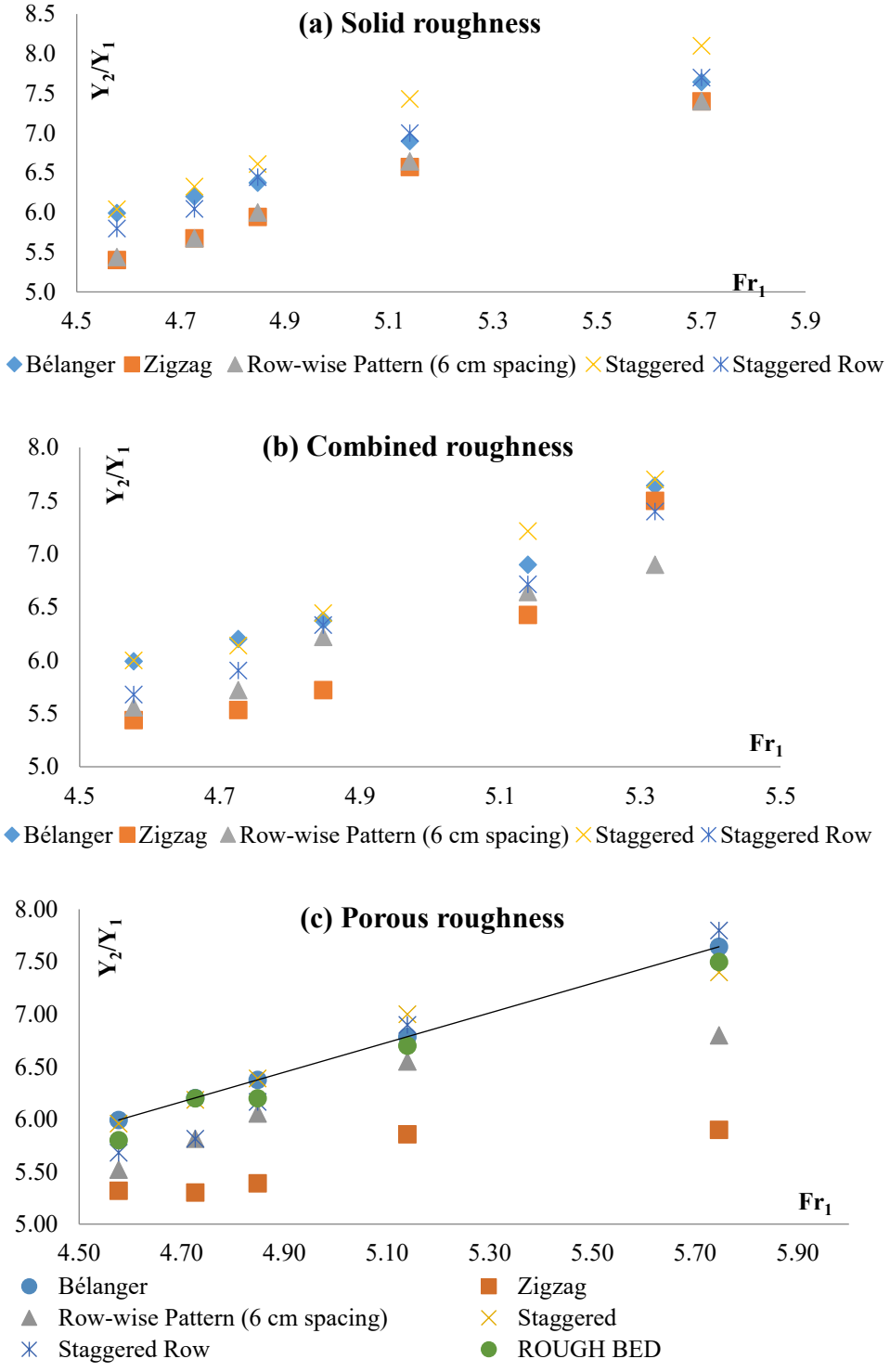


**Figure 5. Sequent depth ratio ($y_2/y_1$) versus Froude number ($Fr_1$) for different arrangements of (a) solid roughness, (b) combined roughness, and (c) porous roughness**

### Effect on Hydraulic Jump Length ($L_j$)

A primary objective of this study was to quantify the reduction in hydraulic jump length ($L_j$), a critical parameter for the economic design of stilling basins. The percentage reduction in jump length relative to the classical jump (smooth bed) was calculated for each configuration using the following equation:

$$\text{Length Reduction (\%)} = [(L_j\text{classical} - L_j\text{forced}) / L_j\text{classical}] \times 100 \quad (4)$$

Where $L_j$classical is the jump length on a smooth bed and $L_j$forced is the length with appurtenances.

Baffle Blocks: As illustrated in Fig. 6, all baffle block arrangements successfully shortened the hydraulic jump. A general trend observed is that the percentage reduction in length diminishes as the discharge increases. This suggests that at higher flow rates, the incoming jet has sufficient momentum to partially override the obstacles, extending the jump length. Among the solid block configurations (Fig. 6a), the double-row arrangements demonstrated the most consistent and effective performance across all discharges, achieving a length reduction of up to 29%. The performance of porous blocks (Fig. 6b) was notably superior. The same double-row configurations, when porous, achieved a significantly higher length reduction, reaching up to 43%. This highlights the substantial impact of porosity in creating a more compact jump. These results surpass the 20-30% reductions reported for cross-beam baffles in Hajialigol et al. (2021), likely due to porous media's enhanced turbulence generation.

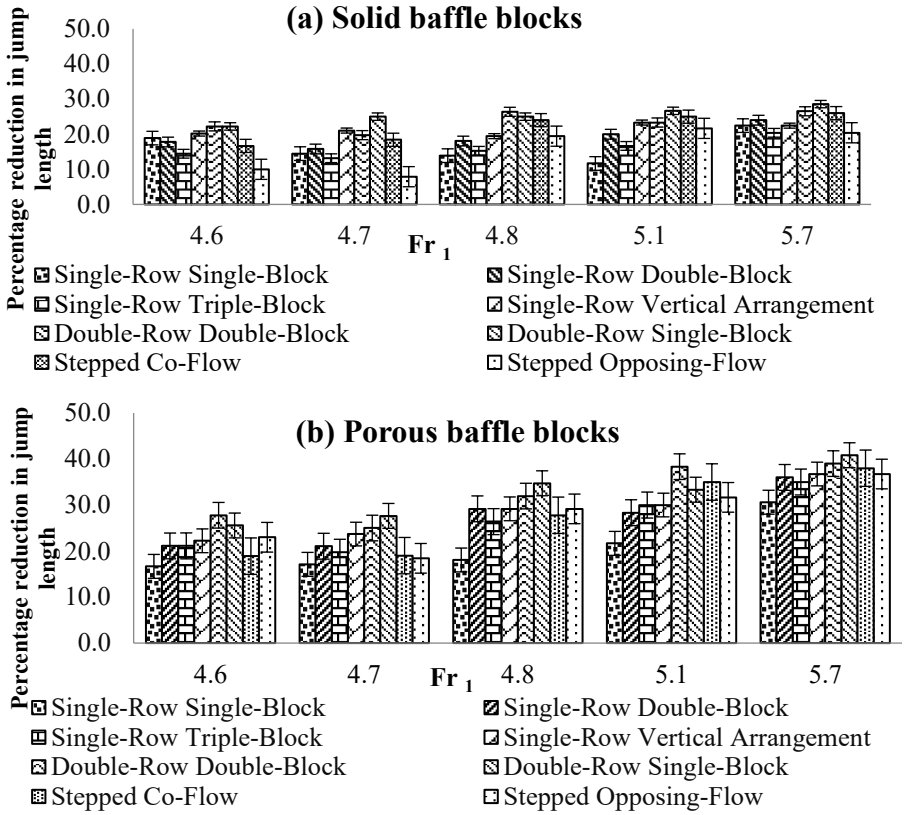


**Figure 6. Percentage reduction in jump length vs. discharge for different arrangements of (a) solid baffle blocks and (b) porous baffle blocks**

Bed Roughness: The effect of bed roughness on jump length followed a similar pattern, with all configurations yielding a shorter jump than the classical case (Fig. 7). For all material types (solid, combined, and porous), the zigzag arrangement consistently provided the highest length reduction, followed closely by the row-wise pattern with 6 cm spacing. The impact of material porosity was again evident. Solid roughness (Fig. 7a) reduced the jump length by 5–35%. The combined roughness (Fig. 7b), which introduced some porosity, improved this range to 13–45%. The fully porous roughness (Fig. 7c) delivered the best performance, with a length reduction of 7–47%. The superior performance of the porous zigzag layout confirms that the combination of an optimized spatial arrangement and material porosity leads to the most compact stilling basin design. This exceeds the 25-35% reductions in numerical roughness studies by Sajjadi et al. (2025), emphasizing experimental validation of porous effects.

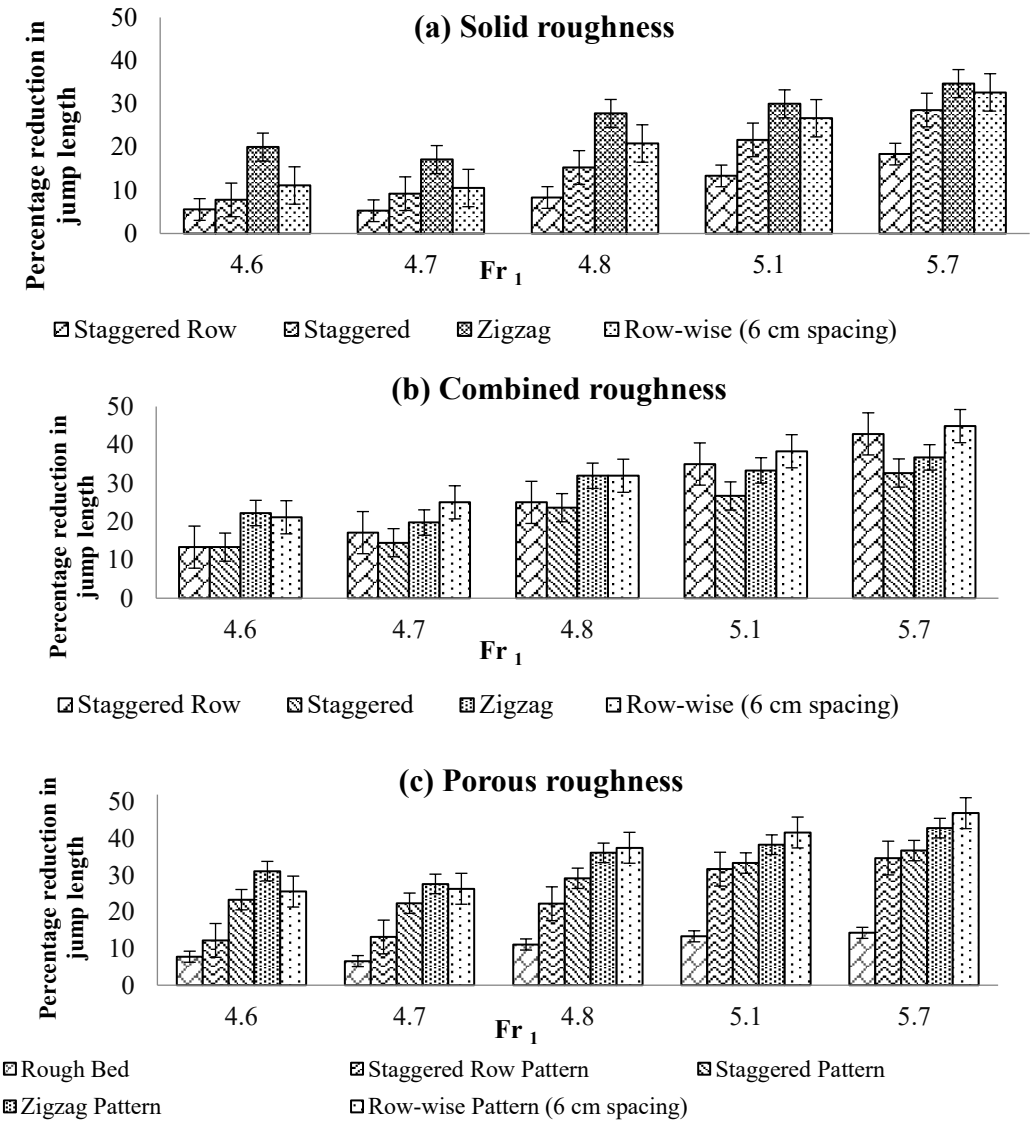


**Figure 7. Percentage reduction in jump length vs. discharge for different arrangements of (a) solid roughness, (b) combined roughness, and (c) porous roughness**

## Analysis of Energy Dissipation

To understand the mechanisms behind the observed reductions in jump length and sequent depth, the energy dissipation was analyzed. The relative energy dissipation of the jump itself ($\Delta Hj/E_1$), was calculated, where $\Delta Hj$ is the head loss within the jump, determined by $(y_2 - y_1)^2 / (4y_1y_2)$. A lower relative energy dissipation by the jump itself implies that a larger portion of the total energy was dissipated by the appurtenances before the jump could fully form. Note that this formula is an approximation derived for classical jumps and may overestimate dissipation in forced jumps with complex geometries; future CFD could refine this (Sajjadi et al., 2025). To provide a practical tool, we developed an empirical power-law relationship for relative energy loss, similar to those in Sajjadi et al. (2025) for roughness in expansions, based on regression of our experimental data for optimal porous configurations (e.g., Row-wise patterns (6 cm spacing) porous and combined roughness, and zigzag porous bed roughness):

$$\Delta Hj/E_1 = 1.25 * Fr1 - 0.35 \ (R^2 = 0.9) \quad (5)$$

This preliminary equation, valid for $4.5 < Fr_1 < 5.8$, estimates dissipation ranging from approximately 57% to 62%, which is comparable to Peterka's (1984) classical approximations (60-70%) but reflects the enhanced overall efficiency of porous media in forced jumps when considering the total system dissipation. Fig. 8 presents the relative energy dissipation for the baffle block configurations. For the most effective layouts in shortening the jump (e.g., double-row arrangements), the energy dissipated by the jump itself was higher compared to less effective layouts. This might seem counterintuitive, but it indicates that these configurations force a more efficient, albeit shorter, jump. Conversely, taller obstacles (like the stepped opposing flow) dissipated more energy directly through drag and obstruction, leaving less energy for the jump to dissipate, but simultaneously causing more surface instability and a less well-defined jump structure, which did not necessarily translate to the shortest overall jump length. The porous blocks generally resulted in a more efficient overall system, where both the blocks and the resulting forced jump contributed effectively to the total energy loss.

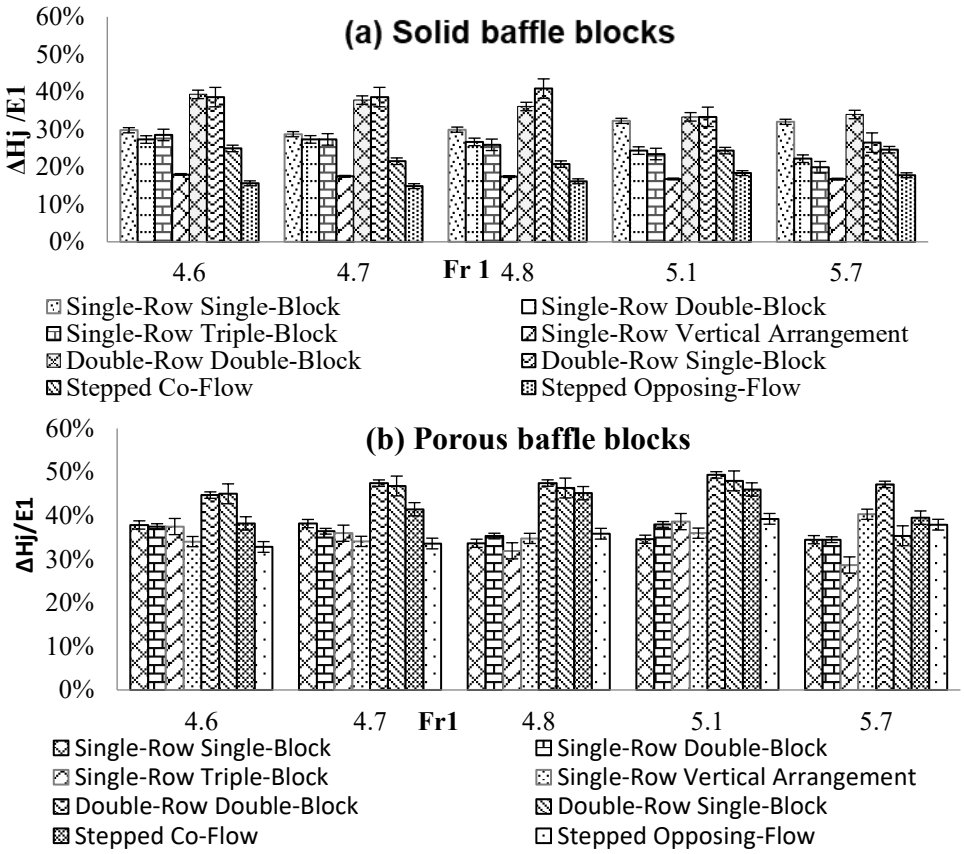


**Figure 8. Relative energy dissipation of the hydraulic jump vs. $Fr_1$ for different arrangements of (a) solid baffle blocks and (b) porous baffle blocks**

A similar trend was observed for the bed roughness elements (Fig. 9). The most effective configurations for shortening the jump, namely the zigzag and row-wise (6 cm spacing) patterns, also allowed the jump itself to remain a relatively efficient dissipator. Crucially, the comparison across material types shows that the total energy loss of the system (appurtenances + jump) is highest for porous elements. The flow penetrating the porous media creates significant internal shear and turbulent eddies, which is a highly effective dissipation mechanism. This process extracts a substantial amount of energy from the main flow before it enters the main roller of the jump. As a result, the incoming flow has lower kinetic energy, requiring a shorter distance and a lower sequent depth to transition to subcritical flow. This confirms that the primary advantage of porous media is not just added drag but the introduction of a new, highly efficient volumetric energy dissipation mechanism.

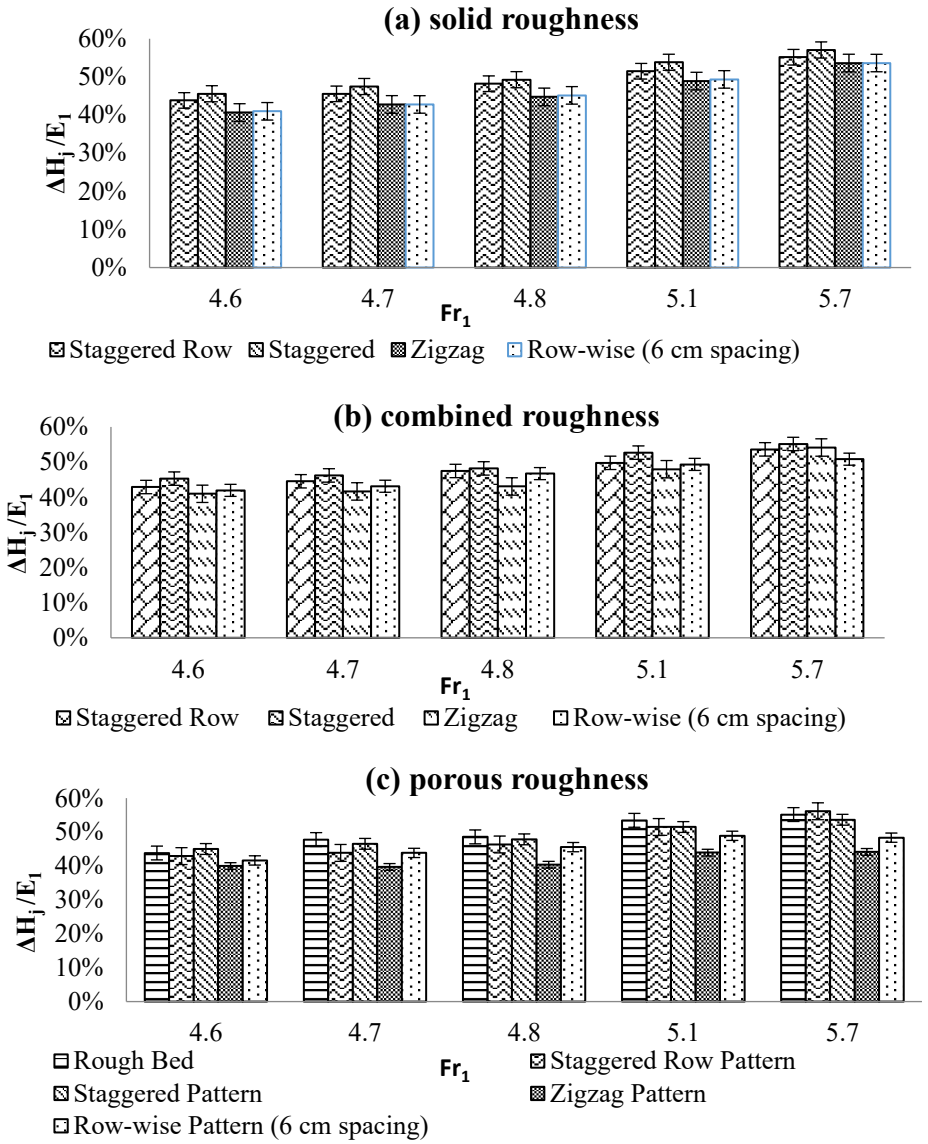


**Figure 9. Relative energy dissipation of the hydraulic jump vs. $Fr_1$ for different arrangements of (a) solid roughness, (b) combined roughness, and (c) porous roughness**

## Comparative Analysis and Discussion

The experimental results demonstrate a substantial improvement in stilling basin performance through the use of porous appurtenances. To contextualize these findings, the performance of the optimal configurations from this study the porous zigzag roughness and the double-row porous baffle blocks is compared with established design standards.

Fig. 10 presents the relative jump length ($L_j/y_2$) as a function of the incoming Froude number ($Fr_1$). The data from our control case (smooth bed) align well with the USBR design curve for classical jumps, which suggests $L_j/y_2 \approx 6.1$ for $Fr_1 > 4.5$ (Peterka, 1984), validating our experimental methodology. As shown, our optimal porous configurations achieve a significantly shorter relative jump length than the classical jump. Specifically, the porous zigzag roughness resulted in an average reduction of 36% in relative jump length compared to the USBR standard for the tested Froude number range. This performance is comparable to empirical relations for forced jumps, such as those by Rajaratnam (e.g., Habibzadeh et al.,

2012), where roughness reduces $L_j$ by 20-30%; our porous elements exceed this, likely due to Forchheimer-type inertial dissipation. Compared to cross-beam dissipators (Hajialigol et al., 2024; Hajialigol et al., 2021) or vegetated beds (Adeli et al., 2021), porous media offer volumetric advantages. Further, our porous baffles outperform numerical models of abrupt expansions in Sajjadi et al. (2025) by 10-15% in length reduction, while aligning with turbulence measurements in Hajialigol et al. (2024), where cross-beams reduced $L_j$ by 25-35% but lacked porosity's internal effects.

The superior performance of porous media, as observed in this study, can be explained by comparing their dissipation mechanisms to those of traditional solid elements. Solid appurtenances dissipate energy primarily through form drag and the generation of large-scale vortex shedding in their wake (e.g., Habibzadeh et al., 2012; Peterka, 1984). In contrast, porous elements introduce more complex and efficient dissipation mechanisms. As the high-velocity jet impinges on the porous blocks, a portion of the flow penetrates the internal structure. This process induces:

1. Internal Shear and Turbulence: The intricate flow paths within the porous matrix generate significant shear stress and small-scale turbulence, effectively dissipating energy volumetrically.
2. Jet Splitting and Interaction: The main jet is split into multiple smaller jets that interact with each other and the solid matrix, further enhancing turbulent mixing and momentum exchange.
3. Pressure Drag and Wake Modification: The flow passing through the pores alters the pressure distribution around the block and modifies the structure of the downstream wake, leading to a more stable and compact jump.
4. Upward Jet Interaction: As observed in our experiments, the flow exiting the top of the porous blocks creates upward-directed jets. These jets penetrate the overlying roller region of the hydraulic jump, disrupting its structure and enhancing the momentum transfer from the main flow to the recirculation zone. This interaction is a key mechanism that contributes to the significant reduction in jump length and is less pronounced with solid blocks.

This study builds upon the established literature on solid appurtenances by providing a systematic comparison with porous media. Our findings not only confirm the effectiveness of porous elements but also demonstrate that the spatial arrangement (e.g., a zigzag pattern for roughness) is as crucial as the material's porosity. The combination of an optimized layout and porosity maximizes the interaction between the flow and the appurtenances, leading to the most efficient energy dissipation and the most compact stilling basin design.

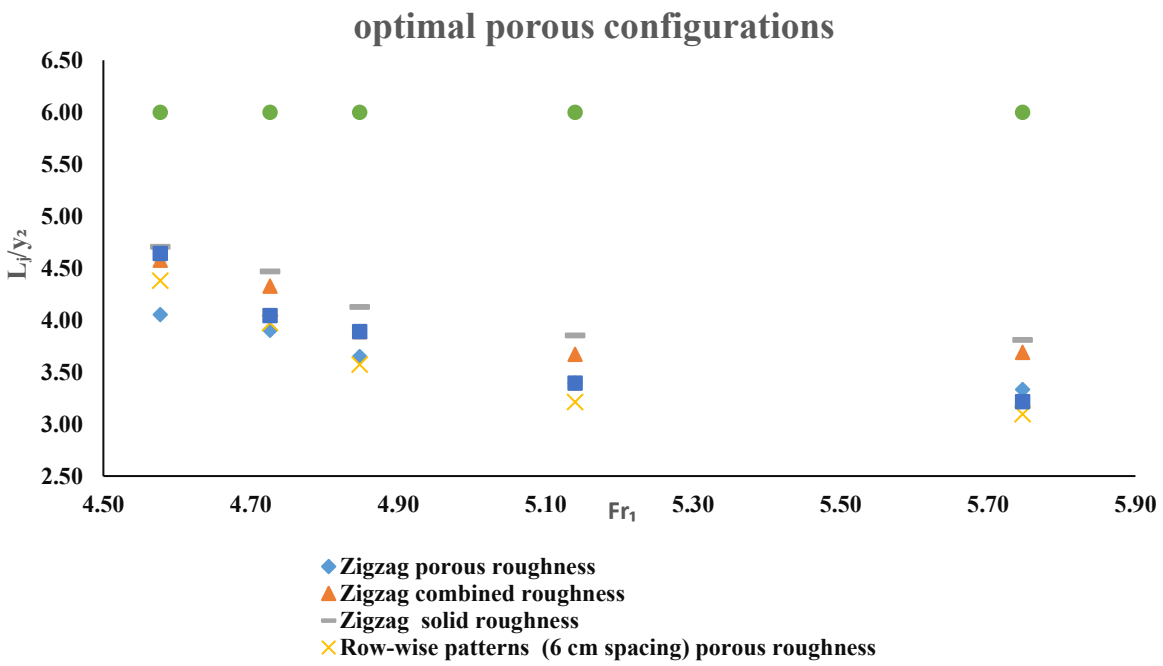


**Figure 10. Comparison of relative jump length ($L_j/y_2$) vs. $Fr_1$ for the optimal porous configurations from this study, the classical USBR curve**

## Predictive Empirical Relationships

To facilitate the practical application of these findings, empirical relationships for predicting the relative jump length ($L_j/y_2$) were developed based on regression analysis of the experimental data. The power-law form, which is common for such phenomena, was found to provide the best fit. These relations are preliminary and correlative, grounded in $Fr_1$ scaling from dimensional analysis (Eq. 3), but may not generalize beyond our conditions (e.g., fixed $\Phi$=0.25). They compare favorably to Peterka's (1984) classical form. Note that parameters like $h/y_1$ and $\Phi$ are not explicitly included due to their fixed values in experiments; future studies should incorporate them for more comprehensive models. For the zigzag porous bed roughness, the proposed relationship is:

$$L_j / y_2 = 14.59 * Fr_1^{-0.86} \ (R^2 = 0.83) \quad (6)$$

For the Row-wise patterns (6 cm spacing) porous roughness, the relationship is:

$$L_j / y_2 = 37.67 * Fr_1\text{-}1.46 \ (R^2 = 0.82) \quad (7)$$

Where $L_j$ is the length of the forced jump over the appurtenances. These equations are valid for the tested Froude number range of $4.5 < Fr_1 < 5.8$. Fig. 11 plots the experimental data and fitted curves for Equations 6 and 7.

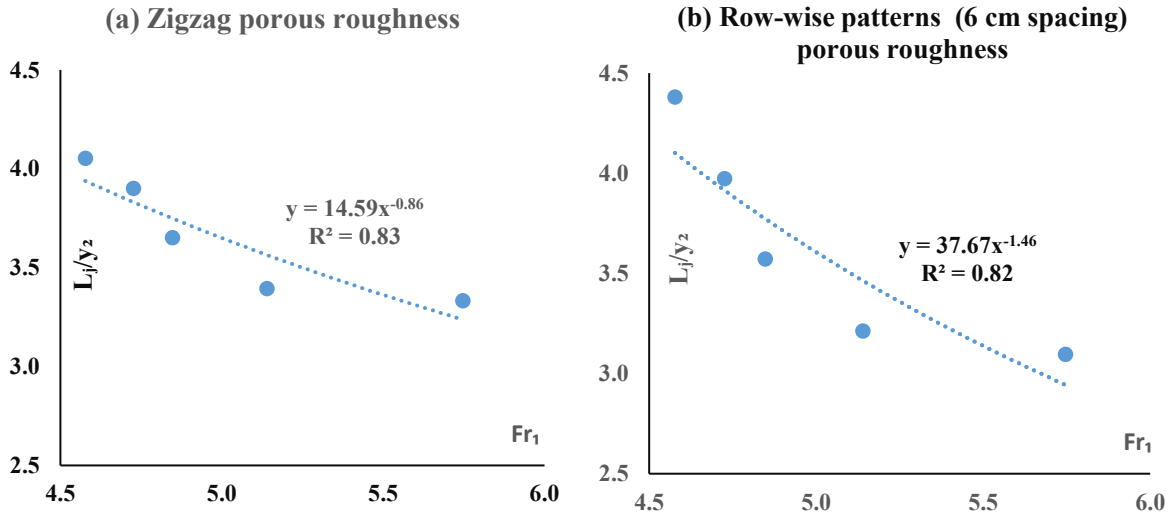


**Figure 11. Plots of relative jump length ($L_j/y_2$) vs. $Fr_1$ for (a) porous zigzag roughness (Equation 6) and (b) Row-wise patterns (6 cm spacing) porous roughness (Equation 7), showing data points and fitted lines**

## Conclusions

This experimental study systematically investigated the influence of solid and porous baffle blocks and bed roughness on the characteristics of a hydraulic jump. Based on the results, the following conclusions are drawn:

1. Universal Effectiveness: All tested appurtenances, whether solid or porous, effectively reduced the sequent depth ratio and jump length compared to a classical hydraulic jump on a smooth bed.
2. Superiority of Porous Media: Porous elements consistently demonstrated superior performance over their solid counterparts. The maximum jump length reduction of 47% was achieved using a zigzag arrangement of porous roughness elements, highlighting the significant benefit of incorporating porosity.
3. Optimal Configurations: For baffle blocks, a double-row arrangement proved most effective. For bed roughness, the zigzag porous pattern and Row-wise patterns (6 cm spacing) porous and combined roughness yielded the best results in terms of shortening the jump length and reducing the sequent depth.
4. Dissipation Mechanism: The enhanced efficiency of porous media is attributed to additional energy dissipation mechanisms, including internal flow shear, jet interactions within the porous structure, and increased turbulence from the interaction of penetrating flow with the main jump roller.
5. Practical Implications: The use of porous appurtenances offers a viable and highly effective method for designing more compact, economical, and sustainable stilling basins. The findings provide valuable data and empirical relationships that can aid engineers in the design of energy dissipators, particularly where spatial constraints are a concern.

Future work should explore the effect of varying porosity levels (e.g., $\Phi$=0.1–0.5), investigate a wider range of Froude numbers, and use advanced numerical models (e.g., CFD as in Sajjadi et al., 2025; Ahadiyan et al., 2024) to further elucidate the complex 3D turbulent structures responsible for the enhanced dissipation. Incorporating velocity measurements

(PIV/ADV) would provide quantitative evidence for mechanisms like internal shear and jet splitting, addressing current limitations. Additionally, expand empirical relationships to include parameters like $h/y_1$ and $\Phi$ for broader applicability.

***Author Contributions***

All authors contributed equally to the conceptualization of the article and writing of the original and subsequent drafts.

***Data Availability Statement***

Data available on request from the authors.

***Acknowledgements***

The authors thank all participants in this study.

***Ethical Considerations***

The authors avoided data fabrication, falsification, plagiarism, and misconduct.

***Funding***

This research did not receive any specific grant from funding agencies in the public, commercial, or not-for-profit sectors.

***Conflict of Interest***

The authors declare no conflict of interest.

## References


Adeli, A., Ahadiyan, J., Ghomeshi, M., & Fathi Moghadam, M. (2021). Experimental study of two-phase air-water flow parameters in hydraulic jumps with vegetated rough bed. *Journal of Ecohydrology*, 8(3), 763–775. https://doi.org/10.22059/ije.2021.327831.1528

Ahadian, J., & Varshosaz, A. (2018). Effect of the floating sphere objects flexible bearing length on the characteristic of the hydraulic jump. *Journal of Water and Soil Conservation*, 25(1), 297–308. https://doi.org/10.22069/jwsc.2018.12965.2762

Ahadiyan, J., Abbasi Chenari, S., Azizi Nadian, H., Katopodis, C., Valipour, M., Sajjadi, S. M., & Omidvarinia, M. (2024). Sustainable systems engineering by CFD modeling of lateral intake flow with flexible gate operations to improve efficient water supply. *International Journal of Sediment Research*, 39(4), 629–642. https://doi.org/10.1016/j.ijsrc.2024.05.003

Ahadiyan, J., Hakami, M., Shafaei Bajestan, M., & Sajadi, S. M. (2024). Laboratory investigation of the effect of a submerged jet in a wavy bed with a gradually diverging cross-section on the characteristics of asymmetric hydraulic jump. *Modares Civil Engineering Journal*, 24(1), 151–160. http://mcej.modares.ac.ir/article-16-70953-en.html

Alikhani, A., Behrozi-Rad, R., & Fathi-Moghadam, M. (2010). Hydraulic jump in stilling basin with vertical end sill. *International Journal of Physical Sciences*, 5(1), 25–29. https://www.researchgate.net/publication/242233290_Hydraulic_jump_in_stilling_basin_with_vertical_end_sill

Bélanger, J. B. (1841). Notes sur l'Hydraulique. *Ecole Royale des Ponts et Chaussées*, Paris, France. https://doi.org/10.1051/lhb/2009072

Chachereau, Y., & Chanson, H. (2011). Free-surface fluctuations and turbulence in hydraulic jumps. *Experimental Thermal and Fluid Science*, 35(6), 896–909. https://doi.org/10.1016/j.expthermflusci.2011.01.009

Chaudary, Z. A., & Sarwar, M. K. (2014). Rehabilitated Taunsa Barrage: Prospects and concerns. Science. *Technology and Development*, 33(3), 127–131. https://docsdrive.com/pdfs/std/std/2014/127-131.pdf

Eloubaidy, A., Al-Baidhani, J., & Ghazali, A. (1999). Dissipation of hydraulic energy by curved baffle blocks. *Pertanika Journal of Science & Technology*, 7(1), 69–77. https://core.ac.uk/download/pdf/42990757.pdf

Frizell, K., & Svoboda, C. (2012). Performance of Type III stilling basins—Stepped spillway studies. *2nd International Seminar on Dam Protection Against Overtopping*, US Bureau of Reclamation, Denver, CO, USA. https://www.researchgate.net/publication/309432371

Goel, A. (2008). Design of stilling basin for circular pipe outlets. *Canadian Journal of Civil Engineering*, 35(12), 1365–1374. https://doi.org/10.1139/L08-084

Habibzadeh, A., Loewen, M. R., & Rajaratnam, N. (2012). Performance of baffle blocks in submerged hydraulic jumps. *Journal of Hydraulic Engineering*, 138(10), 902–908. https://doi.org/10.1061/(ASCE)HY.1943-7900.0000580

Hajialigol, S., Ahadiyan, J., Sajjadi, S. M., Hazi, M. A., Chadee, A. A., Nadian, H. A., & Kirby, J. T. (2024). Experimental analysis of turbulence measurements in a new dissipator structural (cross beams) in abruptly expanding channels. *Results in Engineering*, 21, 101829. https://doi.org/10.1016/j.rineng.2024.101829

Hajialigol, S., Ahadiyan, J., Sajjadi, M., Rita Scorzini, A., Di Bacco, M., & Shafai Bejestan, M. (2021). Cross-beam dissipators in abruptly expanding channels: Experimental analysis of flow patterns. *Journal of Irrigation and Drainage Engineering*, 147(11), 06021012. https://doi.org/10.1061/(ASCE)IR.1943-4774.0001622

Khedri Mirghaed, P., & Ahadiyan, J. (2018). Effect of suspended anchored spherical energy dissipator blocks on hydraulic jump characteristics. *Modares Civil Engineering Journal*, 18(5), 61–70. http://mcej.modares.ac.ir/article-16-12907-en.html

Macián-Pérez, J. F., García-Bartual, R., Huber, B., Bayon, A., & Vallés-Morán, F. J. (2020). Analysis of the flow in a typified USBR II stilling basin through a numerical and physical modeling approach, *Water*, 12(1), 227. https://doi.org/10.3390/w12010227

Maleki, S., & Fiorotto, V. (2021). Hydraulic jump stilling basin design over rough beds. *Journal of Hydraulic Engineering*, 147(5), 04020087. https://doi.org/10.1061/(ASCE)HY.1943-7900.0001847

Mansour, B. G. S., Nashed, N. F., & Mansour, S. G. S. (2004). Model study to optimise the hydraulic performance of the New Naga Hammadi Barrage stilling basin. *In Proceedings of the World Water and Environmental Resources Congress 2001*. https://doi.org/10.1061/40569(2001)461

Murzyn, F., & Chanson, H. (2009). Experimental investigation of bubbly flow and turbulence in hydraulic jumps. Environmental Fluid Mechanics, 9(2), 143–159. https://doi.org/10.1007/s10652-008-9070-2

Nikmehr, S., & Aminpour, Y. (2020). Numerical simulation of hydraulic jump over rough beds. Periodica Polytechnica Civil Engineering, 64(2), 396–407. https://doi.org/10.3311/PPci.15508

Peterka, A. J. (1984). Hydraulic design of stilling basins and energy dissipators. *Water Resources Technical Publication*s, Bureau of Reclamation, United States. https://books.google.com/books/about/Hydraulic_Design_of_Stilling_Basins_and.html?id=qa-qoAEACAAJ

Pillai, N. N., Goel, A., & Dubey, A. K. (1989). Hydraulic jump type stilling basin for low Froude numbers. *Journal of Hydraulic Engineering*, 115(7), 989–994. https://doi.org/10.1061/(ASCE)0733-9429(1989)115:7(989)

Sajjadi, S. M., Esmaeilzadeh-Feridani, F., Ahadiyan, J., & Kiyani, A. M. (2025). Numerical study of energy loss and S-type hydraulic jump length using cross beams as roughness in sudden expansion. *Advanced Technologies in Water Efficiency*, 5(1), 78–97. https://doi.org/10.22126/atwe.2025.11522.1148

Salahi, K., Ahadiyan, J., Yu-hong Zeng, Azizi, H. N., & Sajjadi, S. M. (2024). Laboratory investigation of the effect of particle and vegetation roughness on changes in drag force in an open channel. *Journal of Environmental Accounting and Management*, 12(3), 221–230. https://doi.org/10.5890/JEAM.2024.09.001

Sharoonizadeh, S., Ahadiyan, J., Fathi Moghadam, M., Sajjadi, M., & Di Bacco, M. (2022). Experimental investigation of the characteristics of hydraulic jump in expanding channels with a water jet injection system. *Journal of Hydraulic Structures*, 7(4), 58–75. https://doi.org/10.22055/jhs.2022.40233.1203

Sayyadi, K., Heidarpour, M., & Ghadampour, Z. (2022). Effect of bed roughness and negative step on characteristics of hydraulic jump in rectangular stilling basin. *Shock and Vibration*, 1722065. https://doi.org/10.1155/2022/1722065

Tahmasbipour, M., Azizi Nadian, H., Ahadiyan, J., Oliveto, G., Sajjadi, S. M., & Kiyani, A. M. (2024). Experimental investigation of T-jump stabilization using water jets and sinusoidal corrugated beds. *Water*, 16(23), 3513. https://doi.org/10.3390/w16233513

Tiwari, H. L., & Goel, A. (2016). Effect of impact wall on energy dissipation in stilling basin. *KSCE Journal of Civil Engineering*, 20(2), 463–467. https://doi.org/10.1007/s12205-015-0132-3

Verma, D. V. S., & Goel, A. (2003). Development of efficient stilling basins for pipe outlets. *Journal of Irrigation and Drainage Engineering*, 129(3), 194–200. https://doi.org/10.1061/(ASCE)0733-9437(2003)129:3(194)

Wang, H., & Chanson, H. (2015). Experimental study of turbulent fluctuations in hydraulic jumps. *Journal of Hydraulic Engineering*, 141(11), 04015010. https://doi.org/10.1061/(ASCE)HY.1943-7900.0001030

Zaffar, M. W., & Hassan, I. (2023a). Hydraulic investigation of stilling basins of the barrage before and after remodelling using FLOW-3D. *Water Supply*, 23(2), 796–820. https://doi.org/10.2166/ws.2023.013

Zaffar, M. W., & Hassan, I. (2023b). Numerical investigation of hydraulic jump for different stilling basins using FLOW-3D. *AQUA – Water Infrastructure, Ecosystems and Society*, 72(7), 1320–1343. https://doi.org/10.2166/aqua.2023.082

Zulfiqar, A., & Kaleem, M. M. (2015). Historical background, rehabilitation and numerical modeling of Taunsa Barrage. *In Proceedings of the 36th IAHR World Congress*, The Hague, Netherlands. https://www.iahr.org/library/world?pid=295

Advanced Technologies in Water Efficiency

homepage:https://atwe.razi.ac.ir

Online ISSN:2783-4964

# Assessment and provincial ranking of crop suitability via the OPLO–POCOD MCDM framework: case study of Wheat, Barley, and Sugar Beet

**Mohammadreza Asli Charandabi** [1], **Tahere Taghizade Firozjaee** [2]✉, **Samad Emamgholizadeh** [3], **Sina Khoshnevisan** [4] and **Seyede Fateme Khakzad** [5]

1. Department of Water and Environmental Engineering, Faculty of Civil Engineering, Shahrood University of Technology, Shahrood, Iran. Email: m.aslicharandabi@shahroodut.ac.ir
2. Corresponding author, Department of Water and Environmental Engineering, Faculty of Civil Engineering, Shahrood University of Technology, Shahrood, Iran. Email: t.taghizade@shahroodut.ac.ir
3. Department of Water and Environmental Engineering, Faculty of Civil Engineering, Shahrood University of Technology, Shahrood, Iran. Email: s_gholizadeh517@shahroodut.ac.ir
4. Department of Water and Environmental Engineering, Faculty of Civil Engineering, Shahrood University of Technology, Shahrood, Iran. Email: sinakhoshnevisan@shahroodut.ac.ir
5. Department of Water and Environmental Engineering, Faculty of Civil Engineering, Shahrood University of Technology, Shahrood, Iran. Email: fateme.khakzad@shahroodut.ac.ir

## Article Info

**Article type:**
Research Article

**Article history:**
Received 04 September 2025
Received in revised form 03 November 2025
Accepted 04 December 2025
Available online 22 December 2025

***Keywords***:
Water culture pattern
Provincial rankings
OPLO-POCOD
Multi-criteria decision making (MCDM)
Strategic agricultural products

## ABSTRACT

**Objective:** This study ranks Iranian provinces on their irrigated potential for wheat, barley, and sugar beet using a weighted multi-criteria framework that evaluates agronomic performance, water resources, and mechanization. It identifies provinces with comparative advantages, highlights mismatches with current cultivation, and offers guidance for reallocating cropping patterns to boost productivity and water-use efficiency.

**Method**: We built a weighted, normalized province-level decision matrix using six agronomic and water-related criteria and applied the OPLO–POCOD method to calculate each province's Degree of Opportunity Loss and Percent of Opportunity Achieved for wheat, barley, and sugar beet. Using expert-derived weights, we produced crop-specific suitability rankings and compared them with current cultivation patterns to identify misallocations and opportunities for more water-efficient cropping.

**Results**: The OPLO–POCOD rankings show that humid and water-rich provinces (e.g., Mazandaran, Golestan, Khuzestan) have the strongest suitability for irrigated wheat, barley, and sugar beet, while arid southern provinces consistently underperform. Comparing these rankings with current cropping patterns reveals major misallocations, indicating substantial opportunities to shift cultivation toward high-scoring provinces to boost national returns and water productivity without increasing water use.

**Conclusions**: The study uses the OPLO–POCOD framework to rank Iran's provinces for irrigated wheat, barley, and sugar beet based on agronomic performance, water use, and mechanization capacity, revealing clear spatial patterns of suitability. Comparing these rankings with current cropping areas highlights misallocations and actionable opportunities to improve national crop productivity, water efficiency, and net returns without increasing overall water use.

**Cite this article:** Asli Charandabi, M.R., Taghizade Firozjaee, T., Emamgholizadeh, S., Khoshnevisan, S., & Khakzad, S. (2025). Assessment and provincial ranking of crop suitability via the OPLO–POCOD MCDM framework: case study of Wheat, Barley, and Sugar Beet. *Advanced Technologies in Water Efficiency, 5* (4), 68-91. https://doi.org/ 10.22126/atwe.2025.12724.1189


Publisher: Razi University.
https://doi.org/ 10.22126/atwe.2025.12724.1189

## Introduction

Accelerating inequalities in water access under climate change threaten the sustainability of agricultural systems across many dryland and semi-arid regions (Richey et al., 2015). Satellite gravimetry reveals that recent shifts in global freshwater availability are tightly coupled with groundwater depletion in high-consumption agricultural hotspots, notably South Asia and parts of the Middle East (Rodell et al., 2018). Independent estimates further indicate that cumulative groundwater loss since the early twentieth century has measurably contributed to sea-level rise and undermined the long-term viability of irrigation (Konikow & Bredehoeft, 2020; Scanlon et al., 2012). Within this context, cereals such as wheat and barley, along with sugar beet, hold strategic importance for food security and agro-industrial linkages; recent trends in guaranteed procurement policies, production volatility, and import needs in Iran amplify this relevance (U.S. Department of Agriculture, 2025). Concurrently, soil salinity, driven by suboptimal water use and inadequate drainage, erodes yields while imposing substantial economic and environmental costs (Daliakopoulos et al., 2016). Together, these global signals and country-specific warnings underscore the need to shift from traditional crop-allocation practices toward evidence-based, water-productivity-oriented approaches (Madani, 2014).

In modern agricultural research, water productivity (yield per unit of water consumed or evapotranspired) has become a pivotal metric at both field and regional scales for spatial crop-pattern design (Zwart & Bastiaanssen, 2004; Bouman, 2007). Because crop-allocation decisions are inherently multi-criteria, balancing yield potential, water requirements, surface/groundwater access, rainfall and climate, mechanization, and salinity/quality risks, multi-criteria decision analysis (MCDA) has gained systematic traction, moving from qualitative judgments to defensible quantitative rankings (Chen et al., 2010; Malczewski, 2006; Mendoza & Martins, 2006). Methodologically, newer MCDM[1] formulations can enhance the robustness of provincial rankings; the Opportunity-Loss–Polar-Distance framework (OPLO–POCOD) has shown competitive performance relative to established methods (Sheikh & Senfi, 2024). Given Iran's pronounced climatic heterogeneity, ranging from arid to semi-arid zones to humid temperate regions, substantial spatial variability in irrigation-based crop suitability is expected, motivating the development of province-level rankings supported by integrative decision frameworks.

Illustratively, One study developed a spatial MCDA for rainfed wheat in Kurdistan Province, delineating homogeneous zones with comparable yield potential. Phenological timing (germination, flowering, and grain filling) was determined using growing-degree-days. Four primary criteria (rainfall, temperature, soil, and topography) and 20 sub-criteria were selected based on literature and expert judgment. Factor weights were assigned using fuzzy AHP, and aggregation was performed through a weighted linear combination. Suitability classes followed the FAO scheme (S1, S2, S3, N1, N2), with spatial shares of ~1.2% (S1), 37.8% (S2), 24.7% (S3), 19.2% (N1), and 4.4% (N2). Validation against 2018–2019 to 2020–2021 farm data showed a ratio of observed-to-potential yield of ~75% in S1 and 20% in N2, with a correlation of 0.94 between the computed potential and observed yields. These results highlight the value of spatial MCDA for precision agriculture, crop planning, risk transfer (e.g., insurance), and sustainable water management under scarcity (Pooya et al., 2025).

In another study, researchers prioritized the sustainability of rice cultivation in three provinces, Mazandaran, Fars, and Khuzestan, using an integrated approach. Eco-efficiency was defined as the ratio of "net income" to "environmental burden" per hectare, combined with the

[1] Multi-criteria decision making

Best–Worst Method to weight criteria across energy, labor, economic, and environmental dimensions. The methodological framework applied a life cycle assessment (LCA) that covered the entire process, from land preparation to harvest. Emissions were separated into foreground and background categories and quantified using the Ecoinvent 3.5 and Agri-footprint 5.0 databases, with the IMPACT World+ method implemented in SimaPro software (Alijani et al., 2025). Regarding energy flows, total energy consumption was approximately 9,018,689,923 and 97,549 MJ per hectare in Mazandaran, Fars, and Khuzestan, respectively. Diesel fuel accounted for more than half of the total energy use across all regions, followed by irrigation water. Economically, Mazandaran achieved the highest gross production value, net income, and benefit–cost ratio. Eco-efficiency results similarly placed Mazandaran first (~8,988 USD per environmental burden unit), followed by Fars and Khuzestan. Final Best–Worst rankings indicated that economic (≈0.33) and environmental (≈0.31) criteria carried the most significant weight, yielding composite scores of 0.98, 0.93, and 0.85 for Mazandaran, Fars, and Khuzestan, respectively. The study concludes that all three regions suffer from energy inefficiencies; however, Mazandaran demonstrates superior energy efficiency, reduced losses, and higher profitability, though at the cost of a greater environmental burden. This misalignment underscores the need for targeted management interventions.

In a study aimed at providing a comprehensive overview of potato-producing provinces in Iran, They used efficiency as the first step toward sustainability, applying Data Envelopment Analysis (DEA) for ranking and TOPSIS for integrating results for the 2018 cropping year. In this framework, “yield” and “gross profit” were selected as indicators of production and profitability. Findings showed that when “gross profit” was used as the output, mean technical, pure, and scale efficiencies were lower compared to when “yield” served as the output. Results also indicated that different DEA models produced varying rankings, underscoring the need for multi-model integration to achieve more accurate assessments. In the final integrated ranking, Mazandaran, Kerman, and West Azerbaijan consistently ranked among the top provinces under both output measures, serving as benchmarks for improving efficiency. Correlation analysis revealed negative relationships between efficiency scores (under both outputs) and the use of seed, potash fertilizer, and pesticides, suggesting that biofertilizers and integrated pest management are preferable alternatives. Notably, several major producers, Hamedan, Ardabil, Isfahan, South Kerman, Fars, and Kurdistan, did not rank highly in efficiency. This indicates that producers in these provinces have prioritized higher yields over profitability, highlighting the necessity of cost management and input-use optimization to enhance sustainability (Esfahani & Barikani, 2022).

In another study analyzing environmental management strategies in Iran’s agricultural sector, applied the Analytic Hierarchy Process (AHP) with input from 117 managers, experts, and researchers to compare three management paradigms: Frontier Economics, Eco-development, and Deep Ecology. The findings revealed that formal managers preferred the Frontier Economics paradigm and independent reactive strategies. At the same time, researchers and the private sector leaned toward Eco-development, and environmental specialists favored Deep Ecology. The study emphasized the need to align paradigms with practical strategies to ensure more sustainable management of natural resources and the environment. Recent research also highlights climate variables as key drivers of variability in irrigated crop yields across Iran. Wheat yields peak in provinces with cold winters, where the seasonal mean temperatures range between –3.5 and 0.98 °C, reaching up to 3.88 t/ha under irrigation (Ebrahimi Sirizi et al., 2023). By contrast, spring rainfall exceeding 153 mm is identified as the main factor driving higher barley yields (Kheyruri et al., 2024). Areas with high evaporation (>227 mm), especially in southeastern Iran, are largely unsuitable for barley

and lentil cultivation. Sugar beet demonstrates strong adaptation to moderate temperatures and adequate relative humidity; in land suitability assessments in Fars Province, some physiographic units were classified as highly suitable (S1) under qualitative evaluation methods (Azadi & Baghernejad, 2018).

Agro-climatic zoning studies further underscore the substantial spatial variability of crop potential. In Kermanshah Province, a GIS-based multi-criteria analysis using the Analytic Hierarchy Process (AHP) identified elevation, precipitation, slope, and crop water requirement as the principal determinants of sugar beet suitability, and classified the province into four classes: high potential, moderate potential, low potential, and non-potential (Parmah & Negaresh, 2014). Similar climate-driven patterns have been reported at the national scale for wheat; the impacts of climate change on irrigated wheat differ significantly between arid and semi-arid provinces, with limited temporal adaptation and higher vulnerability of irrigated wheat in arid regions to warming and reduced rainfall (Pakrooh & Kamal, 2023). Efficiency studies provide additional insight into provincial disparities. Using Stochastic Frontier Analysis, estimated technical, allocative (price), and economic efficiencies for irrigated wheat across 27 provinces at 69%, 63%, and 45%, respectively, indicating substantial scope for policy and technological interventions. A separate econometric analysis in the three Khorasan provinces found constant returns to scale for wheat and barley, while sugar beet in South Khorasan exhibited decreasing returns, highlighting the need for localized production planning (Koopahi et al., 2008).

Within agriculture, MCDM techniques have been applied to both production optimization and resource prioritization. In Mazandaran, linear programming under land and profitability constraints identified wheat, barley, and sugar beet as components of an export-oriented optimal cropping pattern (Moazzez & Habibi, 2014). Integrated GIS–MCDM frameworks have been utilized for siting renewable energy sources, demonstrating methodological versatility. Despite their utility, conventional MCDMs face two common limitations that the recently proposed OPLO–POCOD approach addresses (Zandi & Lotfata, 2025). High water use and low productivity remain significant challenges in Iran; MCDM models that jointly consider climatic, edaphic, and topographic indicators can identify optimal cultivation zones, selecting provinces with lower water requirements and higher yields, thereby reducing misallocation and pressure on water resources (Rashidi & Sharifian, 2022; Radmehr et al., 2022). Avoiding cultivation on unsuitable lands also mitigates risks such as soil salinization, groundwater decline, and biodiversity loss, as corroborated internationally (Abuzaid et al., 2025; Gurara, 2020) while enabling the use of underutilized lands and more balanced spatial opportunities (Nabiollahi et al., 2024).

This study integrates various criteria, including yield, crop water requirement, agricultural water use, mean precipitation, mechanization capacity, and productivity, to assess provincial suitability for three strategically important irrigated crops wheat, barley, and sugar beet and to derive a province-level ranking relative to current sown-area rankings. We employ the OPLO–POCOD MCDM framework. The contribution lies in applying this recent MCDM to rank Iranian provinces by crop suitability and directly comparing the outputs with the existing pattern to reveal gaps and recommend cropping pattern adjustments, ultimately identifying provincial comparative advantages for the target crops.

## Method

### Study Area

Iran lies at the junction of the Iranian Plateau and the broader Middle East in Southwest Asia. Its climate is predominantly arid to semi-arid, with hot, dry summers and cold winters across the interior, except along the Caspian littoral and parts of the west. Seasonally, most precipitation occurs from November to May, with a dry period from June to October. Long-term mean annual rainfall is reported at roughly 240–250 mm nationwide, with a steep spatial gradient from <100 mm in central/eastern deserts (Lut) to >1,000 mm on the Caspian plain and windward Alborz slopes (exceeding 1,500–1,800 mm at some stations). Century-scale time series indicate means near 228–246 mm.

In this study, Iran is analyzed at the provincial scale for three strategic irrigated crops: wheat, barley, and sugar beet. Wheat yield is evaluated across 31 provinces, while sugar beet and barley yields are evaluated across 23 and 31 provinces, respectively. Yield (t $ha^{-1}$) and related data were sourced from the Ministry of Agriculture Jihad. Given water and land-use constraints, a multi-criteria decision-making (MCDM) framework is employed to rank provinces for irrigated cultivation based on key indicators: yield per hectare, crop water use, mean precipitation, agricultural water availability, mechanization, and water productivity (yield per unit water). Fig. 1 shows the provincial map of Iran.

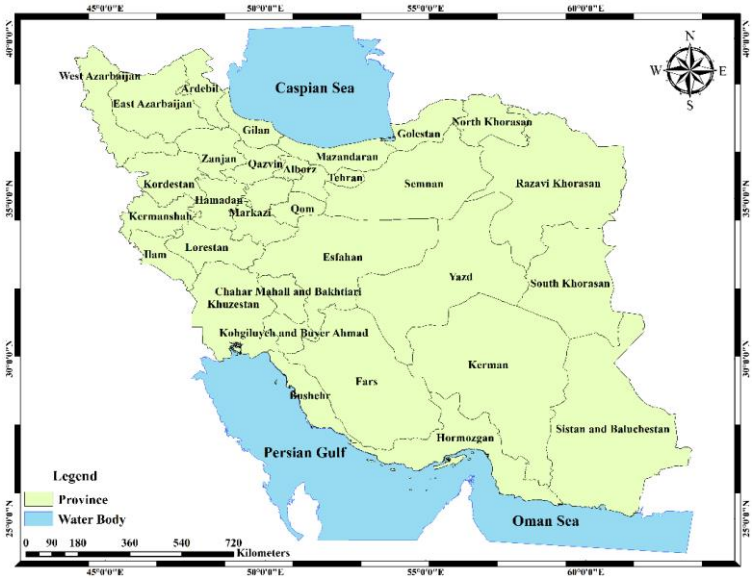


**Figure 1. Location pf Provinces in Iran**

Multi-Criteria Decision-Making (MCDM) methods are recognized as effective tools for addressing complex problems that require the simultaneous consideration of multiple criteria. Their main advantage lies in enabling the evaluation of various alternatives based on a diverse set of indicators. By providing a structured framework for comparing operational objectives through the assessment of different criteria, these approaches facilitate the ranking process and support the selection of the most suitable option among a range of alternatives.

### Opportunity Loss Technique Based on Polar Coordinate Distance

The Opportunity Loss Technique, based on polar coordinate distance, is a key concept in economics and management, serving as a foundation for assessing the value of information.

First introduced by Sheikh and Senfi in 2024, this approach builds on the core idea of opportunity loss. By calculating the degree of loss associated with each alternative, it compares the condition of that alternative with the optimal state using distance measures in polar coordinate space.

## Steps of the OPLO–POCOD Approach

The calculation steps of this method are explained as follows.

Step 1: Construction of the initial decision matrix

The initial decision matrix *A*, comprising m alternatives and n criteria, is formed based on the data and information collected from the decision-makers.

$$X=\begin{bmatrix} x_{11} & \cdots & x_{1j} & \cdots & x_{1n} \\ \vdots & \ddots & \vdots & \ddots & \vdots \\ x_{i1} & \cdots & x_{ij} & \cdots & x_{in} \\ \vdots & \ddots & \vdots & \ddots & \vdots \\ x_{m1} & \cdots & x_{mj} & \cdots & x_{mn} \end{bmatrix}_{m\times n} , \quad i=1 \text{ to } m ; \quad j=1 \text{ to } n. \tag{1}$$

Step 2: Normalization

For data normalization, the following formula is applied, utilizing logarithmic normalization with linear scaling.

$$N_{ij}=\frac{\log_{10}(x_{ij})-\log_{10}(\min_i x_{ij})}{\log_{10}(\max_i x_{ij})-\log_{10}(\min_i x_{ij})}\times 0.9+0.1 \tag{2}$$

In the above formula, *i* and *j* represent the alternative number and the criterion number, respectively. Moreover, the *max* and *min* of each criterion correspond to the highest and lowest values of that criterion across all alternatives. Finally, the output of the formula, applied independently to all criteria, falls within the range of 0.1 to 1.

$$n_{ij}=\frac{X_{ij}}{\sum_{i=1}^{m} X_{ij}} \quad \text{Benefit-Nature}$$

$$n_{ij}=\frac{1/X_{ij}}{\sum_{i=1}^{m} 1/X_{ij}} \quad \text{Cost-Nature}$$

Step 3: Construction of the Opportunity Loss Matrix

In this step, the opportunity loss of each alternative is calculated for all criteria. The calculation is based on the difference between each value in a column and the maximum value of that column (if the criterion has a positive or benefit nature), and the difference between each value in a column and the minimum value of that column (if the criterion has a negative or cost nature).

$$X=\begin{matrix} c_1 & c_j & c_n \\ \end{matrix}\begin{bmatrix} x_{11} & \cdots & x_{1j} & \cdots & x_{1n} \\ \vdots & \ddots & \vdots & \ddots & \vdots \\ x_{i1} & \cdots & x_{ij} & \cdots & x_{in} \\ \vdots & \ddots & \vdots & \ddots & \vdots \\ x_{m1} & \cdots & x_{mj} & \cdots & x_{mn} \end{bmatrix}_{m\times n}, \quad i=1 \text{ to } m \text{ ; } j=1 \text{ to } n. \tag{3}$$

$$\begin{matrix} x_{i1}^* & x_{ij}^* & x_{in}^* \end{matrix}$$

The best value is achieved by maximizing the benefit criteria and minimizing the cost criteria.

$$X=\begin{matrix} c_1 & c_j & c_n \\ \end{matrix}\begin{bmatrix} x_{11-x_1^*} & \cdots & x_{1j-x_j^*} & \cdots & x_{1n-x_n^*} \\ \vdots & \ddots & \vdots & \ddots & \vdots \\ x_{i1-x_1^*} & \cdots & x_{ij-x_j^*} & \cdots & x_{in-x_n^*} \\ \vdots & \ddots & \vdots & \ddots & \vdots \\ x_{m1-x_1^*} & \cdots & x_{mj-x_j^*} & \cdots & x_{mn-x_n^*} \end{bmatrix}_{m\times n}, \quad i=1 \text{ to } m \text{ ; } \quad j=1 \text{ to } n. \tag{4}$$

$$\text{Opportunity Loss (opl)}=\left|x_{ij}-x_{best}\right| \quad \text{for } \forall\, x_{ij} \quad i=1 \text{ to } m; \quad j=1 \text{ to } n. \tag{5}$$

Based on Equations (3) to (5), the matrix is constructed using the obtained opportunity losses.

$$OPL=\begin{matrix} c_1 & c_j & c_n \\ \end{matrix}\begin{bmatrix} opl_{11} & \cdots & opl_{1j} & \cdots & opl_{1n} \\ \vdots & \ddots & \vdots & \ddots & \vdots \\ opl_{i1} & \cdots & opl_{ij} & \cdots & opl_{in} \\ \vdots & \ddots & \vdots & \ddots & \vdots \\ opl_{m1} & \cdots & opl_{mj} & \cdots & opl_{mn} \end{bmatrix}_{m\times n}, \quad i=1 \text{ to } m \text{ ; } j=1 \text{ to } n. \tag{6}$$

Step 4: Construction of the Ordered-Pair Matrix

The ordered-pair matrix is created by combining the elements of the initial decision matrix and the opportunity loss matrix.

$$X_{pair_{ij}}=(x_{ij}, OPL_{ij}), \quad i=1 \text{ to } m ; \quad j=1 \text{ to } n$$

$$X_{pair}=\begin{bmatrix} (x_{11}, opl_{11}) & \cdots & (x_{1j}, opl_{1j}) & \cdots & (x_{1n}, opl_{1n}) \\ \vdots & \ddots & \vdots & \ddots & \vdots \\ (x_{i1}, opl_{i1}) & \cdots & (x_{ij}, opl_{ij}) & \cdots & (x_{in}, opl_{in}) \\ \vdots & \ddots & \vdots & \ddots & \vdots \\ (x_{m1}, opl_{m1}) & \cdots & (x_{mj}, opl_{mj}) & \cdots & (x_{mn}, opl_{mn}) \end{bmatrix}_{m\times n} \quad i=1 \text{ to } m ; \quad j=1 \text{ to } n. \tag{7}$$

Step 5: Construction of the Distance Matrix in Polar Space

In this step, the distance of each alternative from the best value of the same criterion is calculated. For this purpose, each alternative is represented as $(x_{ij}, opl_{ij})$, while the best value of the corresponding criterion is denoted as $(x_{best}, opl_{x_{best}})$. It should be noted that the opportunity loss for the best value is always equal to zero. The distance between these two points in the coordinate space is then computed using the following formula:

$$d_{ij}=\sqrt{A_{ij}^2+B_{ij}^2-2A_{ij}B_{ij}\cos(\theta_2-\theta_1)},$$

$$A = (x_{ij}, opl_{ij}) \text{ and } B = (x_{best}, opl_{x_{best}}) \text{ and } (A, \theta_1) \text{ and } (B, \theta_2). \tag{8}$$

$$A.B = \| A \| \| B \| \cos\theta \tag{9}$$

The cosine of the angle between the two vectors is also obtained from Equation (9).

$$\cos(\theta_2-\theta_1)=\frac{A.B}{\|A\| \|B\|}=\frac{\sum_{i=1}^{n} A_i B_i}{\sqrt{\sum_{i=1}^{n} A_i^2}\sqrt{\sum_{i=1}^{n} B_i^2}} \tag{10}$$

Finally, based on the obtained values, the distance matrix **D** is constructed.

$$D=\begin{bmatrix} d_{11} & \cdots & d_{1j} & \cdots & d_{1n} \\ \vdots & \ddots & \vdots & \ddots & \vdots \\ d_{i1} & \cdots & d_{ij} & \cdots & d_{in} \\ \vdots & \ddots & \vdots & \ddots & \vdots \\ d_{m1} & \cdots & d_{mj} & \cdots & d_{mn} \end{bmatrix}_{m\times n} \quad , \quad i=1 \text{ to } m ; \quad j=1 \text{ to } n. \tag{11}$$

Step 6: Construction of the Weighted Distance Matrix

$$\bar{d}_{ij} = w_j * d_{ij} \tag{12}$$

$$D_w=\begin{bmatrix} \bar{d}_{11} & \cdots & \bar{d}_{1j} & \cdots & \bar{d}_{1n} \\ \vdots & \ddots & \vdots & \ddots & \vdots \\ \bar{d}_{i1} & \cdots & \bar{d}_{ij} & \cdots & \bar{d}_{in} \\ \vdots & \ddots & \vdots & \ddots & \vdots \\ \bar{d}_{m1} & \cdots & \bar{d}_{mj} & \cdots & \bar{d}_{mn} \end{bmatrix}_{m\times n} \quad , \quad i=1 \text{ to } m ; \quad j=1 \text{ to } n. \tag{13}$$

Step 7: Calculation of the Total Distance for Each Alternative

$$S_i=\sum_{j=1}^{n} \bar{d}_{ij} \ , \ i=1 \text{ to } m. \tag{14}$$

$$S_T=\sum_{i=1}^{m} S_i \tag{15}$$

Step 8: Calculation of the Degree of Opportunity Loss (DOL) and the Percentage of Opportunity Achieved (POA)

$$(DOL_i)=\frac{S_i}{S_T}, \tag{16}$$

In this relation:

$$\sum_{i=1}^{m} DOL_i =1.$$

$$(POA_i)=1\text{-}DOL_i. \tag{17}$$

Step 9: Ranking of Alternatives

It should be noted that the value of DOL always lies within the range of 0 to 1. A value of zero indicates that the alternative has achieved the best performance across all criteria and has incurred no opportunity loss. The closer this value is to zero, the fewer the opportunity losses and, consequently, the higher the relative ranking of that alternative compared with others. In contrast, the POL index behaves inversely: values closer to 100 reflect greater success and higher utilization of available opportunities. To determine the weights of the criteria within the OPLO–POCOD framework, a structured expert elicitation process was conducted, fully aligned with the computational components of the method (opportunity loss matrices, polar distances, and weighted aggregation). Six criteria, including yield per hectare, water consumption, mean

precipitation, available agricultural water, mechanization, and water productivity (output per unit of water), were defined operationally and categorized by effect type (benefit/cost) for expert evaluation. Each expert then assigned a score between 0 and 100 to represent the marginal effect of moving from the worst to the best state of each criterion (without pairwise comparisons). Scores were normalized at the individual level (divided by each expert's total score) and then aggregated by calculating the mean of the normalized values. To mitigate the influence of extreme judgments, a 5% trimmed mean was applied, along with content-based constraints relevant to irrigated cropping. Specifically, the weight of available water was set higher than that of other factors, while precipitation and mechanization were assigned lower weights, given their secondary role in irrigation systems.

After normalization, the final weights were: available agricultural water = 0.30, yield = 0.20, water consumption = 0.20, water productivity = 0.20, precipitation = 0.05, and mechanization = 0.05. These weights were directly incorporated into the construction of the weighted distance matrix in the OPLO–POCOD method. Subsequently, weighted polar distances, Degree of Opportunity Loss (DOL), and Percentage of Opportunity Achieved (POA/POL) were computed for each alternative. The resulting weights for each indicator, derived through the integrated OPLO–POCOD approach, are presented in Table 1.

**Table 1. Weights of the criteria derived using the integrated OPLO–POCOD method**

| Criterion | Weight |
|---|---|
| Yield Per Hectare | 0.2 |
| Water consumption | 0.2 |
| Mean precipitation | 0.05 |
| Available agricultural water | 0.3 |
| Mechanization | 0.05 |
| Water productivity | 0.2 |

## Results

### Comprehensive Ranking Analysis Based on Multi-Criteria Decision-Making for Sugar Beet Cultivation in the Provinces of Iran

In this study, the performance of 23 provinces in Iran during the 2022–2023 agricultural year was evaluated for sugar beet cultivation, using the most recent official data released by the Ministry of Jihad Agriculture in September 2024. Based on key indicators such as water consumption, precipitation, agricultural mechanization ratio, and product price, the final ranking of provinces was determined through the OPLO–POCOD multi-criteria decision-making technique. The results revealed substantial differences in agricultural capacity across provinces.

Khuzestan (Rank 1) was placed at the top with a significant margin. Its remarkably low water consumption per hectare, high availability of agricultural water resources, and favorable productivity provided optimal conditions for sugar beet cultivation, despite its relatively weak mechanization ratio. Razavi Khorasan (Rank 2) and Kermanshah (Rank 3) also ranked highly

due to balanced performance across multiple indicators, reflecting minimal opportunity losses. Provinces such as Fars, West Azerbaijan, Golestan, and Mazandaran followed, indicating considerable potential, although they often faced challenges in sub-indicators, such as the availability of agricultural water. At the other end, Ardabil (Rank 23) exhibited the highest opportunity loss, performing poorly in terms of productivity and yield per hectare, despite relatively low water consumption, making it the least suitable province. East Azerbaijan, Lorestan, and North Khorasan also ranked low. Notably, provinces such as Semnan and Alborz, although among the best in yield per hectare, were classified in mid-level rankings due to limitations in available agricultural water, average precipitation, and water consumption per hectare. Fig. 2 illustrates the applied indicators and their respective weights for sugar beet in each province.

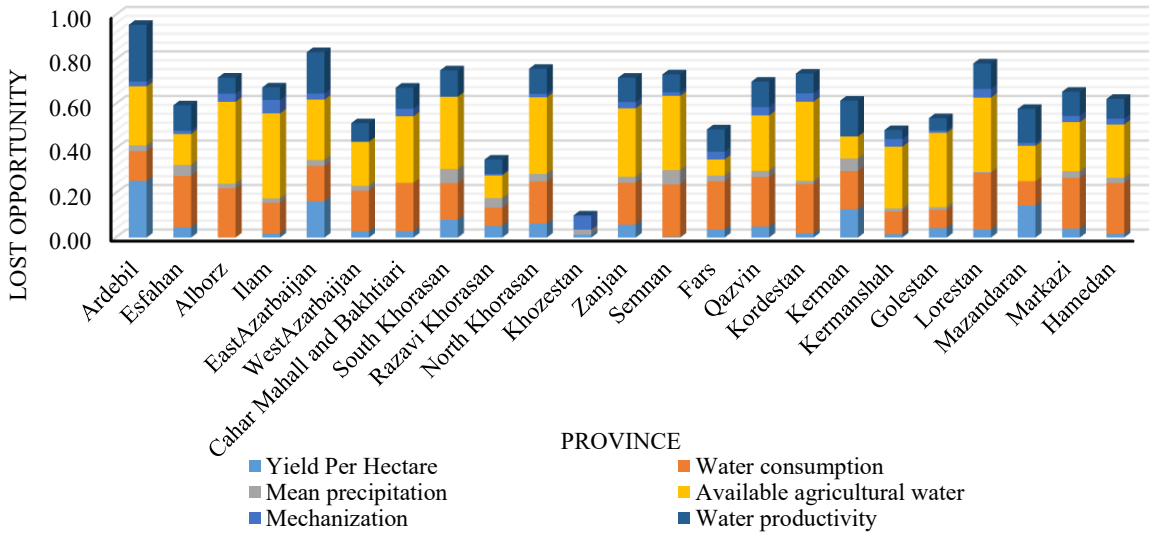


**Figure 2. Applied indicators and their weights in each province for sugar beet cultivation**

## Ranking Based on the Current Cultivated Area of Sugar Beet in the Provinces of Iran

The ranking of Iranian provinces based on the current cultivated area of sugar beet shows that West Azerbaijan ranks first with 27,907 hectares. Razavi Khorasan (20,536 ha) and Khuzestan (17,962 ha) follow in second and third place, respectively. These three provinces account for the largest cultivated areas of sugar beet in the country. Next in rank are Fars (8,777 ha), North Khorasan (2,141 ha), Golestan (2,042 ha), and Isfahan (1,831 ha). Provinces such as Semnan (1,797 ha), Ardabil (1,611 ha), Chaharmahal and Bakhtiari (1,563 ha), Kurdistan (1,389 ha), and Markazi (1,016 ha) fall within the mid-level group (Ministry of Agriculture Jihad Statistical Yearbook, 2024).

Conversely, several provinces have very limited cultivation areas. Qazvin (554 ha), Ilam (496 ha), and South Khorasan (480 ha) belong to the low-cultivation group. Moreover, Mazandaran, East Azerbaijan, Alborz, Zanjan, and Kerman each report an area of less than 100 hectares, with Kerman recording the lowest area at only 3 hectares. Accordingly, provinces can be grouped into three categories: (1) high cultivation (>10,000 ha), represented by West Azerbaijan, Razavi Khorasan, Khuzestan, and Kermanshah; (2) medium cultivation (1,000–10,000 ha), including provinces such as Fars, Golestan, and North Khorasan; and (3) low cultivation (<1,000 ha), which comprises a considerable number of provinces. Fig. 3 presents

the ranking of provinces by sugar beet cultivated area, based on the OPLO–POCOD method, using the cultivated area (hectares) as the input variable.

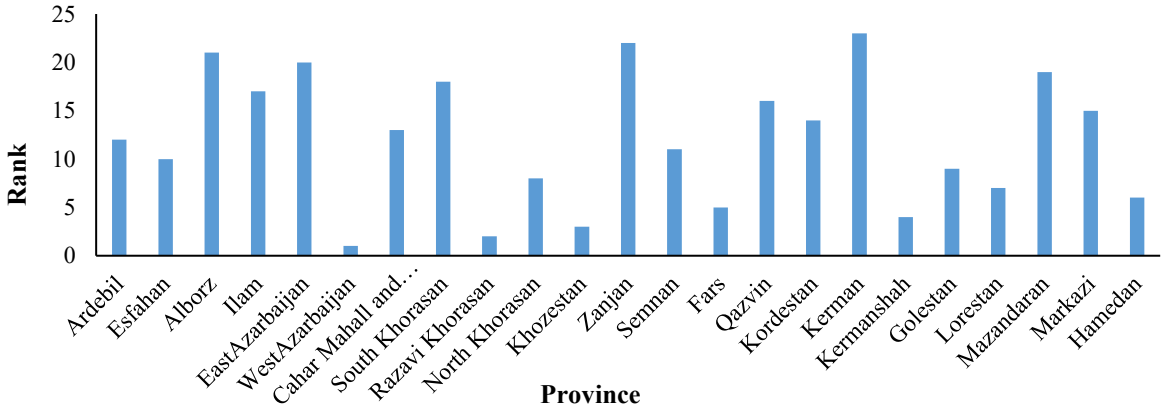


**Figure 3. Ranking of Provinces by Sugar Beet Cultivated Area**

The subsequent step involved comparing the ranking based on the actual cultivated area of provinces with the ranking derived from the OPLO–POCOD multi-criteria decision-making method. This comparison provides a clearer understanding of the degree of alignment between the current distribution of sugar beet cultivation and the actual desirability of provinces in terms of performance indicators.

The results showed that some provinces, such as Fars, Razavi Khorasan, Golestan, and Lorestan, occupy relatively similar positions in both rankings. For instance, Fars ranked fourth in both systems. At the same time, Razavi Khorasan held second place in both OPLO–POCOD and cultivated-area rankings, indicating a degree of alignment between current practices and optimal conditions. Conversely, Khuzestan ranked first under the OPLO–POCOD method but only third in cultivated area. This discrepancy suggests that, despite its strong potential, the province has not yet fully utilized its capacity. Similarly, Kermanshah ranked third in the OPLO–POCOD evaluation but nineteenth in terms of cultivated area, reflecting a significant mismatch between suitability and current cropping patterns. West Azerbaijan, ranked first by cultivated area, fell to fifth in the OPLO–POCOD ranking, demonstrating that extensive cultivation does not necessarily equate to optimal suitability. Other provinces, such as Ardabil, East Azerbaijan, and North Khorasan, ranked low in the OPLO–POCOD results but significantly higher in cultivated area. For example, North Khorasan placed fifth in cultivated area but only twentieth in OPLO–POCOD. Provinces like Alborz and Semnan, by contrast, ranked mid-to-low in both systems, a reflection of relatively good yield per hectare offset by severe constraints in water availability and precipitation.

## Comprehensive Ranking Analysis Based on Multi-Criteria Decision-Making for Irrigated Wheat Cultivation in the Provinces of Iran

The final results indicate substantial structural and ecological differences among provinces in terms of suitability for irrigated wheat cultivation. In the overall ranking, Mazandaran secured first place with a clear margin. Despite only moderate performance on some indicators, this province achieved the lowest opportunity loss, the lowest water consumption, and favorable rainfall conditions, making it the most suitable region for wheat cultivation in Iran. Following Mazandaran, the provinces of Fars (Rank 2), Kermanshah (3), Gilan (4), and West Azerbaijan (5) were placed at the top. These provinces generally exhibited strong performance in indicators

such as yield per hectare, water productivity, and efficient resource use. Within the top ten provinces, a clear geographical pattern emerged: most are located in northern, western, and southern regions, reflecting the influence of relatively wetter climates or better access to water resources compared with other areas. For example, Khuzestan, despite having a lower yield per hectare, ranked 11th due to its high agricultural water availability and favorable water consumption per hectare. Provinces such as Isfahan, Ardabil, and Tehran also ranked relatively high, driven by balanced performance across multiple indicators.

By contrast, South Khorasan (Rank 31), Bushehr (30), Hormozgan (29), and Sistan and Baluchestan (28) occupied the lowest positions. Although some of these provinces benefit from relatively acceptable water availability or water consumption per hectare, they suffer from low productivity and weak yield per unit area. This highlights the greater opportunity losses and unsuitability of provinces located in arid southern regions. Fig. 4 illustrates the applied indicators and their respective weights for wheat in each province.

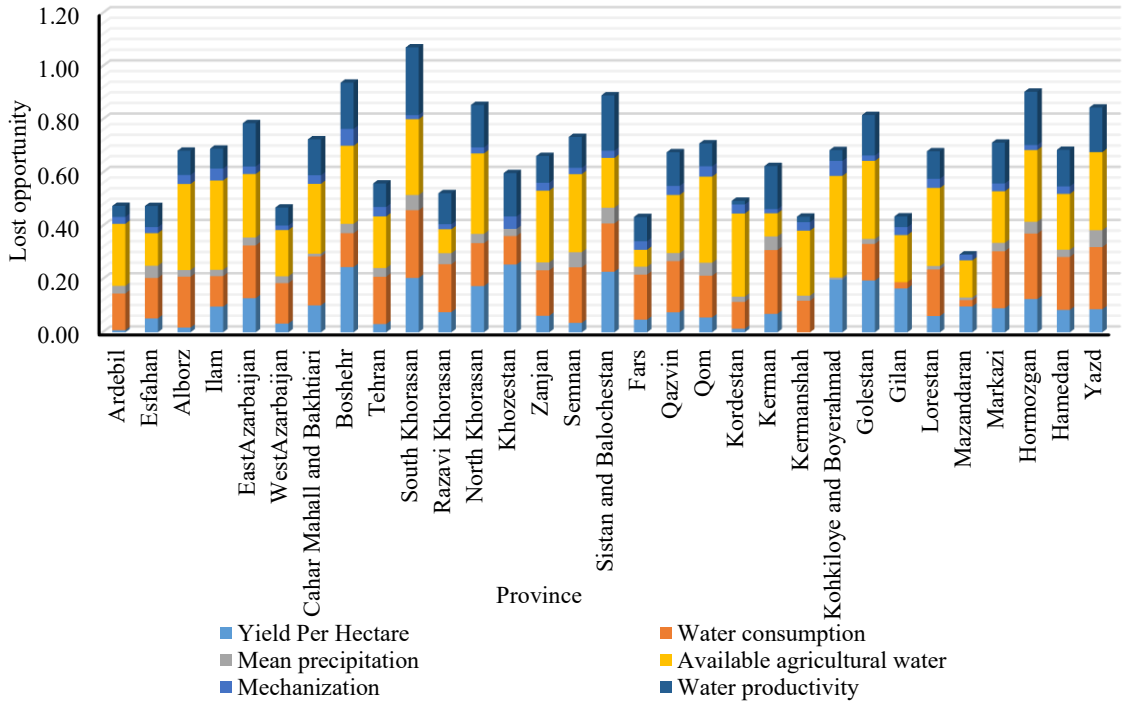


**Figure 4. Applied indicators and their weights in each province for irrigated wheat cultivation**

## Ranking Based on the Current Cultivated Area of Irrigated Wheat in the Provinces of Iran

The analysis of provincial rankings based on the cultivated area of irrigated wheat reveals that Khuzestan, with 742,101 hectares, holds the first place and is recognized as the country's primary hub of wheat production. It is followed by Fars with 291,407 hectares and Razavi Khorasan with 171,476 hectares, ranking second and third, respectively. These three provinces, far ahead of others, account for the largest share of national wheat production.

Subsequently, Golestan (166,284 ha), West Azerbaijan (135,912 ha), Kerman (129,852 ha), Kermanshah (128,799 ha), and East Azerbaijan (85,269 ha) occupy ranks four through eight, confirming their roles as other key production areas. Ardabil (84,214 ha), Hamedan (84,058 ha), and Sistan and Baluchestan (79,966 ha) are placed ninth to eleventh. On the other hand,

some provinces have extremely limited cultivation. Gilan ranks last (31st) with only 53 hectares under wheat, followed by Qom (5,731 ha), Alborz (9,587 ha), Yazd (14,210 ha), and South Khorasan (17,186 ha).

Accordingly, provinces can be categorized into three groups: (1) high-cultivation provinces (>150,000 ha), including Khuzestan, Fars, Razavi Khorasan, and Golestan, located mainly in the southwest, south, and northeast; (2) medium-cultivation provinces (50,000–150,000 ha), such as West Azerbaijan, Kerman, Kermanshah, East Azerbaijan, Ardabil, Hamedan, Sistan and Baluchestan, Isfahan, Ilam, Qazvin, Lorestan, North Khorasan, Bushehr, and Tehran; and (3) low-cultivation provinces (<50,000 ha), including Kurdistan, Kohgiluyeh and Boyer-Ahmad, Markazi, Mazandaran, Zanjan, Semnan, Hormozgan, Chaharmahal and Bakhtiari, Yazd, South Khorasan, Alborz, Qom, and Gilan. Fig. 5 presents the provincial ranking of irrigated wheat cultivated area, calculated based on hectares of sown land.

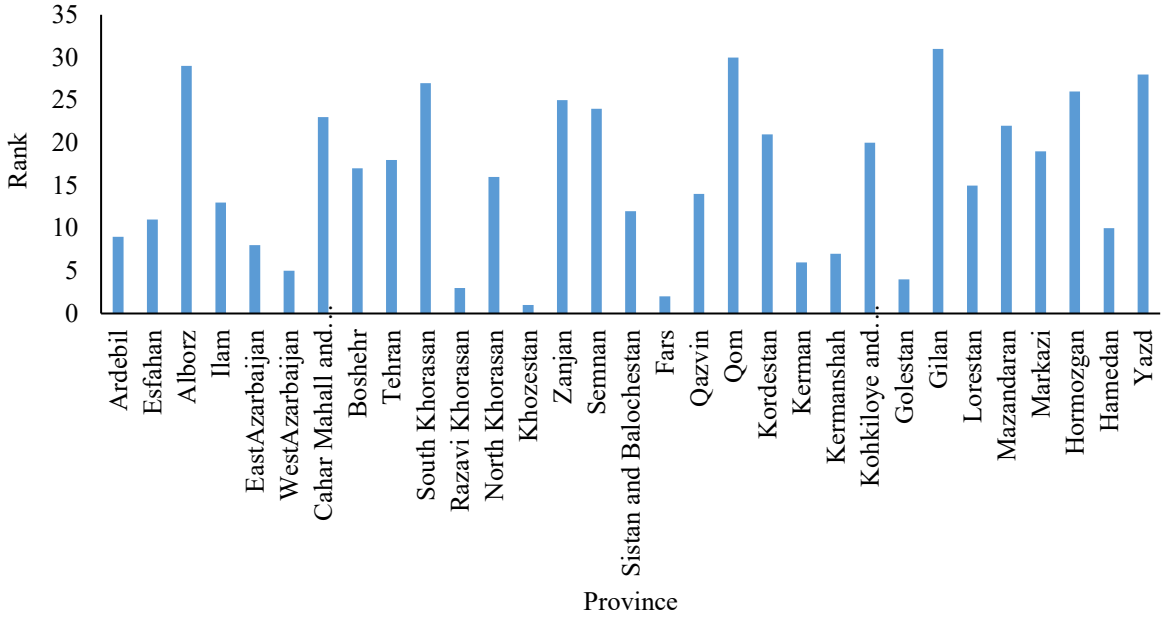


**Figure 5. Ranking of Provinces by Irrigated Wheat Cultivated Area**

From a geographical perspective, provinces with the largest cultivated areas of irrigated wheat are predominantly located in the western, southern, and northeastern regions of Iran. In contrast, provinces with smaller cultivated areas are mostly found in central and northern parts of the country; for example, Gilan, Alborz, Qom, and Yazd, which rank at the bottom of the list, have limited wheat cultivation due to climatic constraints, high population density, restricted arable land, or prioritization of other crops. To assess the degree of alignment between the current distribution of wheat cultivation across provinces and the optimal conditions defined by performance and resource indicators, a comparison was made between the rankings based on actual cultivated area and those derived from the OPLO–POCOD multi-criteria decision-making framework. This comparison provides a clear picture of whether current wheat distribution corresponds with the climatic, water resource, and economic capacities of each province.

The results show that some provinces occupy relatively similar positions in both rankings. For example, West Azerbaijan, ranked fifth by cultivated area, is also among the top provinces in the multi-criteria ranking, indicating that decisions there are fairly aligned with actual

environmental capacities and potential. Similarly, Fars and Kermanshah appear in the upper tier in both rankings, reflecting consistency between cultivated area, climatic suitability, infrastructure, and economic conditions. However, notable discrepancies exist in some provinces. For instance, Sistan and Baluchestan ranks 28th in the multi-criteria evaluation but 12th in cultivated area. This misalignment suggests that cultivation expansion has occurred in ecologically suboptimal conditions, likely driven by regional policies, land availability, or misinformed decisions. Conversely, provinces such as Yazd, Hormozgan, Semnan, and Qom consistently appear at the bottom of both rankings, indicating that limited cultivation corresponds with weak environmental and resource conditions, making wheat production less viable in these areas.

### Comprehensive Ranking Analysis Based on Multi-Criteria Decision-Making for Irrigated Barley Cultivation in the Provinces of Iran

Based on the results of the OPLO–POCOD multi-criteria decision-making method, the suitability of Iranian provinces for irrigated barley cultivation was evaluated. The final assessment was conducted using seven key indicators: yield per hectare, water consumption, agricultural rainfall, available agricultural water, mechanization, water productivity, and opportunity loss. In the overall ranking, Mazandaran achieved first place, earning the highest score across all combined indicators. This province recorded the lowest water consumption per hectare, high productivity, and the least opportunity loss, making it the most suitable region for irrigated barley cultivation. Tehran ranked second, surpassing many central producing provinces due to its balanced performance in terms of yield per hectare and productivity. Fars (Rank 3), Gilan (4), Kurdistan (5), and West Azerbaijan (6) were also among the top ten provinces. The geographical distribution of these leading provinces shows that most are located in the northern and western regions of the country, which benefit from more humid climates or better access to water resources.

At the lower end, provinces such as Kohgiluyeh and Boyer-Ahmad (Rank 31), Hormozgan (30), South Khorasan (29), Bushehr (28), and Sistan and Baluchestan (27) ranked the lowest. Despite relatively strong performances in some indicators, such as mechanization, these provinces performed poorly in terms of yield per hectare and water productivity, coupled with high opportunity loss, resulting in weak final rankings. In the middle of the ranking table, provinces such as Hamedan (Rank 8), Kermanshah (9), Markazi (10), Lorestan (11), Qom (12), and Zanjan (13) demonstrated relatively balanced performance across most indicators. Fig. 6 illustrates the applied indicators and their respective weights for barley in each province.

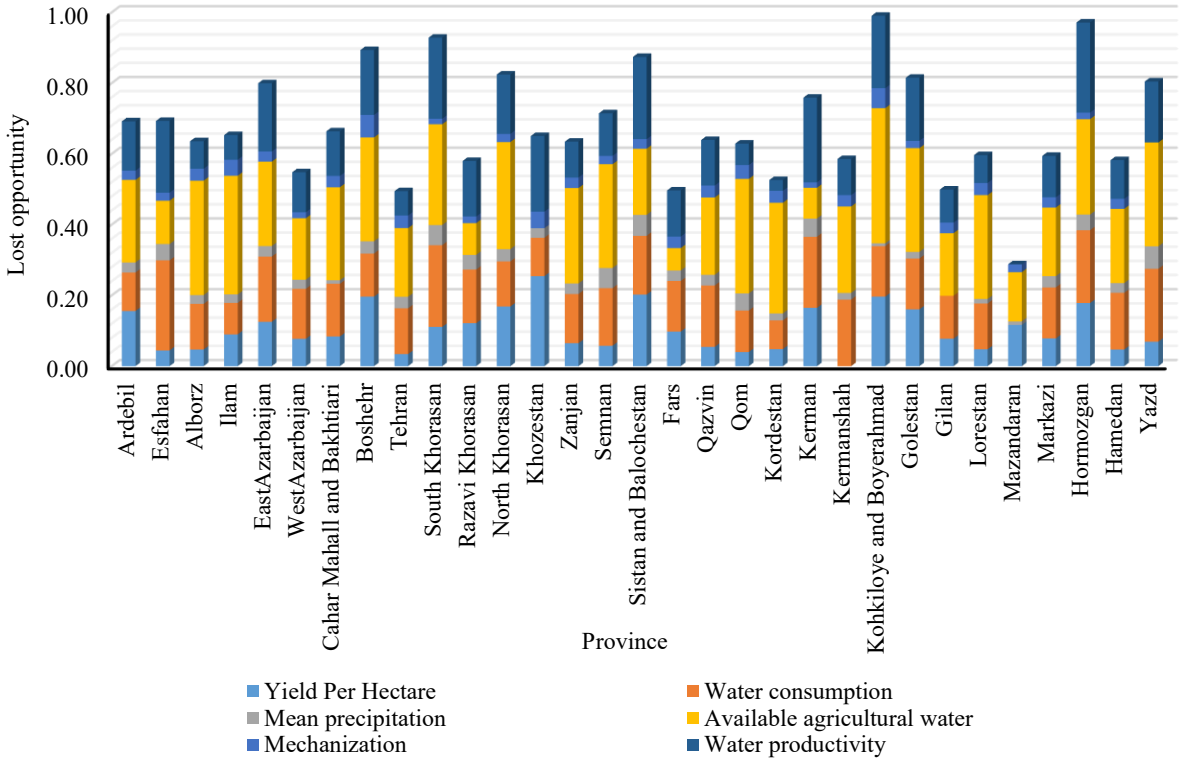


**Figure 6.** Applied indicators and their weights in each province for irrigated barley cultivation

## Ranking Based on the Current Cultivated Area of Irrigated Barley in the Provinces of Iran

Analysis of barley cultivated areas across Iranian provinces shows that Razavi Khorasan ranks first with more than 110,000 hectares, making it the country's primary hub for this crop. Fars follows with 105,000 hectares, while Isfahan ranks third with approximately 59,000 hectares. Provinces such as Hamedan, Markazi, Qazvin, Ardabil, Sistan and Baluchestan, Tehran, and Khuzestan occupy positions 4 through 10, contributing significantly to national barley production.

On the other hand, provinces such as Gilan, Hormozgan, Ilam, Kohgiluyeh and Boyer-Ahmad, Kurdistan, and Yazd account for the lowest cultivated areas. Gilan, with only 28 hectares, ranks last. Based on these findings, provinces can be grouped into three categories: (1) high-cultivation provinces (>50,000 ha), including Razavi Khorasan, Fars, Isfahan, Hamedan, and Markazi, primarily located in the northeast, south, west, and central regions; (2) medium-cultivation provinces (20,000–50,000 ha), including Qazvin, Ardabil, Sistan and Baluchestan, Tehran, Khuzestan, Qom, East Azerbaijan, North Khorasan, Zanjan, Semnan, and Lorestan; and (3) low-cultivation provinces (<20,000 ha), such as West Azerbaijan, Kermanshah, Chaharmahal and Bakhtiari, Golestan, Mazandaran, Kurdistan, Kerman, Yazd, Alborz, Bushehr, Kohgiluyeh and Boyer-Ahmad, Hormozgan, Ilam, and Gilan. Fig. 7 presents the provincial ranking of irrigated barley cultivated area, calculated based on hectares of sown land.

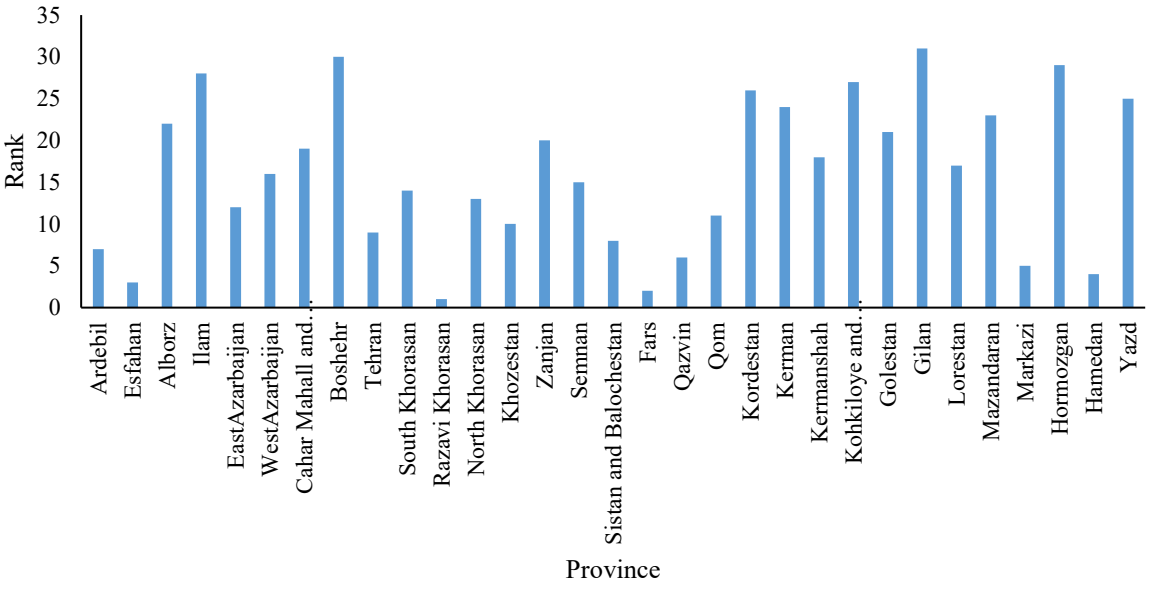


**Figure 7. Ranking of Provinces by Irrigated Barley Cultivated Area**

From a geographical perspective, provinces with large cultivated areas of barley are mainly concentrated in central, western, and northeastern parts of Iran. In contrast, provinces with smaller cultivated areas are located primarily in southern and northern coastal regions.

To evaluate the degree of alignment between the current distribution of barley cultivation and the optimal suitability of provinces based on performance, climatic, and resource indicators, a comparison was made between the rankings derived from actual cultivated area and those obtained using the OPLO–POCOD multi-criteria decision-making method. This comparison provides clearer insights into the consistency or inconsistency of current cropping patterns with the potential capacities of each region. The results show that certain provinces hold relatively similar positions in both rankings. Examples include Hamedan, Yazd, Hormozgan, Qom, Fars, and Chaharmahal and Bakhtiari, which indicate alignment of cultivation decisions with favorable climatic, water resource, and infrastructural conditions. Conversely, notable discrepancies exist in some provinces. For instance, Khuzestan ranks tenth in terms of cultivated area but performs significantly lower in the OPLO–POCOD ranking, suggesting that barley cultivation in this region may not fully align with resource- and indicator-based suitability. Other provinces, such as West Azerbaijan, Qazvin, Kermanshah, South and North Khorasan, Sistan and Baluchestan, Ardabil, and Lorestan, also display wide gaps between their actual cultivated-area ranking and their optimal position in the OPLO–POCOD model, reflecting a relative misalignment between cropping policies and real capacities. Fig.s 8–10 illustrate the comparison between the actual cultivated-area rankings and the OPLO–POCOD rankings for sugar beet, wheat, and barley, respectively.

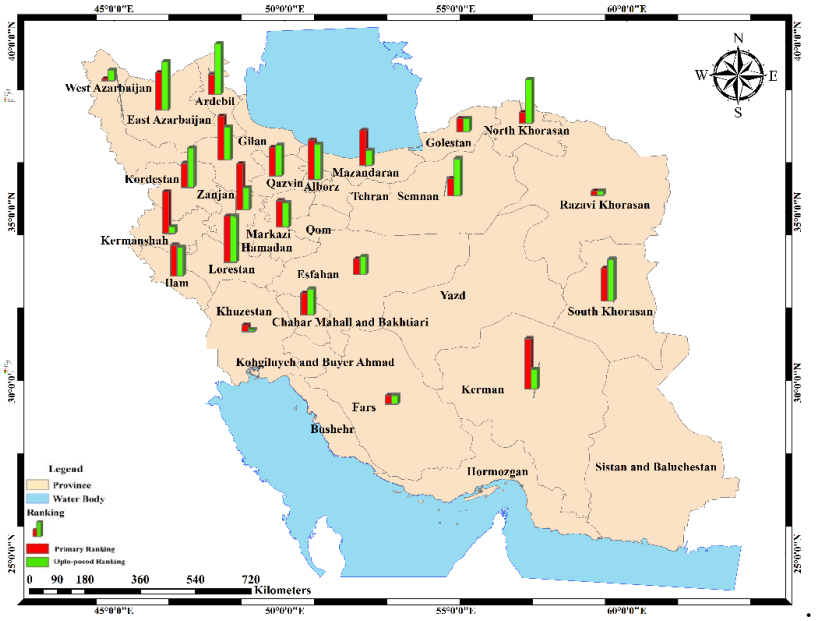


**Figure 8. Comparison of Actual Cultivated-Area Ranking and OPLO–POCOD Ranking by Province (Sugar Beet)**

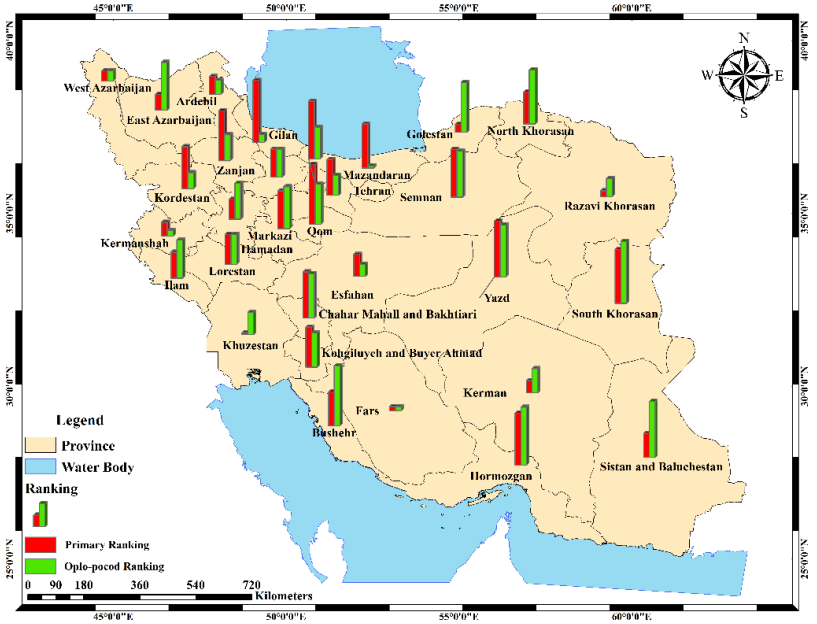


**Figure 9. Comparison of Actual Cultivated-Area Ranking and OPLO–POCOD Ranking by Province (Wheat)**

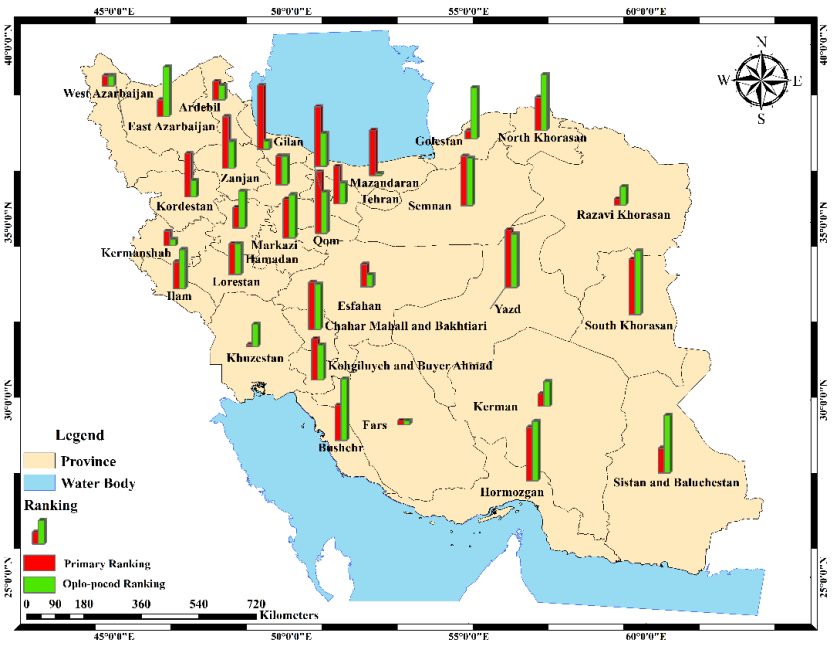


**Figure 10. Comparison of Actual Cultivated-Area Ranking and OPLO–POCOD Ranking by Province (Barley)**

Although the OPLO–POCOD multi-criteria decision-making method highlights provinces such as Mazandaran and Gilan as highly suitable for cultivating sugar beet, wheat, and barley in terms of resource and performance indicators, their actual cultivated area for these crops remains low. This outcome is primarily due to regional agricultural policies, prevailing cropping structures, and specific climatic characteristics. Mazandaran and Gilan are among the few provinces with sufficient climatic and water resources to support rice cultivation, which, given its higher economic value in these areas, has become the dominant crop. As a result, despite favorable potential for wheat and barley, financial priorities and policy choices have limited the exploitation of this capacity. Such cases are exceptional and restricted mainly to provinces with unique climatic advantages or policy-driven mandates, making shifts in their cropping patterns neither feasible nor reasonable in the short term.

The comparative analysis between OPLO–POCOD rankings and actual cultivated-area rankings for sugar beet, wheat, and barley reveals substantial and sometimes stark discrepancies among provinces. These differences underscore the fact that in many regions, the existing cultivated areas are not optimally aligned with climatic, water, and economic conditions. In other words, some provinces possess strong potential but remain underutilized. For example, Khuzestan excels in sugar beet cultivation, while Kermanshah excels in irrigated barley. Others, such as West Azerbaijan, which has high cultivation areas but low suitability scores, demonstrate inefficient resource use and weak agricultural policy frameworks. These mismatches highlight the urgency of revisiting regional cropping policies and resource management strategies to ensure more efficient and productive use of resources.

A major factor contributing to low productivity and excessive water consumption in Iran's agricultural sector, beyond traditional farming practices and outdated technologies, is the mismatch between cropping patterns and the actual ecological and resource capacities of provinces. Results show that in certain high-potential areas, cultivated land remains underutilized, while in unsuitable regions, cultivation is excessive. This misalignment contributes to water overuse and reduced overall efficiency. Optimizing cropping patterns through multi-criteria analysis offers a viable solution for enhancing water use efficiency and agricultural productivity. The OPLO–POCOD approach, in particular, provides an effective

tool to assess the degree of consistency between actual cultivation and provincial potential. Such analyses help identify regions with the most significant mismatches, guiding policymakers to prioritize adjustments in cropping systems and resource allocation. Where discrepancies exist, reforms in agricultural policies and water management are essential to enhance productivity and secure the sustainability of agricultural production.

## Conclusions

Iranian agriculture underpins food security, economic development, and the livelihoods of rural communities. Given the strategic importance of wheat, barley, and sugar beet, a scientific assessment of provincial potential for these crops is essential. In recent years, low efficiency, limited productivity, and mismatches between cultivated areas and actual capacity have led to resource losses, particularly water, and reduced economic returns. This study employed the OPLO–POCOD multi-criteria decision-making approach to evaluate and rank provinces based on their suitability for the three crops. Key indicators included yield per unit area, water consumption per hectare, mean precipitation, agricultural water availability, mechanization capacity, and water productivity per unit area. The indicator values reflect current conditions, which may change over time. Data were obtained from the National Statistics Portal and the Ministry of Agriculture Jihad. Results showed that in many provinces, current cultivation patterns do not align with relative potential; some highly capable provinces contribute little, while others with lower suitability cultivate extensively. Such mismatches contribute to production inefficiencies. By integrating technical, economic, and environmental indicators, MCDM methods provide a more comprehensive and reliable framework for managing scarce land and water resources compared with single-criterion approaches. They also highlight structural inconsistencies between potential and cultivated areas, offering a foundation for optimizing cropping patterns, reducing waste, and enhancing productivity and sustainability, thus serving as a direct tool for policymaking and resource allocation.

For future research, the inclusion of soil quality, long-term climatic trends, market-based economic indicators, and the effects of agricultural support policies is recommended. Remote sensing can improve data accuracy for climate, land use, and water resources, while longer time-series analyses would aid in forecasting future conditions. Comparing different MCDM methods and integrating them with neural networks and multi-objective optimization could further enhance accuracy. Evaluating the impacts of cropping-pattern adjustments, particularly in provinces with significant mismatches, is also essential for guiding policy reforms.

In this study, the OPLO–POCOD framework incorporated expert-derived weights for six indicators: yield, water consumption, precipitation, available water, mechanization, and water productivity to rank provincial suitability for irrigated wheat, barley, and sugar beet. Subsequently, the Degree of Opportunity Loss (DOL) and Percentage of Opportunity Achieved (POA) were calculated, and final rankings were determined by minimizing opportunity loss. The results indicated that Mazandaran leads in irrigated wheat and barley, with northern humid provinces such as Golestan and West Azerbaijan generally ranking higher. In contrast, arid southern provinces (e.g., South Khorasan, Bushehr, Hormozgan, Kohgiluyeh and Boyer-Ahmad) ranked lower. For sugar beet, Khuzestan held the top position. The comparison between potential rankings and actual cultivated areas revealed significant discrepancies. For example, Khuzestan's strong suitability for sugar beet contrasts with its relatively small current share, highlighting opportunities for spatial reallocation of cropping.

***Author Contributions***

Data collection: Sina Khoshnevisan, Mohammadreza Asli Charandabi, Samad Emamgholizadeh.
Research report preparation: Sina Khoshnevisan, Mohammadreza Asli Charandabi.
Data analysis: Sina Khoshnevisan, Tahereh Taghizadeh.
The contribution of authors to the article was approximately as follows:
First Author: Preparation and processing of samples, conducting experiments and data collection, performing calculations, statistical analysis of data, analysis and interpretation of information and results, drafting the manuscript.
Second Author: Research design, supervision of research stages, validation and control of results, revision, review, and finalization of the manuscript.
Third Author: Contribution to research design, supervision of the study, reviewing and revising the manuscript.
Fourth and Fifth Authors: Writing and revising the manuscript, collaboration in data collection.

***Data Availability Statement***

Data available on request from the authors.

***Acknowledgements***

The authors would like to thank all participants in the present study.

The authors thank all participants in this study.

***Ethical Considerations***

The authors ensured that their work was free from data fabrication, falsification, plagiarism, and misconduct.

***Funding***

This research did not receive any specific grant from funding agencies in the public, commercial, or not-for-profit sectors.

***Conflict of Interest***

The authors declare no conflict of interest

## References


Abuzaid, A. S., Abbas, H. H., Mostafa, M. A., El Ghonamy, Y. K., Rebouh, N. Y., & Shokr, M. S. (2025). A comprehensive crop suitability assessment under modern irrigation system in arid croplands. *PLOS ONE*, 20(6), e0326183. https://doi.org/ 10.1371/journal.pone.0326183

Alijani, M., Feizabadi, Y., & Goudarzi, M. (2025). Comparative analysis of paddy cultivation sustainability through integrating eco-efficiency and best–worst method approaches. *Journal of Agriculture and Food Research*, 19, 101479. https://doi.org/10.1016/j.jafr.2024.101479

Azadi, H., & Baghernejad, M. (2018). Qualitative land suitability assessment and estimating land production potential for main irrigated crops in northern Fars province. *Agriculture and Forestry*, 64(4), 237–250. https://doi.org/10.17707/agricultforest.64.4.26

Bouman, B. A. M. (2007). A conceptual framework for the improvement of crop water productivity at different spatial scales. *Agricultural Systems*, 93(1-3), 43–60. https://doi.org/10.1016/j.agsy.2006.04.004

Chen, Y., Yu, J., & Khan, S. (2010). Spatial sensitivity analysis of multi-criteria weights in GIS-based land suitability evaluation. *Environmental Modelling & Software*, 25(12), 1582–1591. https://doi.org/10.1016/j.envsoft.2010.06.001

Daliakopoulos, I. N., Tsanis, I. K., Koutroulis, A., Kourgialas, N. N., Varouchakis, E. A., Karatzas, G. P., & Ritsema, C. J. (2016). The threat of soil salinity: A European review. *Science of the Total Environment*, 573, 727–739. https://doi.org/10.1016/j.scitotenv.2016.08.177

Ebrahimi Sirizi, M., Taghavi Zirvani, E., Esmailzadeh, A., Khosravian, J., Ahmadi, R., Mijani, N., Soltannia, R., & Jokar Arsanjani, J. (2023). A Scenario-Based Multi-Criteria Decision-Making Approach for Allocation of Pistachio Processing Facilities: A Case Study of Zarand, Iran. *Sustainability*, 15(20), 15054. https://doi.org/10.3390/su152015054

Esfahani, S. M. J., & Barikani, E. (2022). Ranking production units by integrating data envelopment analysis and multi-criteria decision-making: The case of potato-producing provinces in Iran. *Iran Agricultural Research*, 41(1), 49–60. https://doi.org/10.22099/iar.2022.42629.1473

Gurara, M. A. (2020). Evaluation of Land Suitability for Irrigation Development and Sustainable Land Management Using ArcGIS on Katar Watershed in Rift Valley Basin, Ethiopia. *Journal of Water Resources and Ocean Science*, 9(3), 56–63. https://doi.org/ 10.11648/j.wros.20200903.11

Kheyruri, Y., Neshat, A., Sharafati, A., & Hameed, A. S. (2024). Identifying the most effective climate parameters on crop yield in rain-fed agriculture and irrigated farming in Iran. *Physics and Chemistry of the Earth*, 103744. https://doi.org/10.1016/j.pce.2024.103744

Konikow, L. F., & Bredehoeft, J. D. (2020). Groundwater Resource Development: Effects and Sustainability. *The Groundwater Project Publications*, Ontario, Canada. https://doi.org/ 10.21083/978-1-7770541-4-4

Koopahi, M., Barikani, S. H. S., Asgari, M., & Shahbazi, H. (2008). Econometric estimates of scale economies in Iranian agriculture (Case study: Three Khorasan provinces). *World Applied Sciences Journal*, 5(3), 340-344 .http://www.idosi.org/wasj/wasj5(3)/12.pdf

Madani, K. (2014). Water management in Iran: What is causing the looming crisis?. *Journal of Environmental Studies and Sciences*, 4(4), 315–328. https://doi.org/10.1007/s13412-014-0182-z

Malczewski, J. (2006). GIS-based multicriteria decision analysis: A survey. International *Journal of Geographical Information Science*, 20(7), 703–726. https://doi.org/10.1080/13658810600661508

Mendoza, G. A., & Martins, H. (2006). Multi-criteria decision analysis in natural resource management: A critical review of methods and new modelling paradigms. *Forest Ecology and Management*, 230(1-3), 1–22. https://doi.org/10.1016/j.foreco.2006.03.023

Moazzez, H., & Habibi, A. (2014). Optimization of agricultural products export with use of linear programming model in Mazandaran province. *Indian Journal of Fundamental and Applied Life Sciences*, 4(S4), 3219-3224. https://www.cibtech.org/sp.ed/jls/2014/04/JLS-380-S4-391-5.pdf

Nabiollahi, K., Kebonye, N. M., Molani, F., Tahari-Mehrjardi, M. H., Taghizadeh-Mehrjardi, R., Shokati, H., & Scholten, T. (2024). Assessment of Land Suitability Potential Using Ensemble Approaches of Advanced Multi-Criteria Decision Models and Machine Learning for Wheat Cultivation. *Remote Sensing*, 16(14), 2566. https://doi.org/10.3390/rs16142566

Pakrooh, P., & Kamal, M. A. (2023). Modeling the potential impacts of climate change on wheat yield in Iran: Evidence from national and provincial data analysis. *Ecological Modelling*, 110513. https://doi.org/10.1016/j.ecolmodel.2023.110513

Parmah, E., & Negaresh, H. (2014). Agroclimatic zoning of sugar beet in Kermanshah province using GIS. *J. Biodiv. & Environ. Sci*, 4(4), 345-354. https://innspub.net/agroclimatic-zoning-of-sugar-beet-in-kermanshah-province-using-gis/

Pooya, M. R., Hasankhani, A., Fathololomi, S., & Karimi Firozjaei, M. (2025). A spatial multi-criteria decision-making approach to evaluating homogeneous areas for rainfed wheat yield assessment. *Water*, 17, 1045. https://doi.org/10.3390/w17071045

Radmehr, A., Bozorg-Haddad, O., & Loáiciga, H. A. (2022). Integrated strategic planning and multi-criteria decision-making framework with its application to agricultural water management. *Scientific Reports*, 12(1), 8406. https://doi.org/10.1038/s41598-022-12194-5

Rashidi, F., & Sharifian, S. (2022). A comparative analysis of three multi-criteria decision-making methods for land suitability assessment. *Environmental Monitoring and Assessment*, 194(9), 657. https://doi.org/10.1007/s10661-022-10259-6

Richey, A. S., Thomas, B. F., Lo, M. H., Reager, J. T., Famiglietti, J. S., Voss, K., Swenson, S., & Rodell, M. (2015). Quantifying renewable groundwater stress with GRACE. *Water Resources Research*, 51(7), 5217–5238. https://doi.org/10.1002/2015WR017349

Rodell, M., Famiglietti, J. S., Wiese, D. N., Reager, J. T., Beaudoing, H. K., Landerer, F. W., & Lo, M. H. (2018). Emerging trends in global freshwater availability. *Nature*, 557(7707), 651–659. https://doi.org/10.1038/s41586-018-0123-1

Scanlon, B. R., Faunt, C. C., Longuevergne, L., Reedy, R. C., Alley, W. M., McGuire, V. L., & McMahon, P. B. (2012). Groundwater depletion and sustainability of irrigation in the US High Plains and Central Valley. *Proceedings of the National Academy of Sciences*, 109(24), 9320–9325. https://doi.org/10.1073/pnas.1200311109

Sheikh, R., & Senfi, S. (2024). A Novel Opportunity Losses-Based Polar Coordinate Distance (OPLO-POCOD) Approach to Multiple Criteria Decision-Making. *Journal of Mathematics*, 2024, 8845886. https://doi.org/10.1155/2024/8845886

U.S. Department of Agriculture, F. A. S. (2025). Grain: World Markets and Trade . *Foreign agricultural service Publications*, Washington- DC, United States. https://esmis.nal.usda.gov/publication/grain-world-markets-and-trade

Zandi, I., & Lotfata, A. (2025). Evaluating solar power plant sites using integrated GIS and MCDM methods: A case study in Kermanshah Province. *Scientific Reports*, 15, 87476. https://doi.org/10.1038/s41598-025-87476-9

Zwart, S. J., & Bastiaanssen, W. G. M. (2004). Review of measured crop water productivity values for irrigated wheat, rice, cotton and maize. *Agricultural Water Management*, 69(2), 115–133. https://doi.org/10.1016/j.agwat.2004.04.007

Advanced Technologies in Water Efficiency
homepage:https://atwe.razi.ac.ir
Online ISSN:2783-4964

# Investigating fluid-structure interaction and transient flow dynamics for enhanced pipeline fault detection

**Alireza Sabetimani[1], Seyed Mohsen Sajjadi[2]✉, Manoochehr Fathi Moghadam[3], Alireza Keramat[4], and Javad Ahadiyan[5]**

1. Department of Hydraulic Structures, Shahid Chamran University of Ahvaz, Ahvaz, Iran. E-mail: alireza.sabetimani@yahoo.com
2. Corresponding author, Department of Hydraulic Structures, Faculty of Water and Environmental Engineering, Shahid Chamran University of Ahvaz, Ahvaz, Iran. E-mail: sajjadi.mohsen@gmail.com
3. Department of Hydraulic Structures, Faculty of Water and Environmental Engineering, Shahid Chamran University of Ahvaz, Ahvaz, Iran. E-mail: fathi49@gmail.com
4. Department of Civil Engineering, University of Hong Kong, Hong Kong. E-mail: keramat.alireza@gmail.com
5. Department of Hydraulic Structures, Faculty of Water and Environmental Engineering, Shahid Chamran University of Ahvaz, Ahvaz, Iran. E-mail: j.ahadiyan@scu.ac.ir

## Article Info

**Article type:**
Research Article

**Article history:**
Received 01 July 2025
Received in revised form 02 November 2025
Accepted 08 December 2025
Available online 22 December 2025

***Keywords***:
pipeline fault detection,
water hammer,
viscoelastic pipe walls,
unsteady friction,
poisson coupling,
junction coupling.

## ABSTRACT

**Objective:** The objective of this study is to investigate how fluid–structure interaction (FSI), along with unsteady friction, viscoelastic wall behavior, and potential column separation, affects transient pressure signals in pipelines and influences the accuracy of fault detection.

**Method**: To achieve this, a controlled experimental pipeline loop was employed, and simulations were performed using the Method-of-Characteristics (MOC). The study examined the effects of FSI through Poisson and junction coupling, valve maneuvers, and both elastic and viscoelastic pipe models.

**Results**: The results show that FSI systematically amplifies transient pressure fluctuations and can mimic the signatures of leaks or blockages. Sensor placement, valve-closure time, and axial support stiffness significantly influence the magnitude of FSI effects. Moreover, viscoelastic pipe models dissipate energy and attenuate oscillations, leading to better agreement with experimental measurements and enhanced system robustness.

**Conclusions**: The study highlights that accurate transient-based fault detection requires explicit modeling of FSI and careful consideration of measurement layout, actuation timing, and structural support in the design of fault-detection systems to ensure reliability.

**Cite this article:** Sabetimani, A., Amer., Sajjadi, S.M., Fathi Moghadam, M., Keramat, A., & Ahadiyan, J. (2025). Investigating fluid-structure interaction and transient flow dynamics for enhanced pipeline fault detection. *Advanced Technologies in Water Efficiency, 5* (4), 92-107. https://doi.org/10.22126/atwe.2025.12399.1175


Publisher: Razi University.
https://doi.org/10.22126/atwe.2025.12399.1175

## Introduction

This study focuses on improving the detection and management of pipeline faults through the analysis of fluid-structure interaction (FSI) and transient flow dynamics. The growing demand for water resources and the increasing complexity of pipeline networks make this an essential area of research. The objective of this work is to address the challenge of accurately identifying pipeline defects such as leakage, blockages, and structural weaknesses, which are critical for ensuring the reliability of water transmission systems (Chen et al., 2022; Islam, 2023).

The literature reveals substantial progress in understanding transient flows, particularly in their application to fault detection. For instance, (Tijsseling, 1996) provided a comprehensive review of water hammer effects, while (Wiggert, & Tijsseling, 2001) explored FSI mechanisms. (Colombo et al., 2009) examined transient-based leak detection methods, highlighting the potential of using transient signals for fault identification. However, there remains a gap in integrating these findings into robust, field-applicable diagnostic systems.

To address this gap, the methodology adopted in this study involves constructing a controlled experimental pipeline system, utilizing state-of-the-art measurement techniques, and validating the results through numerical simulations. Specifically, the method of characteristics (MOC) is employed to analyze transient events (Colombo et al., 2009; Joshi & Jaiman, 2018). By combining experimental and computational approaches, this research aims to bridge the gap between theoretical understanding and practical application.

The key results demonstrate the critical influence of FSI on pressure signal fluctuations during transient events. These fluctuations can mimic fault signals, underscoring the importance of accounting for FSI effects in fault detection systems. The findings highlight the need for improved support designs and advanced modeling techniques to enhance diagnostic accuracy and pipeline resilience.

Various numerical methods, including mathematical, graphical, and implicit methods, have been developed for transient flow analysis. Among these, the method of characteristics (MOC) is widely recognized for its accuracy in modeling unsteady flows (Joshi & Jaiman, 2018).

Factors Influencing Transient Flow Signals:Several factors significantly influence transient flow signals, each contributing uniquely to the complexity of fault detection in pipeline systems.

**Fluid Column Separation (CS):** Fluid column separation occurs when the pressure within a pipeline drops below the vapor pressure of the fluid, leading to cavity formation. This phenomenon can cause severe pressure fluctuations upon cavity collapse, which affects the integrity of the pipeline system. (Adamkowski & Lewandowski, 2009) developed a new method for predicting liquid column separation during hydraulic transients, enhancing the reliability of such predictions. Studies such as (Wiggert, & Tijsseling, 2001) have extensively analyzed the implications of this phenomenon.

**Unsteady Friction (UF):** Unsteady friction refers to transient, non-permanent frictional effects arising during changes in flow conditions. Unlike steady-state friction, these effects are time-dependent and can significantly dampen or amplify transient signals. (Zielke, 1968) introduced a convolution-based model to account for unsteady friction in transient pipe flow, providing a theoretical basis for understanding these effects.

**Viscoelastic Properties of Pipe Walls (VE):** The viscoelastic behavior of pipeline walls influences the propagation of pressure waves during transient events. This property causes energy dissipation and changes in wave speed, which are critical for accurately modeling transient flow (Meniconi et al., 2012). investigated the impact of pipe wall viscoelasticity on water hammer phenomena, highlighting the importance of considering material properties in transient analysis.

**Leakage and Clogging:** Pipeline faults such as leaks and clogs introduce localized pressure variations that interfere with transient signals. Identifying these faults requires distinguishing their effects from other damping mechanisms. (Colombo et al., 2009) conducted a selective literature review of transient-based leak detection methods, discussing techniques for isolating fault-induced fluctuations.

These factors collectively influence the damping and fluctuations in transient flow signals, complicating the process of identifying and analyzing pipeline faults.

**Pressure Head and Sensor Position:**

Fig. 1 illustrates the transient pressure head (H) as a function of time (ms) for varying sensor positions along the pipeline. The position of the sensors is normalized using E1.

$$Ls=\frac{L\_sensor}{L\_pipeline}\times 100 \quad (1)$$

The results show that pressure signals exhibit distinct variations depending on the proximity of the sensors to the transient source (water hammer valve). Sensors closer to the valve capture sharper pressure changes and higher amplitudes, indicating the significant influence of sensor position on capturing transient phenomena.

The schematic demonstrates the experimental setup used to assess the influence of sensor positioning on pressure signal detection (Fig. 2). Sensors are strategically placed along the pipeline, with one near the water hammer valve (downstream) and another near the reservoir (upstream). This arrangement highlights the importance of sensor placement for accurately capturing pressure wave characteristics.

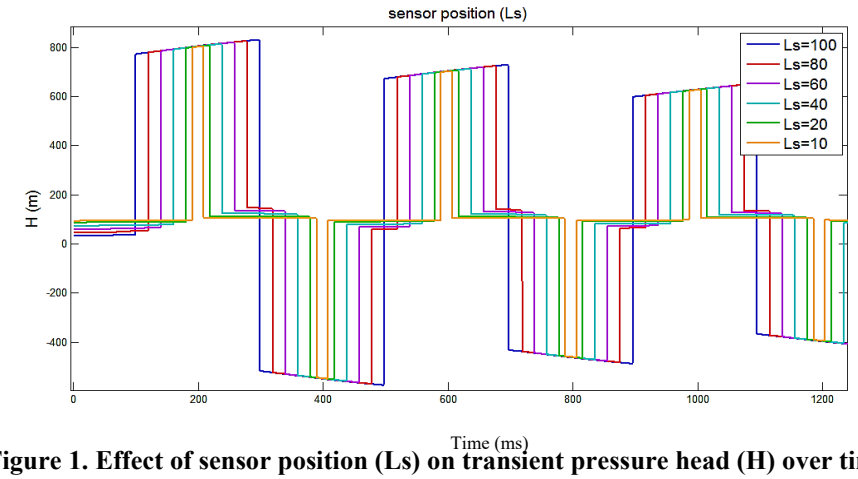


**Figure 1. Effect of sensor position (Ls) on transient pressure head (H) over time**

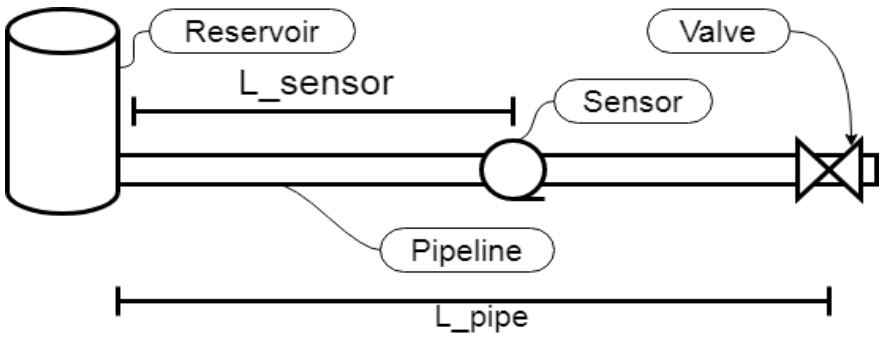


**Figure 2. Schematic diagram of the experimental setup, including the reservoir, pipeline, valve, and sensor**

The analysis confirms that the optimal position for pressure sensors is near the water hammer valve, where the system is most actively stimulated. Pressure waves diminish in intensity as they propagate further from the transient source, making downstream locations more suitable for capturing high-resolution pressure data. Additionally, the placement of a second sensor near the reservoir ensures accurate measurement of baseline pressure conditions, providing a reference for analyzing transient signals.

**Fluid-Structure Interaction (FSI):** Fluid-Structure Interaction (FSI) occurs when the fluid within a pipe interacts significantly with the structural dynamics of the pipe itself. This interaction becomes particularly critical during transient flow events, where sudden changes in flow conditions can amplify the effects. FSI often leads to axial vibrations and propagating stress waves within the pipe, which, if not adequately supported, can result in substantial displacements and potentially compromise the pipeline's integrity. Early studies, such as those by (Wiggert, & Tijsseling, 1996), laid the groundwork for understanding these dynamics in flexible piping systems.One key area of focus in FSI research is the behavior of pressure signals during transient events. These signals are most prominent in the first half-period of the transient flow, where their characteristics can provide insights into the interaction's mechanisms. Studies like (Tijsseling, 1996) emphasize the importance of analyzing this phase to accurately model and predict FSI effects.

**Three primary coupling mechanisms characterize FSI:**

**Poisson Coupling:** This mechanism arises from the pressure-induced axial stress within the pipeline. Poisson coupling influences how axial forces are distributed along the pipe's length, as discussed in early theoretical works by (Zielke, 1968).

**Friction Coupling:** Caused by the fluid friction along the pipe walls, this mechanism affects the transient flow's damping characteristics (Colombo et al., 2009). highlighted the role of friction coupling in modifying the amplitude of pressure waves.

**Junction Coupling:** This mechanism originates from discontinuities or fittings in the pipeline system, such as elbows or valves. Junction coupling's significance in transient flow behavior was explored in depth by (Adamkowski & Lewandowski, 2009), who investigated its impact on pressure wave reflections and refractions.

The Fig. 3 illustrates the propagation of stress waves and pressure waves in a pipeline system during transient flow events. It shows the interaction of these waves when a valve is opened, demonstrating the effects of fluid-structure interaction (FSI) at various stages. Stress waves originate from the pipe walls due to structural dynamics, while pressure waves travel through the fluid, highlighting the coupled nature of the system. This visualization emphasizes how FSI influences transient flow behaviors, such as wave reflection and transmission, which are critical for analyzing pipeline stability and fault detection.

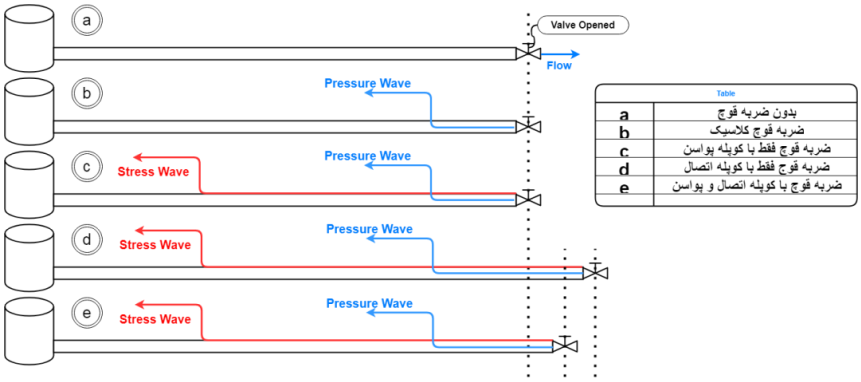


**Figure 3. Wave propagation in a pipeline system during transient flow events, depicting stress waves (red) in the pipe walls and pressure waves (blue) in the fluid after valve operation:(a) Initial state: Valve is opened, and no flow or wave activity occurs. (b) Valve is opened, generating a pressure wave (blue) that propagates through the fluid. (c) Stress wave (red) in the pipe wall begins to interact with the pressure wave. (d) The stress and pressure waves reflect and propagate in the pipeline. (e) Multiple interactions between stress and pressure waves continue as transient flow stabilizes**

**Effect of Valve Closure Time:** Fig.4 illustrates the effect of valve closure time (Tc) on transient pressure signals (H) in a pipeline system. As Tc decreases, represented by the blue curve (Tc=0.01), the pressure signal exhibits sharp and oscillatory peaks, indicating significant water hammer effects due to rapid valve closure. Conversely, as Tc increases (e.g., Tc=0.05, Tc=0.1, and Tc=0.15), the oscillations become smoother and less pronounced, reflecting a gradual dissipation of energy and reduced transient effects. (Colombo et al., 2009) studied the influence of valve closure time on pressure signals caused by water hammer and found that valve closure time plays a critical role in both fluid-structure interaction (FSI) and in detecting leaks and blockages in the system. As shown in the fig. 5, increasing the valve closure time reduces the intensity of the jumps caused by FSI. This trend highlights that longer valve closure times mitigate the intensity of pressure oscillations, leading to a more stable pressure response and reduced stress on the pipeline structure.

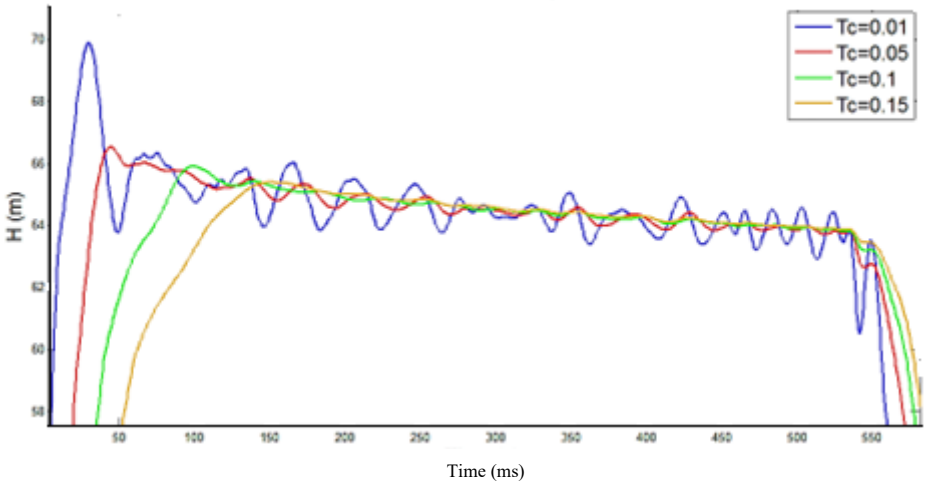


**Figure 4. Effect of valve closure time (Tc) on transient pressure head (H) over time. Rapid closure (Tc=0.01) leads to higher oscillations, while slower closures (Tc=0.05–0.15) reduce oscillation intensity**

**Effect of Pipe Support Stiffness:**The stiffness of pipe supports plays a crucial role in influencing pressure signals during transient flow. Research has shown that higher support stiffness can amplify pressure fluctuations, while inadequate stiffness may result in errors or larger pressure jumps (Wiggert & Tijsseling, 1985). demonstrated that higher support stiffness increases pressure compared to classic cases, highlighting the need for precise stiffness calibration in pipeline designs (Wiggert & Tijsseling, 2001). insufficient support stiffness leads to errors in transient analysis, making accurate stiffness evaluation critical for reliable modeling (Colombo et al., 2009). In another study, (Duan et al., 2010) found that lower support stiffness causes larger pressure jumps during transient events. Their findings underscore the importance of optimizing support design to mitigate such effects (Duan et al., 2010). Moreover, (Monteiro Andrade et al.,2023 ) investigated the impact of fixed and viscoelastic supports on fluid-structure interaction (FSI). Their results showed that support type and material significantly affect transient signal behavior, offering insights for improving pipeline resilience (Keramat et al., 2012;Meniconi et al., 2012).

These studies collectively emphasize the importance of proper support design in mitigating FSI-induced pressure fluctuations and ensuring pipeline system reliability. These findings emphasize the importance of proper support design to mitigate FSI-induced pressure fluctuations.

## Method

The objective of this study is to address the research question: How can fluid-structure interaction (FSI) effects be accurately accounted for to improve pipeline fault detection? The relevance of this question lies in both theoretical advancements in transient flow analysis and practical applications in ensuring the reliability of water transmission systems.

## Research Framework

The research framework combines experimental investigations with numerical simulations. A controlled experimental pipeline system was constructed, allowing for precise manipulation of flow conditions and structural dynamics. High-density polyethylene pipes were used for their viscoelastic properties, which are essential for studying FSI phenomena.

## Experimental Setup

The experimental model was designed in the Hydraulic Laboratory at Shahid Chamran University of Ahvaz (Keramat et al., 2020). It includes a tank-pipe-valve system to simulate transient flow events. The detailed specifications of the pipeline system used in this study are summarized in Table 1. And Fig. 5 provides a comprehensive visual representation of the experimental setup used for investigating transient flow and fluid-structure interaction (FSI). The setup includes key components such as an air vessel, water supply pump, bypass and input water regulator valve, and transient and flow control valves.

**Table 1. Pipeline specifications used in the experimental setup for studying fluid-structure interaction and transient flow behavior.**

| Specification | Pipe Material | Outer Diameter | Length | Wall Thickness | Young's Modulus | Poisson's Ratio |
|---|---|---|---|---|---|---|
| Values | High-density polyethylene | 63 mm | 158 m | 6.5 mm | 1.43 GPa | 0.46 |

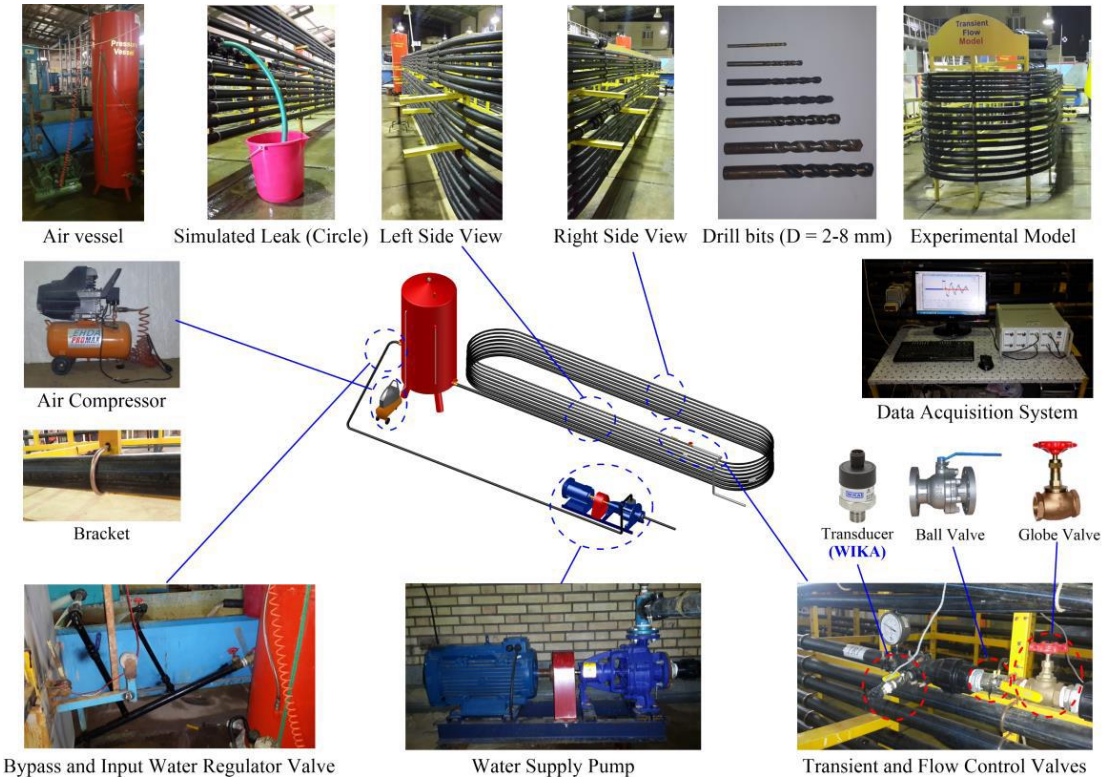


**Figure 5. Overview of the experimental setup for transient flow and fluid-structure interaction (FSI) studies, including an air vessel, water pump, control valves, simulated leaks, and a data acquisition system (Rahmanshahi, 2016)**

The system was installed in a semicircular frame to minimize secondary flows at sharp turns. Metal fasteners with plastic coatings were used to prevent lateral and longitudinal movements of the pipes. The schematic diagram illustrates the experimental setup used for studying transient flow behavior and fluid-structure interaction (FSI) in a pipeline system. The setup includes a pressure vessel with an adjustable water level, inlet flow control, and a pipeline equipped with pressure sensors for data collection. Key components such as a water hammer valve and flow control valve are also shown (Fig. 6), enabling precise manipulation of flow conditions to simulate transient events and analyze their effects on the system.

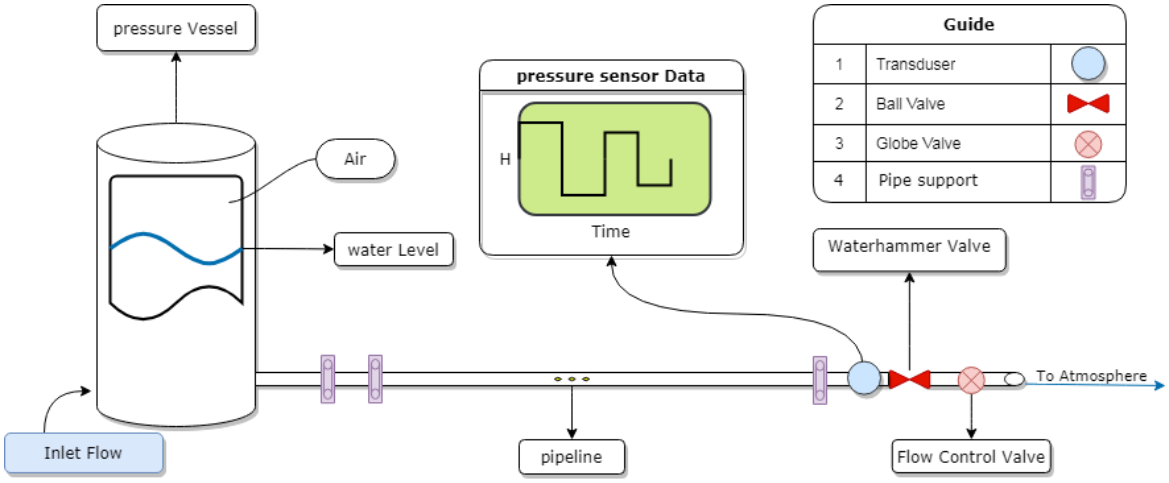


**Figure 6. Schematic of the experimental setup used to study transient flow and fluid-structure interaction (FSI) in pipelines, highlighting the pressure vessel, control valves, and pressure sensors**

## Effect of Structural Vibrations and Noise on Pressure Sensor

Fluid-structure interaction (FSI) causes vibrations in the pipeline, while system noise introduces uncertainty in pressure signal reflections and jumps, reducing the accuracy of identifying weak parameters such as magnitude, length, and location of faults (Duan, 2015). To evaluate the influence of structural vibrations on pressure sensors near the transient flow source, specifically at the valve location, an additional sensor was employed. As shown in the schematic diagram, this second sensor was exclusively attached to the pipeline structure and had no direct contact with the fluid inside the pipe. Additionally, a reference pressure sensor, which was not attached to any part of the system, was used to monitor environmental noise.

After generating the transient flow, the signals from all three sensors were compared. Since pipeline vibrations enter a critical state at high flow rates, the experiment was repeated three times at a flow rate of 2.4 L/s. The results, shown in Fig. 8, reveal that at higher frequencies, oscillations appeared in the sensors. Repeating the experiments confirmed that these oscillations were due to environmental noise, which was mitigated using a low-pass filter in MATLAB to process the data recorded by the data logger.

The experimental results demonstrated that the pressure jumps observed during the first half-period of the transient signal were not influenced by sensor vibrations. Furthermore, the repeatability of the tests indicated that these oscillations were not random but were driven by underlying mechanisms affecting the signal. This finding highlights the importance of accurate noise filtering and structural vibration analysis in transient flow studies.

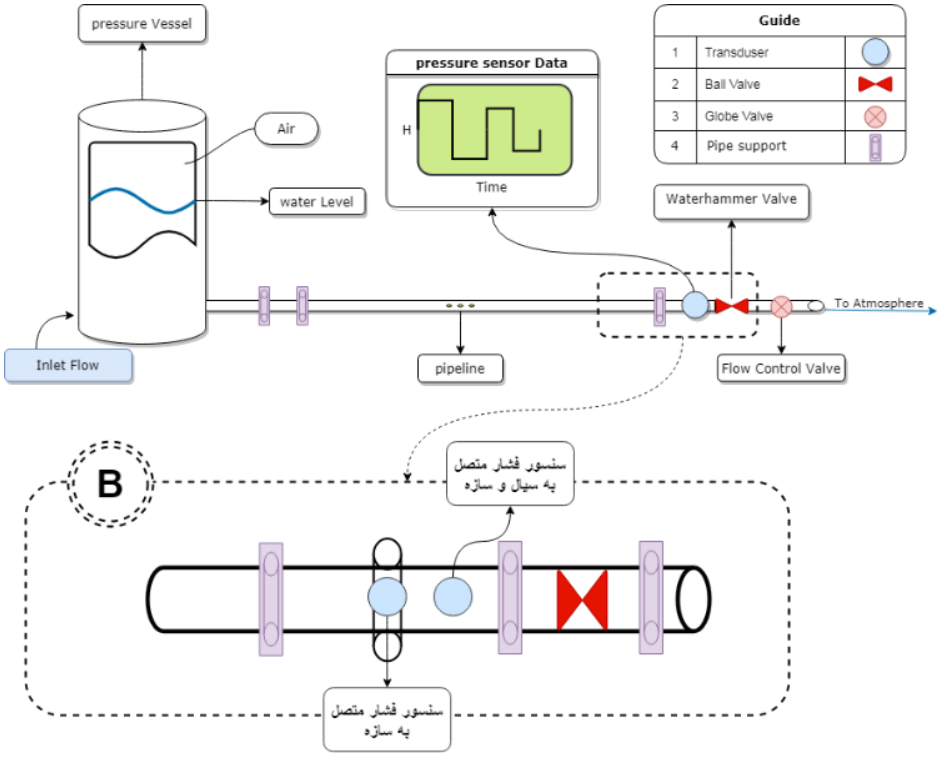


**Figure 7. Schematic of the experimental setup, including the pressure vessel, inlet flow, water level, pipeline, waterhammer valve, flow control valve, and pressure sensors attached to the fluid and structure for transient flow analysis**

## Data Collection and Analysis

To ensure accuracy, noise removal from collected signals was achieved using a low-pass frequency filter. Experiments were repeated three times under each condition to validate repeatability. The transient signals were analyzed to observe the effects of FSI, including damping and pressure fluctuations.

## Numerical Simulation

The Method of Characteristics (MOC) was employed for numerical analysis of transient flow events. This method, recognized for its accuracy, was used to model the interaction between fluid dynamics and structural responses. By integrating experimental results with computational simulations, the study aims to provide a comprehensive understanding of FSI in pipelines.

The chosen methods align with the research objectives, providing both theoretical insights and practical solutions for improving pipeline fault detection systems.

## Governing Equations

The pressure wave occurs due to the phenomenon of ram impact in pressurized channels caused by a sudden change in speed downstream. For practical applications of transient flow in pressurized pipes, the mass and momentum conservation equations are commonly used (Covas et al., 2005). To derive the governing equations for transient flow with fluid-structure interaction (Poisson coupling) under viscoelastic pressure, the following assumptions are made: the pipe is straight, with a thin, homogeneous, and isotropic wall. The material of the pipe behaves linearly, and the fluid is single-phase and non-viscous. Friction effects are neglected,

as the focus is on the first half-period of the pressure head where damping effects are insignificant.

The viscoelastic behavior of the pipe wall is described using the comprehensive Kelvin-Voigt model with a constant Poisson's ratio. These equations, representing one-dimensional flow in a horizontal pipe and ignoring transfer acceleration terms, are based on prior studies (Lavooij & Tijsseling, 1991; Keramat et al., 2012):

Fluid Momentum Equation:

$$\frac{\partial Q}{\partial t}+gA_f\frac{\partial \tilde{H}}{\partial z}=0 \quad (2)$$

Fluid Continuity Equation:

$$\frac{1}{A_f}\frac{\partial Q}{\partial z}+\frac{g}{c_f^2}\frac{\partial \tilde{H}}{\partial t}-2\vartheta\frac{\partial \dot{u}_z}{\partial z}=(\vartheta^2-1)\rho_f g\frac{D}{e}\frac{\partial I_{\tilde{H}}}{\partial t} \quad (3)$$

Axial Vibration of the Tube Wall:

$$\frac{\partial^2 u_z}{\partial t^2}-c_t^2\frac{\partial^2 u_z}{\partial z^2}-g\frac{\rho_f}{\rho_t}\frac{\vartheta D}{2e}\frac{\partial H}{\partial z}=E_0 g\frac{\rho_f}{\rho_t}\frac{\vartheta D}{2e}\frac{\partial I_{\tilde{H}}}{\partial z}-E_0 I_{\ddot{u}_z} \quad (4)$$

In the governing equations for transient flow and fluid-structure interaction (FSI), the variables are
defined as follows:

Q: Volumetric flow rate ($m^3/s$).
H: Total head and perturbation head, respectively (m).
$A_f$: Cross-sectional area of the fluid ($m^2$).
$C_f$: Wave speed of the fluid (m/s).
g: Gravitational acceleration ($m/s^2$).
$\vartheta$: Poisson ratio of the pipe material.
$U_z$: Axial displacement of the pipe wall (m).
$\rho_f$ and $\rho_t$: Densities of the fluid and the pipe material (kg/m3), respectively.
D: Pipe diameter (m).
e: Wall thickness of the pipe (m).
$E_0$: Young's modulus of the pipe material (Pa).
C: Wave speed in the pipe wall (m/s).

Finite element analysis is applied to the pipe wall motion, while the method of characteristics is employed for the fluid. This approach demonstrates how fluid-structure interaction influences water hammer parameters in elastic and viscoelastic pipes, differing from classical theory.

## Results

Experimental results indicate that FSI significantly impacts pressure signal fluctuations during the first half-period of transient flow. These fluctuations closely resemble those caused by pipeline faults such as leakage and clogging. Properly accounting for FSI effects is crucial for accurate fault detection. If FSI is neglected, ensuring adequate stiffness of valve supports can mitigate pressure jumps and improve detection accuracy. The transient pressure head (H) as a function of time (ms) for an elastic pipeline material is presented in Fig. 8. The blue line represents the case with no Poisson coupling, showing a significantly lower pressure response. In contrast, the orange and purple lines correspond to cases with only Poisson coupling and

both Poisson and junction coupling, respectively. The results demonstrate that Poisson coupling substantially increases pressure oscillations, while the addition of junction coupling further amplifies and stabilizes the response. This highlights the significant influence of coupling mechanisms on transient flow dynamics in elastic materials.

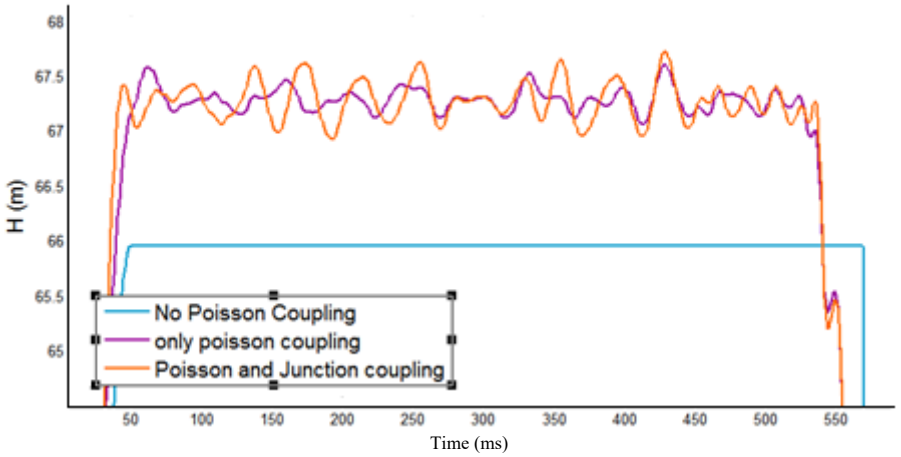


**Figure 8. Comparison of transient pressure head (H) under elastic conditions for different coupling mechanisms: no Poisson coupling, only Poisson coupling, and Poisson with junction coupling.**

Fig. 9 shows the transient pressure head (H) over time for a viscoelastic pipeline material. Compared to the elastic case, the pressure response is notably dampened. The blue line, representing no Poisson coupling, exhibits a significantly reduced pressure head. Meanwhile, the orange and purple lines, corresponding to only Poisson coupling and both Poisson and junction coupling, demonstrate the effect of viscoelasticity in mitigating pressure oscillations. These findings emphasize the energy-dissipating properties of viscoelastic materials, which reduce the intensity of pressure waves.

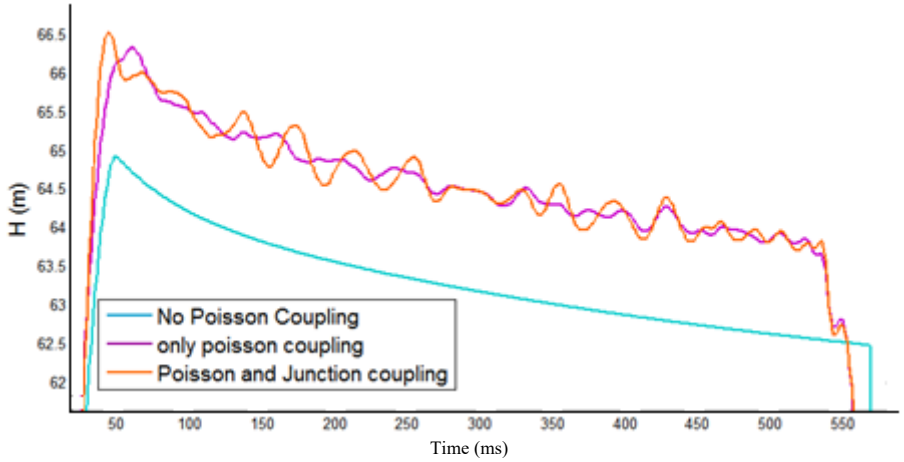


**Figure 2. Comparison of transient pressure head (H) under viscoelastic conditions for different coupling mechanisms: no Poisson coupling, only Poisson coupling, and Poisson with junction coupling.**

The comparison between elastic and viscoelastic cases underscores the critical role of material properties in influencing transient flow behavior. Elastic materials exhibit higher pressure oscillations, making them more prone to structural stress and potential failure under transient conditions. In contrast, viscoelastic materials effectively dampen pressure waves, reducing the risk of high-intensity oscillations. Furthermore, the inclusion of Poisson and junction coupling mechanisms enhances the understanding of dynamic interactions, demonstrating their importance in accurately modeling pipeline systems.

These findings validate the experimental setup and underscore the necessity of considering material properties and coupling mechanisms in the design and analysis of pipeline systems.

Fig. 10 compares the pressure head (H) over time for two scenarios: water hammer with fluid-structure interaction (FSI) and classic water hammer without FSI. The blue line represents the water hammer with FSI, showing significant oscillations and higher amplitude pressure peaks due to the dynamic interaction between the fluid and the pipeline structure. In contrast, the red dashed line represents the classic water hammer, which follows a predictable pressure decay with no additional oscillations. The chart highlights the influence of FSI in amplifying and sustaining pressure oscillations over time, which is critical for understanding the complexities of transient flow in pipeline systems. This comparison underscores the necessity of considering FSI effects in the design and analysis of hydraulic systems to predict and mitigate potential risks effectively.

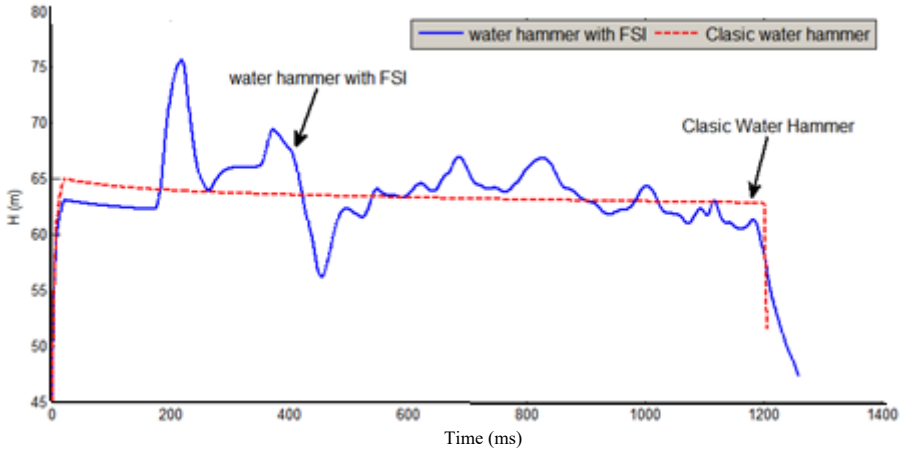


**Figure 3. Comparison of water hammer effects with and without fluid-structure interaction (FSI). The blue line shows water hammer with FSI, exhibiting amplified oscillations, while the red dashed line represents the classic water hammer with a predictable pressure decay.**

Experimental results indicate that FSI significantly impacts pressure signal fluctuations during the first half-period of transient flow. These fluctuations closely resemble those caused by pipeline faults such as leakage and clogging. Properly accounting for FSI effects is crucial for accurate fault detection. If FSI is neglected, ensuring adequate stiffness of valve supports can mitigate pressure jumps and improve detection accuracy.

## Conclusions

This study delineates the coupled fluid–structure mechanisms that govern early-time transients used for pipeline fault detection. We show that fluid–structure interaction (FSI)—

arising from Poisson coupling of circumferential strain to pressure and junction/axial coupling of the pipe to its supports—can amplify or phase-shift pressure responses to valve maneuvers, producing signatures that mask or mimic true faults (e.g., small leaks, incipient blockages). The magnitude of these FSI-induced fluctuations is not a fixed property of the fluid alone; it depends materially on structural boundary conditions. In particular, the stiffness and layout of valve and pipe supports regulate axial wall motion and therefore the local head jump during the first half-period. As a result, nominally identical hydraulic events can yield measurably different transients across installations with different support designs.

These findings have two immediate implications for reliable diagnostics. First, models and detection algorithms should explicitly account for FSI. In practice, that means using transient solvers (e.g., Method of Characteristics) with (i) wave-speed correction for circumferential compliance, (ii) junction/axial coupling to supports, (iii) viscoelastic wall rheology (e.g., Kelvin–Voigt or standard-linear-solid) to capture decay envelopes, and (iv) an appropriate treatment of unsteady friction where relevant. Second, where full FSI modeling is impractical, systems can be engineered to suppress the confounding effects: tune the effective support stiffness in the vicinity of actuated valves, select valve-closure laws that limit high-frequency content, and place sensors at positions that balance sensitivity with robustness to support-induced amplification.

For practitioners, we recommend the following workflow: (1) document and, where possible, estimate effective support stiffness and spacing near the actuation point; (2) calibrate wall viscoelastic parameters from ring-down tests to match measured decay; (3) report quantitative effect sizes for key design choices—sensor location, valve-closure time (Tc), and support stiffness (k)—using peak-to-peak head, time-to-first-extremum, and signal-to-noise ratio; and (4) perform a brief sensitivity/uncertainty analysis to establish how much apparent "fault signal" can be attributed to FSI under site-specific conditions. Taken together, these steps reduce false positives and improve the transferability of detection thresholds across assets.

Future work should integrate advanced modeling and field validation: coupled fluid–structure solvers with identifiable, minimal parameter sets; Bayesian calibration to propagate uncertainty in support stiffness and wall rheology to detection decisions; physics-informed learning to fuse pressure and structural vibration measurements; and multi-site trials to quantify how material (HDPE vs. steel), diameter, and support typologies scale FSI effects. Such developments will enable fault-detection methodologies that remain accurate across the full envelope of hydraulic actuation and structural variability encountered in modern distribution systems.

### *Author Contributions*

All authors contributed equally to the conceptualization of the article and writing of the original and subsequent drafts.

### *Data Availability Statement*

Data available on request from the authors.

### *Acknowledgements*

The authors would like to thank all participants in the present study.

### *Ethical Considerations*

The authors avoided data fabrication, falsification, plagiarism, and misconduct.

***Funding***

This research did not receive any specific grant from funding agencies in the public, commercial, or not-for-profit sectors.

***Conflict of Interest***

The authors declare no conflict of interest.

## References

Adamkowski, A., & Lewandowski, M. (2009). A new method for numerical prediction of liquid column separation accompanying hydraulic transients in pipelines. *Journal of Fluids Engineering*, 131(7), 071302. https://doi.org/10.1115/1.3153365

Adamkowski, A., & Lewandowski, M. (2017). Study on influence of fluid parameters on axial coupled vibration of hydraulic pipelines. *Shock and Vibration*, 4824376. https://doi.org/10.1155/2017/4824376

Chen, Y., Zhao, C., Guo, Q., Zhou, J., & Feng, Y. (2022). Fluid-Structure Interaction in a Pipeline Embedded in Concrete During Water Hammer. *Frontiers in Energy Research*, 10, 956209. https://doi.org/10.3389/fenrg.2022.956209

Colombo, A. F., Lee, P., & Karney, B. W. (2009). A selective literature review of transient-based leak detection methods. *Journal of Hydro-environment Research*, 2(4), 212–227. https://doi.org/10.1016/j.jher.2009.02.003

Covas, D., Ramos, H., & De Almeida, A. B. (2005). Hydraulic transients used for leak detection in water distribution systems. *Water Science and Technology: Water Supply*, 5(2), 95–105. https://www.researchgate.net/publication/263973267_Hydraulic_transients_used_for_leak_detection_in_water_distribution_systems

Duan, H. F., Lee, P. J., & Ghidaoui, M. S. (2010). Unsteady friction and visco-elasticity in pipe fluid transients. *Journal of Hydraulic Research*, 48(3), 354–362. https://doi.org/10.1080/00221681003726247

Duan, M. (2015). Structural and Thermal Analyses of Deepwater Pipes. Springer Cham Publications. Berlin, Germany. https://doi.org/10.1007/978-3-030-53540-7

Islam, M. R. I. (2023). SPH-based framework for modelling fluid-structure interaction problems with finite deformation and fracturing. *Ocean Engineering* ,294(21),116722. https://doi.org/10.1016/j.oceaneng.2024.116722

Joshi, V., & Jaiman, R. K. (2018). A positivity preserving and conservative variational scheme for phase-field modeling of two-phase flows. *Journal of Computational Physics*, 360, 137–166. https://doi.org/10.1016/J.JCP.2018.01.028

Keramat, A., Fathi-Moghadam, M., Zanganeh, R., Rahmanshahi, M., Tijsseling, A. S., & Jabbari, E. (2020). Experimental investigation of transients-induced fluid–structure interaction in a pipeline with multiple-axial supports. *Journal of Fluids and Structures*, 93, 102848. https://doi.org/10.1016/j.jfluidstructs.2019.102848

Keramat, A., Tijsseling, A. S., Hou, Q., & Ahmadi, A. (2012). Fluid–structure interaction with pipe-wall viscoelasticity during water hammer. *Journal of Fluids and Structures*, 28, 434–455. https://doi.org/10.1016/j.jfluidstructs.2011.11.001

Lavooij, C. S. W., & Tijsseling, A. S. (1991). Fluid-structure interaction in liquid-filled piping systems. *Journal of Fluids and Structures*, 5(5), 573–595. https://doi.org/10.1016/S0889-9746(05)80006-4

Meniconi, S., Brunone, B., & Ferrante, M. (2012). Water-hammer pressure waves interaction at cross-section changes in series in viscoelastic pipes. *Journal of Fluids and Structures*, 33, 44–58. https://doi.org/10.1016/j.jfluidstructs.2012.05.007

Monteiro Andrade, D., Bastos de Freitas Rachid, F., & Tijsseling, A. S. (2023). An analysis of fluid–structure interaction coupling mechanisms in liquid-filled viscoelastic pipes subject to fast transients. *Journal of Fluids and Structures*, 121, 103924. https://doi.org/10.1016/j.jfluidstructs.2023.103924

Tijsseling, A. S. (1996). Fluid-structure interaction in liquid-filled pipe systems: A review. *Journal of Fluids and Structures*, 10(2), 109–146. https://doi.org/10.1006/jfls.1996.0009

Wiggert, D. C., & Tijsseling, A. S. (1985). Analysis of liquid and structural transients in piping by the method of characteristics. Journal of Fluids Engineering-transactions of The Asme, 109, 97–102. https://doi.org/10.1115/1.3242638

Wiggert, D. C., & Tijsseling, A. S. (1996). Fluid transients in flexible piping systems: a perspective on recent developments. *Proceedings of the 18th IAHR Symposium on Hydraulic Machinery and Cavitation*, Valencia, Spain. https://link.springer.com/chapter/10.1007/978-94-010-9385-9_5

Wiggert, D. C., & Tijsseling, A. S. (2001). Fluid transients and fluid-structure interaction in flexible liquid-filled piping. *Applied Mechanics Reviews*, 54(5), 455–481. https://doi.org/10.1115/1.1404122

Zielke, W. (1968). Frequency-dependent friction in transient pipe flow. *Journal of Basic Engineering*, 90(1), 109–115. https://doi.org/10.1115/1.3605049

Advanced Technologies in Water Efficiency
homepage:https://atwe.razi.ac.ir
Online ISSN:2783-4964

# The effect of vortex on head loss and pressure fluctuation along the Penstock of Hydroelectric power plant

**Reza Roshan** [1], and **Rasool Ghobadian** [2]✉

1. Department of Water Engineering, Razi University, Kermanshah, Iran. E-mail: rezaroshan2631@gmail.com,
2. Corresponding author, Department of Water Engineering, Razi University, Kermanshah, Iran. E-mail: r_ghobadian@Razi.ac.ir

## Article Info

**Article type:**
Research Article

**Article history:**
Received 30 July 2025
Received in revised form 14 October 2025
Accepted 18 November 2025
Available online 22 December 2025

***Keywords***:
physical model,
vortex,
pressure fluctuations,
anti-vortex plate,
hydroelectric power plant,
penstock.

## ABSTRACT

**Objective:** This study aimed to assess the hydraulic impacts of intake vortices on energy losses and pressure fluctuations in hydropower penstocks and to evaluate the effectiveness of horizontal perforated anti-vortex plates in mitigating these effects.

**Method**: A large-scale laboratory model was used to systematically examine the influence of intake vortices under a wide range of hydraulic conditions. The experiments were conducted by varying the relative submergence depth (S/D = 1.5, 1.75, 2.0, 2.5, and 3.0) and the intake Froude number (Fr = 0.6, 0.8, 1.0, and 1.2) to generate different vortex strengths. Hydraulic parameters, including relative total head loss, relative friction head loss, Darcy–Weisbach friction coefficient, and pressure fluctuations, were measured along the penstock. Pressure fluctuations were recorded at nine measurement sections distributed along the penstock, and the hydraulic performance was compared for cases with and without the installation of an anti-vortex plate.

**Results**: The experimental results clearly demonstrated that the installation of an anti-vortex plate significantly reduced hydraulic losses and pressure fluctuations. On average, the friction coefficient, relative total head loss, and relative friction head loss were reduced to approximately 19.2%, 44.4%, and 20.8% of their corresponding values without the plate, respectively. Increasing the submergence ratio led to a notable increase in relative friction head loss, while the friction coefficient decreased. For a fixed submergence depth, higher Froude numbers intensified vortex strength, resulting in increased total and friction head losses as well as more pronounced pressure fluctuations along the penstock, despite a reduction in the friction coefficient. The dissipation length of vortices was found to depend strongly on vortex class, with weak Class C vortices dissipating within approximately 7 diameters from the intake, Class B vortices persisting up to about 18 diameters, and strong Class A vortices showing no clear dissipation within the tested penstock length.

**Conclusions**: Intake vortices have a substantial adverse effect on the hydraulic performance of hydropower penstocks by increasing energy losses and inducing pressure fluctuations. The results confirm that horizontal perforated anti-vortex plates are an effective and practical solution for mitigating vortex-induced losses and stabilizing flow conditions at intakes. Furthermore, the findings highlight the critical role of submergence depth and intake Froude number in controlling vortex strength and persistence. For strong air-core vortices, considerably longer penstocks or additional mitigation measures may be required to ensure complete vortex attenuation, underscoring the importance of vortex control in the design and operation of hydropower intakes.

**Cite this article:** Sabetimani, A., Amer., Sajjadi, S.M., Fathi Moghadam, M., Keramat, A., & Ahadiyan, J. (2025). Investigating fluid-structure interaction and transient flow dynamics for enhanced pipeline fault detection. *Advanced Technologies in Water Efficiency, 5* (4), 108-128. https://doi.org/10.22126/atwe.2025.12399.1175


Publisher: Razi University.
https://doi.org/10.22126/atwe.2025.12399.1175

## Introduction

Free surface vortices are a common and at the same time limiting phenomenon in all types of industrial intakes and their related hydro mechanical facilities. The formation of strong vortices in all types of intakes, including power plant intakes, is considered as an undesirable phenomenon. Especially in the situation where the vortex causes the entry of air and strong swirling flows into the water intake tunnel (Penstock). The occurrence of this phenomenon will cause severe drops in water intake efficiency, mechanical damages such as intensification of vibrations, corrosion and cavitation, as well as operational problems (Suerich-Gulick et al., 2014; Möller et al., 2012). Considering the importance of this issue, the amount of air influence into the intake caused by air-core vortices during detailed laboratory studies in recent years have been investigated ( Keller et al., 2014 ; Möller et al, 2015). In hydroelectric power plants, at levels lower than the acceptable level, due to the formation of a vortex with the air core and the entry of air into the Penstock, the production of electrical energy faced a serious problem (Amiri et al., 2011). The history of research on the vortex goes back many years ago. In this relation, Rahm published a relatively complete set of records of theoretical studies before 1950 in a report, in which, in addition to describing the mechanism of formation of strong vortices, there are evidences of the decrease in intake efficiency due to the occurrence of strong vortices with air core(Rahm, 1953). Researchers believe that the formation of strong vortices at the water intakes imposes adverse effects on the structure of the water intakes and their adjacent facilities. The vortices formed on the surface of the water physically divided into six types (levels), from 1 to 6, as the level of the vortex increases; its strength also increases (Knauss, 1987). In terms of importance and degree of risk, the six types of vortex classified into three classes A, B and C (Sarkardeh et al., 2010). The relationship between these two types of classification with the physical characteristics of the vortex is shown in Fig. 1.

According to Fig. 1, class A includes vortices through which air enters the intake, so they are at the highest level in terms of importance and degree of risk. On the other hand, class C vortices mainly have surface rotations and have the lowest degree of risk. Class B vortices are also important because they cause the transfer of floating particles into the intake tunnel. In understanding the vortex and the factors affecting it, the contribution of laboratory studies and experimental models is more than other methods. Mechanism of vortex formation was studied by laboratory tests(Gulliver & Rindles, 1987). Using an experimental method, Sarkardeh et al. investigated the effect of the geometric and hydraulic conditions of the intake and reservoir on the strength of the vortices formed at a horizontal intake(Sarkardeh et al., 2012 ; Sarkardeh et al., 2013) . Azarpira et al. also investigated the flow conditions in the reservoir in the presence of a vortex using the laboratory model of the Karun III dam (Azarpira et al., 2014 ).

The most important design indicator of water intakes is critical submergence depth (Sc). The critical submergence depth is a water level at which the created air core is on the threshold of entering the intake (Fig. 2). As long as the submergence depth of the reservoir (Si) is greater than the critical submergence depth(Sc), air core can not enter the intake. On the contrary, in the condition that Si moves towards Sci and is less than Sc, a permanent and continuous air core is formed and enters the the intake. Due to the variety of factors affecting the vortex formation, the exact determination of the critical submergence depth is associated with complications (Knauss, 1987 ), in such a way that the general relationships presented in this field are empirical. Therefore, it is still necessary that the vortex phenomenon and the factors affecting the critical submergence depth is further studied and analyzed. In recent years, with the advancement of computer models, numerical methods have also been used in the study of the vortex phenomenon. As an example, we can refer to the study on the vortex flow created in a cylindrical tank containing a viscous fluid in steady state by direct numerical simulation

method. In this study, it was observed that there is a direct relationship between the parameters of the flow inside the tank and in the intake conduit, so that with the increase in the fluid rotation in the tank, the flow rotation inside the intake conduit also increases (Constantinescu & Patel, 1998 ). Partovi Azar et al.(2010), indicated that the critical submergence would depend on hydraulic conditions in intake structure and using FLUENT model, they showed that the most severe vortex created on the gates of Aydoghmush Dam's intake tower is type 3.

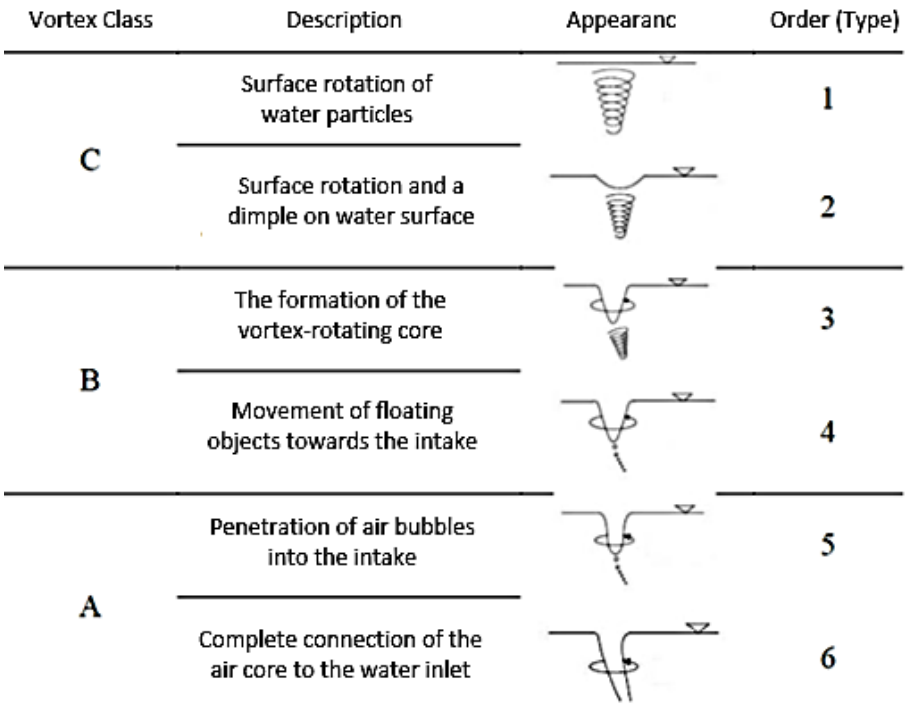


**Figure 1. Vortex type visual classification (Sarkardeh et al. 2010 )**

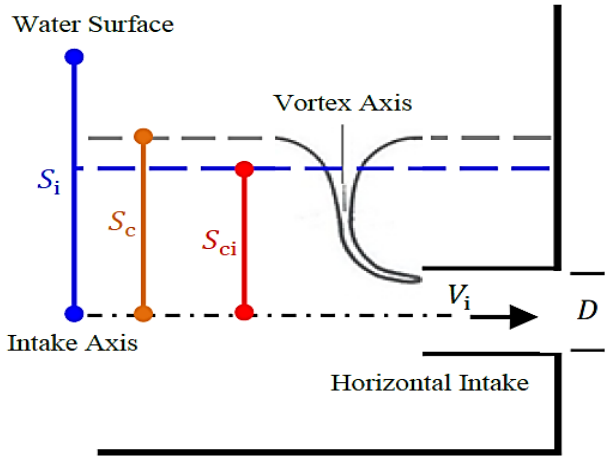


**Figure 2. Critical submergence at a horizontal intake (Knauss, 1987)**

Chelebioglu conducted a study on the friction coefficient and roughness changes in the Penstock of the power plant (ÇELEBIOĞLU, 2019 ). He noticed that when highly calcined water was passed through the Penstock of a hydroelectric plant, it left a residue on the surface of the pipe. The accumulated debris over time change pipe roughness and friction loss in the system and as a result, the head and flow rate on the turbine. He finally concluded that the surface roughness value (ε) equivalent to 0.3 mm could be used for calcined surfaces, which is much higher than steel surfaces but smaller than concrete. Sukhapure et al. conducted a research on head losses and prediction of these losses in two-branch penstocks (Y-Branch) with angles of 30°, 45°, 60° and 90°. Using Computational Fluid Dynamics (CFD) and simulation of branching, they presented a digital reference for head loss calculations for bifurcated penstocks (Sukhapure, 2018). In a research, Moukam et al. used the Colebrook-White equation to evaluate the turbulent boundary layer and friction along the penstock of the Three Gorges Dam, and concluded with 3D simulation in Fluent software that the slope of the penstock pipe has a significant effect on the development of the boundary layer and friction (Moukam et al., 2022 ). Roshan and Ghobadian studied effect of anti-vortex plates on vortex dissipation, discharge coefficient and inlet loss coefficient in hydropower intakes. Their results showed that the intake discharge coefficient reduces 5.9%, 10.5%, and 13.4% by using of perforated anti-vortex plate with openings of 70%, 58% and 50% respectively. It is also caused 12.9%, 24.7% and 33.5% for inlet loss coefficient of the intake, respectively (Roshan and Ghobadian, 2022). Aghajani et al. using image processing method and hydraulic PTV technique, investigated the flow through the horizontal intake with a trashrack. Their results showed that the best performance of the trashrack in reducing the vortex power occurred at the Froude number of one and on average, about 56% of the vortex power was reduced (Agbayani, et al., 2019). Manogaran et al. investigated the effect of two types of anti-vortex plates in mitigation of free-surface vortices in the dam intake using numerical simulation. Their results showed that square plates can be more effective in mitigation the free-surface vortices flow and decay of the vortex class than wedge edge plates (Manogaran et al., 2023). Zheng et al., in a review research work, systematically presented the hydrodynamic characteristics of the gravity surface vortex, including the mechanisms of evolution of flow pattern and the vibrations caused by the vortex. They also examined the future research directions in this matter (Zheng et al., 2023). Roshan and Ghobadian by physical model investigated the effect of reservoir geometric asymmetry, presence of unevenness in the bottom of the reservoir and angle of approach flow on the critical submergence depth (Roshan & Ghobadian, 2023).

A review of previous studies shows that research on power-plant penstocks generally focuses on various design methods aimed at minimizing construction and operating costs (e.g., Singhal & Kumar, 2015), reducing water consumption for hydropower generation (e.g., Leon, 2016), and optimizing geometric parameters of penstocks to increase the efficiency of gravity-fed power plants (e.g., Bajracharya et al., 2020). Although valuable achievements have been collected in these fields, however no specific research has been conducted to investigate the effect of vortex on the head loss and friction coefficient of Penstock of the power plant, as well as the analysis of pressure fluctuations along it in the presence of different type of vortexes. Considering the complexity of the subject and its importance, the conclusion of this findings require further research in this field. Therefore, in this research, using a large-scale laboratory model, the effect of vortex with different classes on energy loss along the horizontal water carrying tunnel (similar to Penstocks in hydroelectric power plants) has been investigated.

## Method

### Dimensional analysis

A review of previous research shows no formula has been provided to calculate the energy loss in the water carrying tunnel under the conditions of vortex entry with and without air core. The relationship between the parameters affecting the amount of head loss( $h_f$ ) in the Penstock can be introduced as follows:

$$h_f=f(D,V,S,g,\rho,\upsilon,\sigma,\Gamma,\varphi,L,\varepsilon) \quad (1)$$

Where inside diameter of the Penstock is D, volumetric mass of water is ρ , V is average velocity of flow in the Penstock, ν is kinematic viscosity of the fluid, gravitational acceleration is g, surface tension of the fluid is σ, Γ indicates circulation of vortex , angle of the approach flow is φ, submergence depth is S, L is the length of the tunnel and $\varepsilon$ signifies the roughness of the tunnel.

by using dimensional analysis and integrating some dimensionless groups with each other, the following relationship is finally obtained to calculate the relative friction loss in the water carrying tunnel in the presence of the entrance vortex:

$$\frac{h_f}{L}=f(\frac{S}{D},Fr,Re,We,N_\Gamma,\frac{\varepsilon}{D},\varphi) \quad (2)$$

where the dimensionless groups in the right side of the relation are relative submergence depth of the intake (S/D), Froude number( $V/\sqrt{gD}$ ), Reynolds number ( $VD/\upsilon$ ), Weber number( $\rho V^2 D/\sigma$ ), circulation number( $\Gamma/VD$ ), relative roughness and angle of the approach flow, respectively.

Typically, Froude number similarity is used in vortex modeling where gravity and inertial forces have significant effects. However, there are effects of viscosity and surface tension, although their amount is small and they should be minimized. These limitations can be considered as criteria for determining the scale of the model. Various researchers have studied the scale effects in vortex physical model and have proposed minimum values for the Reynolds and Weber numbers to prevent scale effects caused by viscosity and surface tension of the fluid. Minimum values of Re≥7.7× 104 and We>600 (Padmanabhan and Larsen, 2001); and We>120 (Jain et al. 1978); Re≥5× 104 (Daggett and Keulegan, 1974) and Re≥1.1× 105 and We>720 (Odgaard, 1986 ) should be considered in the construction of the model. The minimum values of Reynolds and Weber numbers in this study are $1.2\times10^5$ and $1.2\times10^3$, respectively, which are higher than the minimum criteria provided to eliminate the effects of viscosity and surface tension. On the other hand in the experiments conducted in the current research, parameters $\varphi, L, \varepsilon$ and D were considered constant. Additionally, the experiments conducted in (Roshan, 2023) showed that NΓ is a function of the submergence depth and the Froude number( $N_\Gamma = 0.36\ (S/D)^{-0.69} Fr^{0.184}$ ). According to these explanations, in this study only the effect of two parameters, submergence depth (S/D) and Froude number( $V/\sqrt{gD}$ ), on energy loss as well as pressure fluctioation along the Penstock and friction coeeficient have been investigated.

### Laboratory model

Considering that the aim of this research is to investigate the effect of vortex with an air core (vortex of class A) and without air core on the longitudinal head loss of the penstock, the laboratory model should be able to create and develop the vortex of type 6 and different submergence depths (S/D). Achieving this requires that flow with different Froude numbers (Fr) can be generated for a fixed depth inside the water intake tunnel. Obviously, such an issue cannot be achieved in the case of gravity flow, because in gravity flow, the depth of water in the reservoir and the flow velocity (or Froude number) are directly related to each other. To

solve this problem in the model, a pump was directly connected to the end of water intake tunnel. By adjusting the speed of the pump electromotor, flow velocity can be adjusted independently of the water depth in the reservoir. In addition, to keep the water depth of the tank constant, at different flow rates, the return pipe was directed to the model tank, so there is always a constant amount of water circulating in the system. In this way, it is possible to fill the tank with water to a certain depth at the beginning and then by changing the speed of the electromotor, different discharges and as a result different Froude numbers can be created in the Penstock. The main components of the laboratory model are reservoir, water-carrying pipe (Penstock), pump and a device to control electromotor rotation, which are shown in Fig. 3. The model reservoir is 1.3 m wide, 3.5 m long and 2 m high. The intake projected 0.15 meters into the reservoir and placed in such a way that the walls and the bottom of the reservoir do not affect the flow conditions on it. The reason for the projecting of the intake into the reservoir is to simulate the dead zone of flow area above the water intake. The length of the penstock pipe is 4.5 meters and its inside diameter is 0.16 meters. At 2 meters upstream of the intake in the reservoir, there are vertical blades that can change the angle of the incoming flow towards the intake. This makes it possible to strengthen the upstream circulation to reach stronger vortices. This model was made in the Water Research Institute of the Ministry of Energy. Since in all conditions of the experiments, the Reynolds number was much more than 2000 (Table 1), the prevailing flow can be considered turbulent and independent of the Reynolds number. To eliminate the vortex, horizontal perforated plates were used on the forehead of the intake (Fig. 4).

**Table 1. Geometric characteristics of the model and hydraulic parameters of the flow**

| Specifications | Parameters | Signs & Measure Units | Variation Range |
|---|---|---|---|
| Hydraulic | Flow Discharge | Q ($m^3/s$) | $0.015 \le Q \le 0.030$ |
| | Flow Velocity | V (m/s) | $0.75 \le V \le 1.5$ |
| | Submergence Depth | H or S (m) | $0.24 \le S \le 0.40$ |
| | Froude Number | $F_r$ | $0.60 \le F_r \le 1.19$ |
| | Reynolds Number | $R_e$ | $120000 \le R_e \le 240000$ |
| | Relative submergence | S/D | $1.5 \le S/D \le 3.0$ |
| Geometric | Anti-Vortex Plate Length | L (m) | $0.24 \le L \le 0.32$ |
| | Anti-Vortex Plate Width | W (m) | $0.16 \le W \le 0.24$ |
| | Reservoir Height | $H_R$ (m) | 2.0 |
| | Penstock Diameter | D (m) | 0.16 |
| | Anti-Vortex Plate Thickness | T (m) | $0.002 \le T \le 0.006$ |
| | Anti-Vortex Plate Opening | Op (%) | $\%50 \le Op \le \%70$ |
| | Blades Angle | θ (Degree) | $0 \le \theta \le 20$ |

In the table: Froude and Reynolds numbers are defined as $Fr = V/\sqrt{gD}$ and $Re = VD/\nu$ where ν is the kinematic viscosity of the fluid.

For flow discharge measurements, an electromagnetic flow meter (MAGFLO2500) with an accuracy of 1% installed in the path of the water return pipes into the reservoir was used (Fig. 5). To measure pressure fluctuations along the penstock, instantaneous pressure sensors were used (Fig. 6). Pressure fluctuations were measured in 9 sections at a distance of 0.5 meters from each other (Fig. 7). In addition, 4 piezometers in each section were embedded for measuring pressure fluctuations.

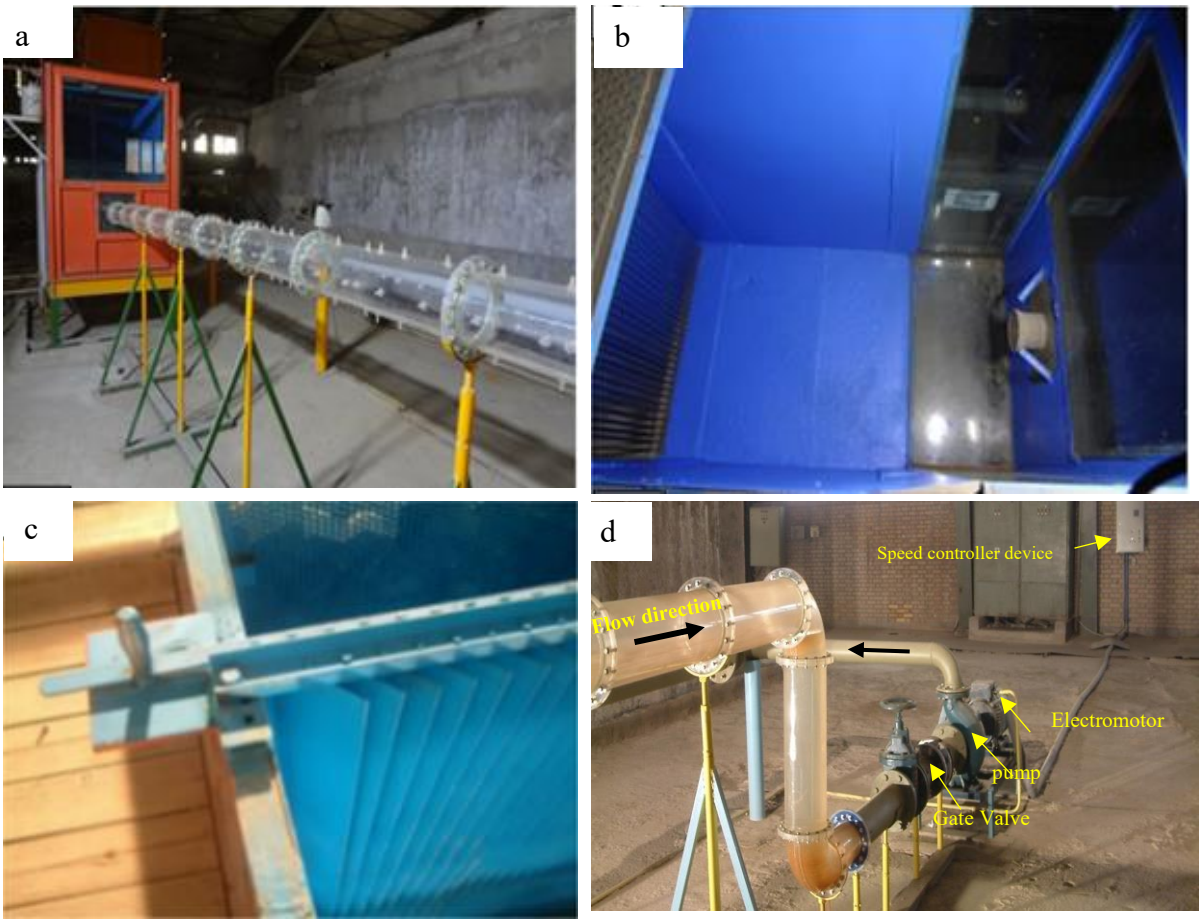


**Figure 3. (a) Reservoir, transparent flow pipe; (b) glass walls of the reservoir and intake; (c) blades installed to create geometric asymmetry in model; (d) pump, electromotor speed controller device in laboratory model**

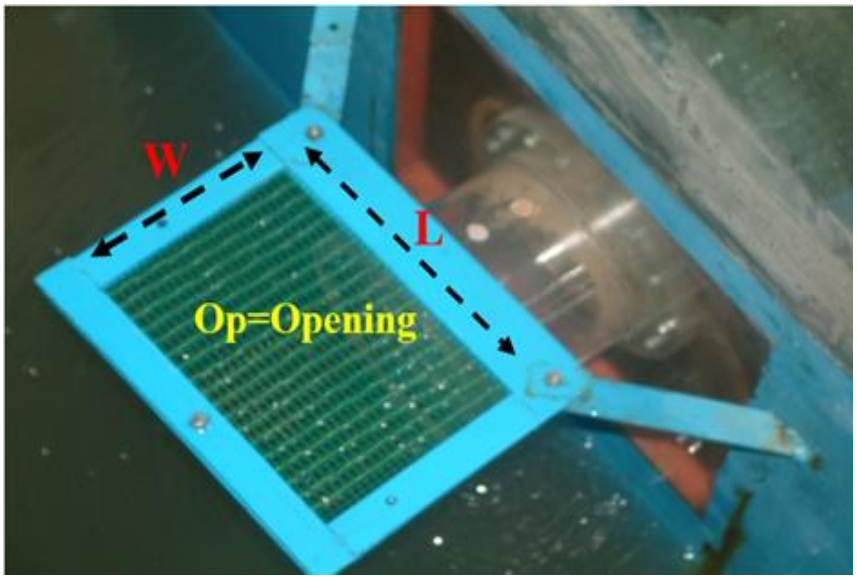


**Figure 4. Perforated Horizontal plate installed on the forehead of the intake**

**Fig. 5. Flowmeter installed in the model**

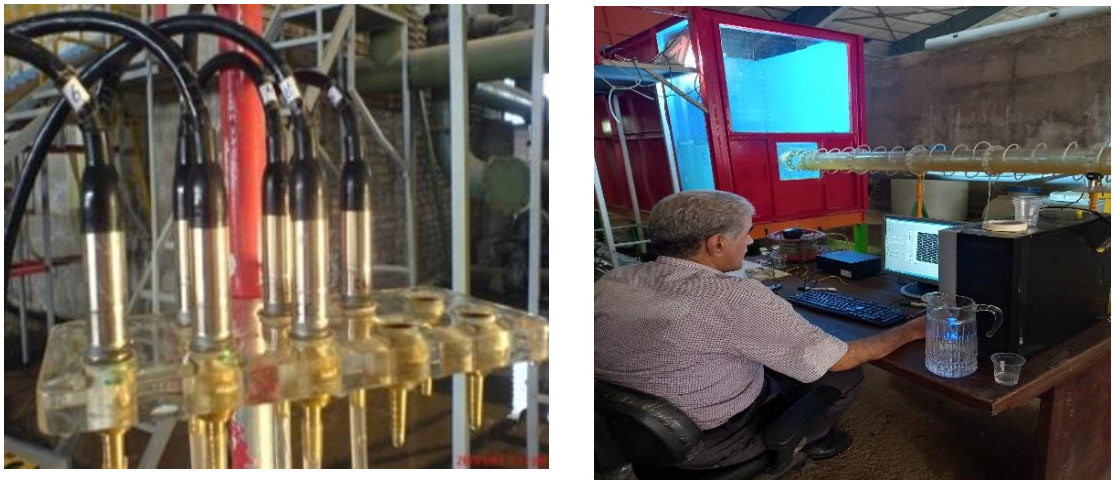

**Figure 6. Instantaneous pressure sensors and dynamic pressure setup in the model**

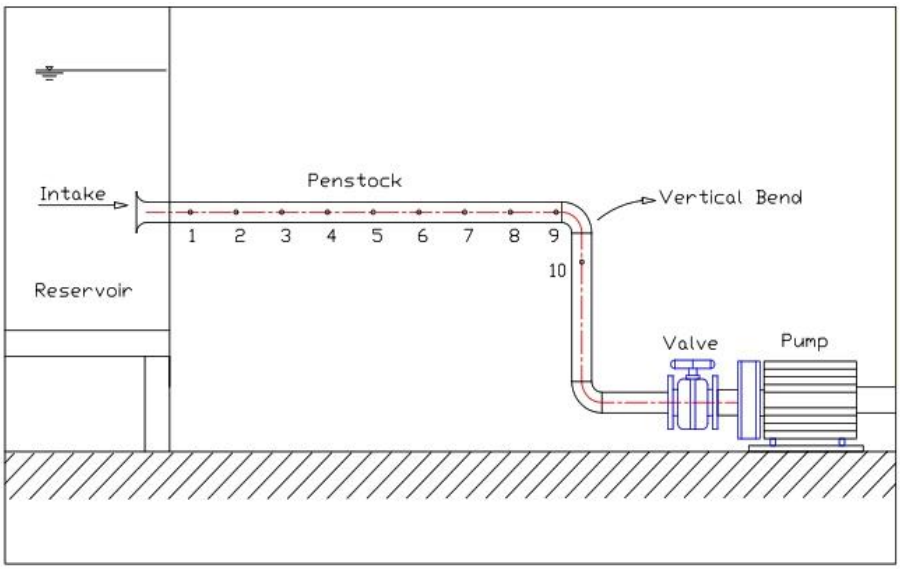


**Figore 7. Dynamic pressure measurement sections along the penstock**

## Results

### Effect of vortex on the head loss along the penstock

The experiments were carried out in the presence of the vortices with different classes. Five different relative submergence depths (S/D) in the reservoir as well as four Froude numbers (Fr) were considered. The selected range of Froude number and submergence depth includes all cases of the absence and the presence of possible weak and strong vortices at the intake. The values of the total head loss (ΔH) along the tunnel and relative total head loss (ΔH/H) are given in Table 2. To calculate the percentage of relative total head loss, the average pressure at section No.9 in Fig.7 was obtained and then the amount of the head loss was calculated from energy relationship between mentioned section and reservoir water surface and divide it by the reservoir head above the tunnel centerline (H or S).

The values in Table 2 indicate that at a certain relative submergence depth (S/D), with increase in Froude number, the amount of ΔH and ΔH/H have increased. The reason is that due to increasing the Froude number flow velocity in the Penstock increases and greater inlet and friction head loss in the presence of the anti-vortex plate is expected. In the condition without

the anti-vortex plate, in addition to the increase in the flow velocity in the Penstock, the increase in the order of the vortex by increasing Froude number is also another reason. For example, by increasing the Froude number from 0.6 to 1.2, the vortex order has increased from 2 to 6 (Roshan and Ghobadian, 2022 ). In other words, the area of the rotating flow inside the tank increases and vortex flow with the air core enters the Penstock, which has a higher energy loss.

Presence of the anti-vortex plate has caused the amount of energy loss to decrease in both absolute and relative forms. Values in tow last column of Table 2 identify that the reduction of ΔH/H due to the presence of the anti-vortex plate is between 1.4 to 6.1% for the reason that the anti-vortex plate plate at any relative submergence depth causes the order of the vortex to decrease or vortex be completely eliminated. In that case, the flow enters penstock with less disturbance and turbulence and as a result, the energy loss is less. Also, in general, with decrease in S/D, the amount of ΔH has increased, and effect of anti-vortex plate has become robust. The research of Roshan showed that with reduction of S/D, the size of the rotating area of the flow towards the Penstock intake increases (Roshan, 2023). In other words, the flow enters the Penstock with more turbulence, which increases the absolute energy loss. However, it is clear that with the increase in S/D, the relative head loss decrease, the main reason of that, is the increase of H (or S) in the denominator of the relative head loss relationship rather than the brief decrease of ΔH.

**Table 2. Values of the total head loss(ΔH) and relative head loss (ΔH / H) along the tunnel in different (Fr) and (S/D)**

| S/D | Fr | Q (m3/s) | Average Press. Piz. 9 Without Plate (m) | Average Press. Piz. 9 With Plate (m) | ΔH (cm) | | ΔH / H (%) | |
|---|---|---|---|---|---|---|---|---|
| | | | | | Without Plate (Strong Vortex) | With Plate | Without Plate (Strong Vortex) | With Plate |
| 1.5 | 0.6 | 0.015 | 0.202 | 0.236 | 0.96 | 0.12 | 4.0 | 0.5 |
| | 0.8 | 0.020 | 0.171 | 0.233 | 1.87 | 0.65 | 7.8 | 2.7 |
| | 1.0 | 0.025 | 0.133 | 0.230 | 2.86 | 1.42 | 11.9 | 5.9 |
| | 1.2 | 0.030 | 0.087 | 0.226 | 3.96 | 2.54 | 16.5 | 10.6 |
| 1.75 | 0.6 | 0.015 | 0.240 | 0.277 | 1.12 | 0.05 | 4.0 | 0.2 |
| | 0.8 | 0.020 | 0.207 | 0.274 | 2.24 | 0.56 | 8.0 | 2.0 |
| | 1.0 | 0.025 | 0.179 | 0.271 | 2.83 | 1.18 | 10.1 | 4.2 |
| | 1.2 | 0.030 | 0.149 | 0.267 | 3.95 | 2.24 | 14.1 | 8.0 |
| 2 | 0.6 | 0.015 | 0.281 | 0.315 | 1.12 | 0.00 | 3.5 | 0.0 |
| | 0.8 | 0.020 | 0.251 | 0.313 | 1.86 | 0.38 | 5.8 | 1.2 |
| | 1.0 | 0.025 | 0.217 | 0.309 | 2.59 | 1.15 | 8.1 | 3.6 |
| | 1.2 | 0.030 | 0.198 | 0.304 | 3.71 | 1.82 | 11.6 | 5.7 |
| 2.5 | 0.6 | 0.015 | 0.364 | 0.393 | 0.76 | 0.00 | 1.9 | 0.0 |
| | 0.8 | 0.020 | 0.336 | 0.388 | 1.20 | 0.40 | 3.0 | 1.0 |
| | 1.0 | 0.025 | 0.305 | 0.377 | 1.84 | 1.24 | 4.6 | 3.1 |
| | 1.2 | 0.030 | 0.279 | 0.371 | 2.80 | 1.68 | 7.0 | 4.2 |
| 3 | 0.6 | 0.015 | 0.444 | 0.472 | 0.72 | 0.00 | 1.5 | 0.0 |
| | 0.8 | 0.020 | 0.420 | 0.463 | 1.10 | 0.43 | 2.3 | 0.9 |
| | 1.0 | 0.025 | 0.391 | 0.454 | 1.92 | 1.01 | 4.0 | 2.1 |
| | 1.2 | 0.030 | 0.370 | 0.444 | 2.83 | 1.82 | 5.9 | 3.8 |

Time (ms)

Fig. 8 shows the variations of the relative friction head loss(hf/L) in competition with Froude number in the absence and presence of anti-vortex plate. As it can be seen from Fig. 8, by increasing S/D, the amount of relative friction head loss (hf/L) increases. For a specific Froude number (constant velocity in the Penstock) with increasing values of S/D, the pressure inside the Penstock increases. Therefore, the fluid particles are in contact with each other and the tunnel wall with a higher pressure, so expect a greater friction loss. For example, in absence of anti-vortex plate, with the increase of the S/D from 1.5 to 3 at the highest Froude number, i.e. 1.2, the value of hf/L has changed from .75 to 1.35%. On the other hand, for the lowest Froude number, i.e. 0.6, with the increase S/D from 1.5 to 3, the relative friction loss has increased from .47% to .635%. On average, in the experiments of this research, by doubling the submergence depth, the amount of relative friction loss has increased by about 64%. Also, Fig. 8 shows for a certain S/D, increasing the Froude number increases the velocity of the flow in the tunnel and, as a result, increases the friction loss. Also, the effect of Froude number on the friction head loss is higher in the greater submergence depth. In general, in the condition of no anti-vortex plate, the Froude number increased from 6 to 1.2, the relative friction head loss increased from 0.57 to 1.05 %.

In addition, Fig. 8 indicate that the presence of the anti-vortex plate due to reduction of vortex effect has reduced the friction loss in the Penstock. The smaller S/D, the greater effect of the anti-vortex plate on the energy loss in the Penstock. The disturbance and turbulence of the flow inside the penstock due to the entry of the vortex with its air core can be the main reason for the increase in friction loss. Moreover, the possibility of the inversion of the flow velocity profile near the tunnel wall may increase the friction loss in the presence of a vortex. In this situation, in addition to steady friction loss, unsteady friction loss is also possible.

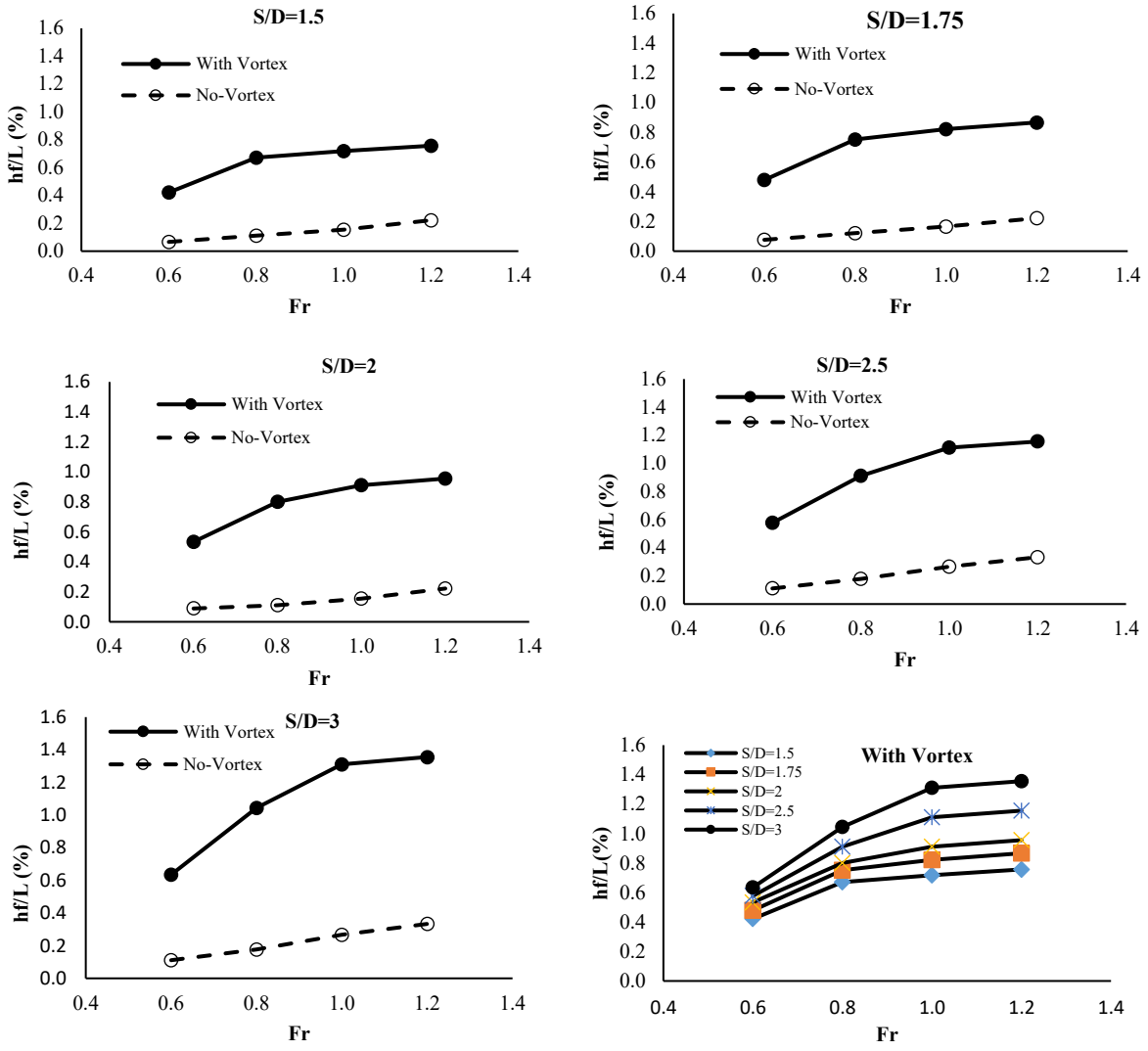


**Figure 8. Variations of relative friction head loss vs. Froude number in different submergence depths with and without the presence of the vorticity control plate**

## Analysis of pressure fluctuations in the presence of vortices

Experiments in different conditions showed that even in the strongest air-core vortices, the swirling flows entering the tunnel concentrate near the tunnel crown. Therefore, among the four pressure sensors installed around each section of the tunnel, the sensor installed on the tunnel crown shows the most intense pressure fluctuations. For this reason, analyzes are presented only for the pressures recorded on the crown of the tunnel. In order to show the pressure fluctuating behavior of the flow along the penstock, the parameter of Fluctuating Intensity (FI) was defined as the following relationship:

$$FI=\frac{\sigma_P}{\bar{P}}=\frac{\sqrt{\frac{\sum_1^n (Pi-\bar{P})^2}{n}}}{\bar{P}} \quad (3)$$

Where standard deviation of the dynamic pressure data at each point is $\sigma_P$ and $\bar{P}$ indicate the mean of the dynamic pressure data at the same point, Pi is each of value of measured

dynamic pressure data and n denote total number of observations. The closer the value of FE is to zero, it indicates less fluctuation in the flow and less deviation from the average pressure. Table 3 includes the absolute values of FI for different S/D and Fr along the tunnel. In this table (l) represents distance from beginning of tunnel and (L) is total length of the tunnel. The values presented in this table show that for the Froude number of 0.6, the maximum value of FI reaches about 2%. The reason for this low value is due to the formation of type 1or 2 vortex in this Froude number. While for the Froude number of 1.2 and the S/D of 1.5, which creates a vortex of order 6 (Roshan & Ghobadian, 2022), the value of FI reaches about 12.9%. As mentioned before, in the 6 order vortex, a strong swirling flow enters intake with an air core, which causes strong turbulence flow in the penstock.

**Table 3. The absolute values of FI for different S/D and Fr along the tunnel**

| l / L (%) | Fluctuation Intensity (FI) - $F_r$ = 0.6 | | | | |
|---|---|---|---|---|---|
| | S/D = 1.5 | S/D = 1.75 | S/D = 2 | S/D = 2.5 | S/D = 3 |
| 5 | 1.00 | 0.30 | 0.75 | 0.60 | 0.20 |
| 10 | 0.90 | 0.51 | 0.65 | 0.65 | 0.30 |
| 20 | 0.81 | 0.75 | 0.60 | 0.70 | 0.52 |
| 30 | 0.68 | 0.61 | 0.65 | 0.68 | 0.45 |
| 40 | 0.90 | 0.63 | 0.81 | 0.70 | 0.50 |
| 50 | 1.50 | 1.15 | 1.35 | 0.90 | 0.62 |
| 60 | 1.65 | 1.25 | 1.40 | 1.00 | 0.75 |
| 70 | 1.38 | 1.30 | 1.25 | 1.10 | 0.80 |
| 80 | 2.00 | 1.60 | 1.60 | 1.35 | 1.00 |
| l / L (%) | Fluctuation Intensity (FI) - $F_r$ = 0.8 | | | | |
| | S/D = 1.5 | S/D = 1.75 | S/D = 2 | S/D = 2.5 | S/D = 3 |
| 5 | 1.40 | 0.65 | 0.80 | 0.45 | 0.30 |
| 10 | 1.55 | 0.90 | 0.90 | 0.55 | 0.44 |
| 20 | 1.65 | 1.45 | 1.10 | 1.00 | 0.85 |
| 30 | 1.80 | 1.55 | 1.25 | 1.35 | 1.10 |
| 40 | 2.10 | 1.80 | 1.50 | 1.65 | 1.20 |
| 50 | 2.40 | 2.10 | 2.15 | 1.60 | 1.30 |
| 60 | 3.15 | 2.50 | 2.40 | 2.00 | 1.75 |
| 70 | 4.20 | 2.80 | 2.20 | 2.25 | 1.90 |
| 80 | 4.90 | 3.15 | 2.75 | 2.40 | 2.00 |
| l / L (%) | Fluctuation Intensity (FI) - $F_r$ = 1.0 | | | | |
| | S/D = 1.5 | S/D = 1.75 | S/D = 2 | S/D = 2.5 | S/D = 3 |
| 5 | 1.60 | 0.95 | 0.80 | 0.45 | 0.40 |
| 10 | 1.85 | 1.15 | 1.10 | 0.90 | 0.80 |
| 20 | 2.10 | 1.80 | 1.70 | 1.65 | 1.55 |
| 30 | 2.08 | 2.00 | 1.55 | 1.90 | 1.55 |
| 40 | 2.50 | 2.40 | 1.65 | 2.15 | 2.00 |
| 50 | 3.50 | 3.25 | 2.80 | 2.55 | 2.20 |
| 60 | 3.95 | 3.50 | 3.00 | 2.85 | 2.35 |
| 70 | 4.45 | 4.25 | 3.30 | 3.05 | 2.75 |
| 80 | 6.75 | 5.40 | 3.95 | 3.75 | 3.10 |
| l / L (%) | Fluctuation Intensity (FI) - $F_r$ = 1.2 | | | | |
| | S/D = 1.5 | S/D = 1.75 | S/D = 2 | S/D = 2.5 | S/D = 3 |
| 5 | 2.20 | 1.30 | 1.10 | 0.80 | 0.70 |
| 10 | 3.15 | 2.20 | 1.95 | 1.20 | 1.00 |
| 20 | 4.00 | 3.30 | 2.75 | 2.20 | 1.95 |
| 30 | 4.20 | 3.25 | 2.90 | 2.30 | 2.00 |
| 40 | 4.85 | 3.30 | 3.30 | 2.40 | 2.15 |
| 50 | 6.25 | 5.00 | 5.20 | 3.10 | 2.30 |
| 60 | 8.95 | 5.60 | 5.60 | 4.00 | 3.10 |
| 70 | 11.10 | 5.95 | 5.85 | 4.20 | 3.60 |
| 80 | 12.90 | 9.60 | 8.10 | 5.20 | 4.30 |

Fig. 9 shows variation of FI along Penstock. As it can be seen from this figure by increasing the distance from beginning of the penstock to the vertical bend, FI and in other words pressure fluctuations have also increased. This increasing trend can be seen for all relative submergence depths and all Froude numbers. However, this trend is greater at higher Froude numbers and smaller relative submergence depths. At higher Froude numbers and submergence depths, the 6 order vortex with the air core is formed and pulled into the water intake opening. When this strong swirling flow advances along the penstock, it moves across the flow to reach the crown of the tunnel and air bubbles are released inside the flow, causing more turbulence and fluctuations in the flow pressure. This issue was also seen through observations with dye injection. Fig. 10 shows a strong vortex with an air core stretching into the penstock in the model. As it can be seen from this figure, the vortex after entering the water intake, first moves downwards (to the vicinity of the tunnel axis) then it reaches the crown of the tunnel through a distance.

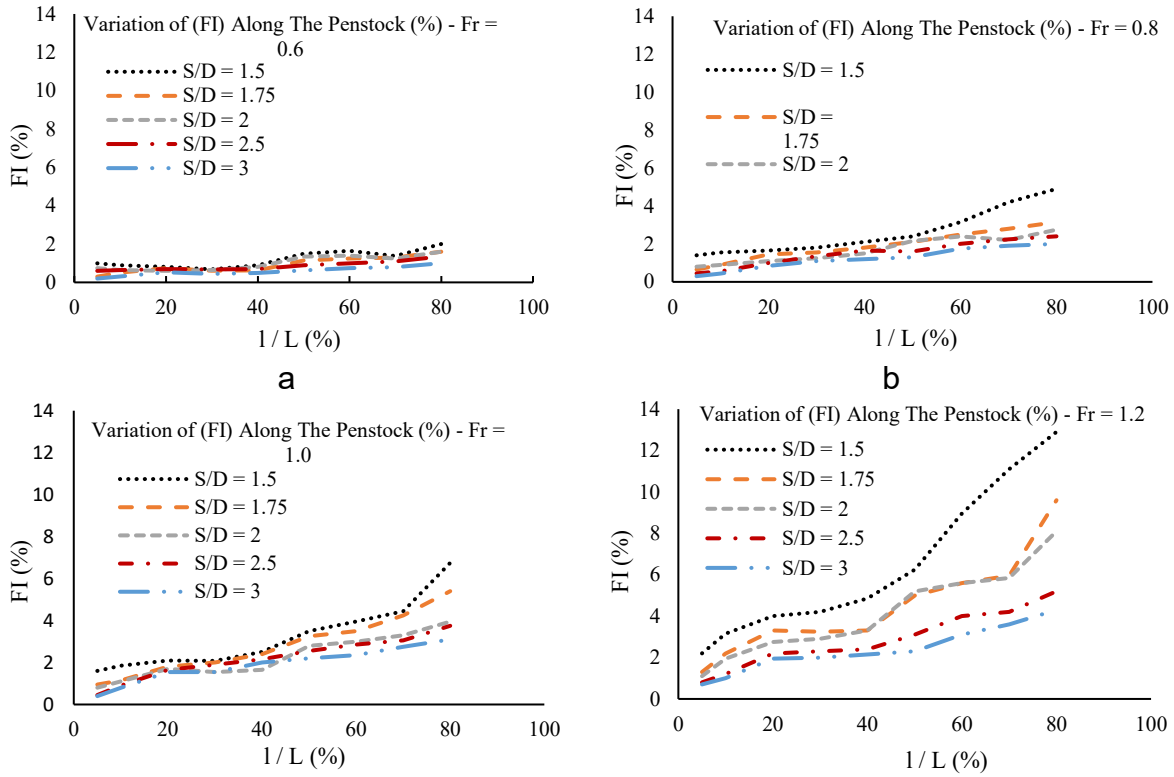


**Figure 9. Variation of Fluctuating Intensity along the tunnel for (a) Fr = 0.6 , (b) Fr = 0.8 , (c) Fr = 1.0 and (d) Fr = 1.2**

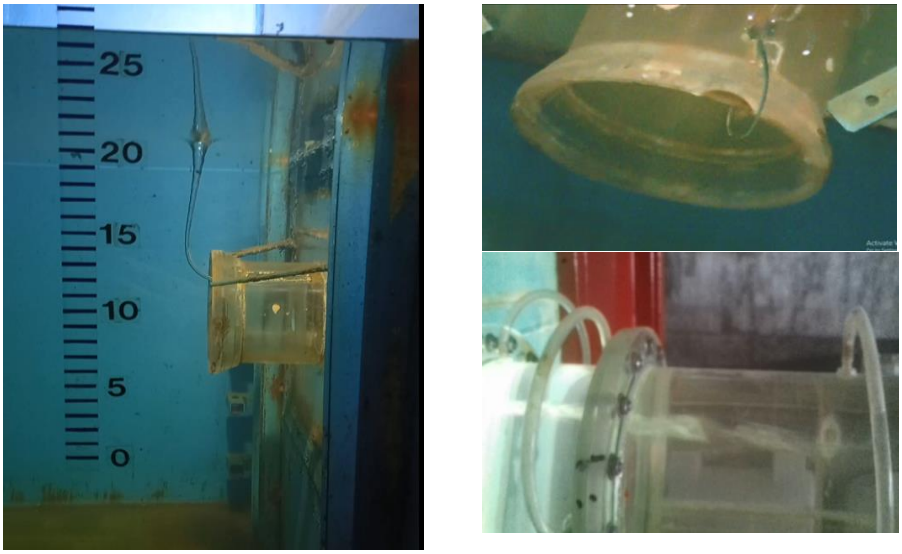


**Figure 10. A strong vortex at the intake and the entry of swirling flow with an air core into the penstock**

## Vortex elimination along the Penstock

The vortex elimination trend was investigated along the tunnel for each of the three vortex groups shown in Fig 1. In order to achieve this goal, the pressure fluctuations were analyzed along Penstock, at any point where the trend of pressure fluctuations was fixed; it was introduced as the location of vortex elimination. In Fig 11, intensity of the pressure fluctuations (FI parameter represents the pressure fluctuation) is plotted against the relative length from the beginning of the Penstock. As shown in this figure, the type C weak vortex has eliminated in a length of about 25% or 7D from the beginning of the tunnel. For type B vortex, the effects of the vortex can be seen up to a relative distance of 65% or 18D from the beginning of the Penstock, and after that, the vortex is depreciated. In the case of strong air-core vortices, class A, by following the air core along the tunnel (as a parameter that shows the presence of the vortex) and reaching it to the bend, it seems that no length can be considered for vortex elimination. For this type of vortex, as shown in Fig 11, until the end of the penstock, which is about 30 times the diameter of the pipe, the pressure fluctuations have maintained their increasing trend. The reason for that is the growth of the flow rotation area and reaching to the inner wall of the pipe, that is, where the pressure sensors are installed.

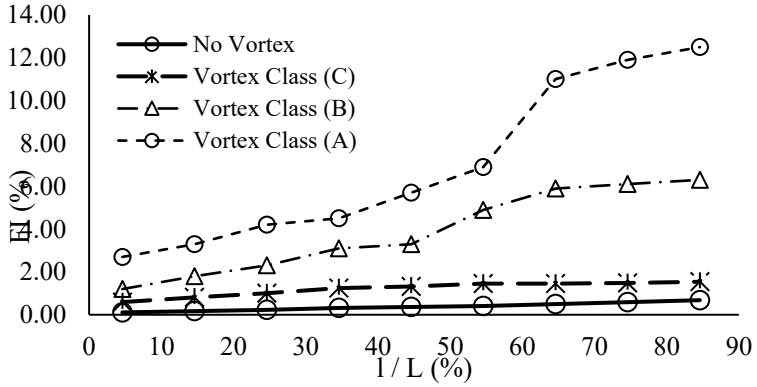


**Figure 11. Fluctuating Intensity for different vortex classes along the tunnel**

## Friction coefficient in the penstock

The average values of the measured fluctuating pressures in piezometers No. 1 and 9 (Fig. 7) were determined to calculate head loss ($h_f$) along the Penstock. Values of friction coefficient ($f$) was determined for all experimental test using the Darcy-Weisbach equation ($h_f = f.\frac{L}{D}.\frac{V^2}{2g}$). Although the use of Darcy-Weisbach relationship is not completely suitable for the conditions of air in the pipe flow, nevertheless, due to the lack of an alternative relationship and its popularity, the aforementioned relationship was used. Variations of friction coefficient ($f$) against the Froude number for different relative submerged depths are presented in Fig 12.

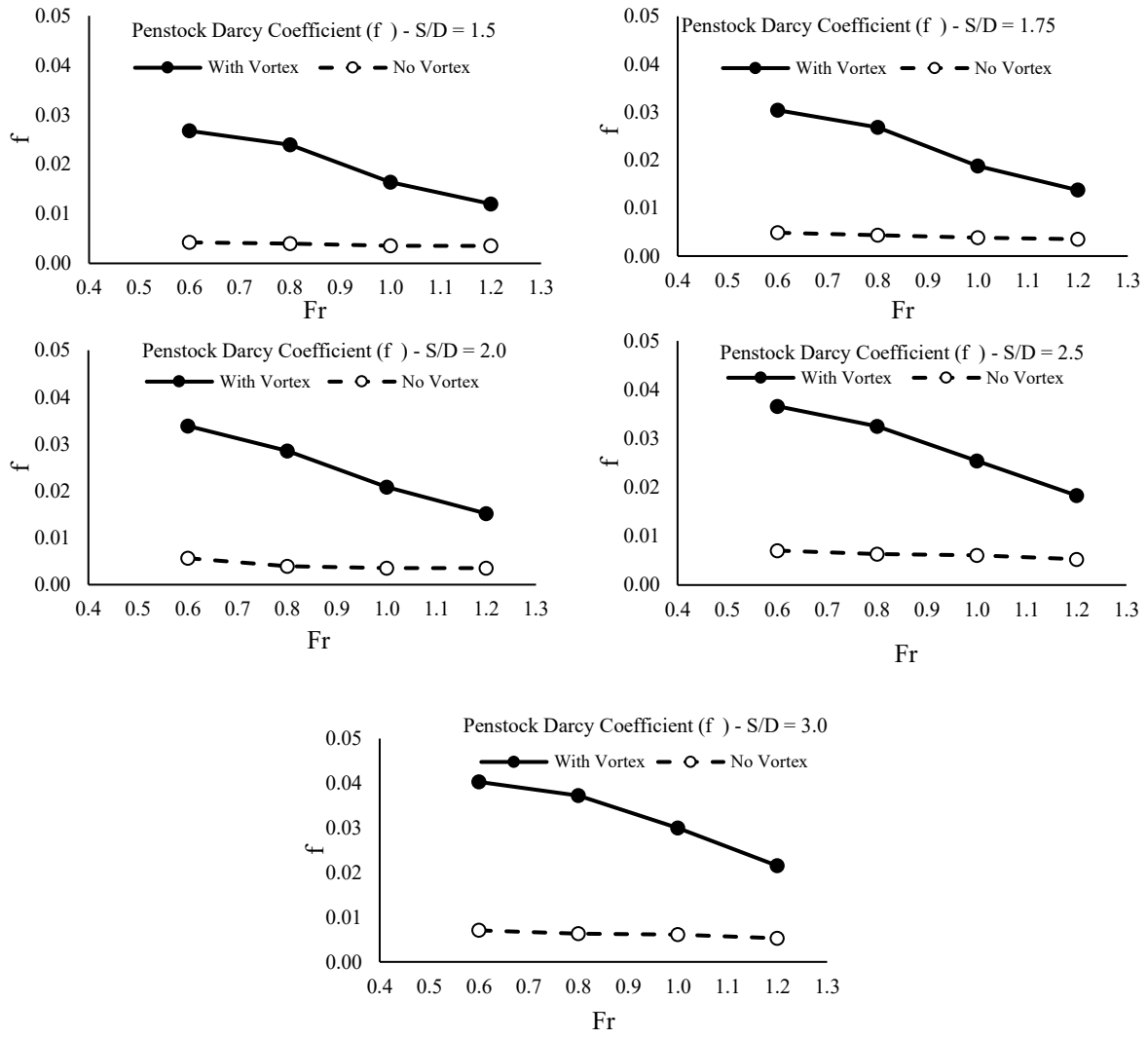


**Figure 12. Variations of friction coefficient ($f$) against the Froude number for different relative submerged depths**

As can be seen in Fig 12, for the condition that the anti-vortex plate is installed on the intake forehead, the formation of the vortex is prevented and the friction coefficient value are almost constant and is not affected by Froude number and submergence depth. Also, on average, the coefficient of friction loss in the state without vortex is 20% of this coefficient in the presence of a vortex, in other words vortex formation causes an increase in the friction coefficient in the tunnel. Furthermore, with the presence of the vortex, the largest values of the friction coefficient have been obtained at lower Fr and higher S/D. For example, in the Fr of 0.6 and the S/D of 3,

the presence of the vortex has increased the friction coefficient about 6 time in comparison with no vortex condition. On the other hand, by decreasing S/D and increasing Fr, where the strong vortices created, the lowest value of the friction coefficient has been obtained. The reason for this could be that increasing the Froude number increases the velocity of the flow in the penstock and makes the flow more turbulent, on the other hand, the decrease in the critical depth also causes the vortex to enter the penstock with a larger order, which also causes more turbulence in the flow. More turbulence means reducing the coefficient of friction loss, as in Moody's diagram, friction coefficient decreases with increasing flow velocity and Reynolds number. On the whole The results state that contribution of increasing Fr in reducing of friction coefficient is more than the reduction of the S/D.

## Conclusions

The present study was conducted using a large-scale laboratory model. To date, no dedicated research has examined the influence of intake vortices on longitudinal head loss and friction coefficient in hydropower penstocks. Therefore, this investigation aimed to evaluate the effects of a wide range of vortex classes on head loss, friction coefficient, and pressure fluctuation intensity along the penstock through carefully controlled experiments.

The results demonstrated that the installation of an anti-vortex plate, designed to eliminate or reduce vortex strength, significantly decreased total energy loss in both absolute and relative terms. The relative total head loss reduction ($\Delta H/H$) achieved with the plate ranged from 1.4 % to 6.1 %. Furthermore, as the relative submergence ratio (S/D) decreased — corresponding to increased flow vorticity and enlargement of the rotating zone near the intake — the absolute head loss ($\Delta H$) increased, and the beneficial effect of the anti-vortex plate became more pronounced.

For a constant Froude number, an increase in S/D led to higher internal pressure within the penstock and greater interaction between fluid particles and the tunnel wall, resulting in elevated relative friction loss (hf/L). In the presence of vortex flow, doubling the submergence depth increased the relative friction loss by approximately 64 % on average. Additionally, for a fixed S/D ratio, higher Froude numbers — associated with greater flow velocity — produced larger friction losses. The influence of the Froude number on friction head loss was found to be more significant at greater submergence depths.

On average, the friction coefficient (f) in vortex-free conditions was approximately 20 % lower than in the presence of vortices. Vortex formation consistently increased the friction coefficient within the penstock, with the highest values observed at lower Froude numbers and higher S/D ratios. Conditions that promoted higher-order vortices (potentially with an air-entraining core) — namely increased Froude number, reduced relative submergence, and removal of the anti-vortex plate — generated greater flow turbulence at the intake. As expected, the friction coefficient decreased with rising turbulence intensity.

Pressure fluctuation behavior along the penstock was analyzed by introducing the fluctuation intensity parameter FI (Equation 3). Strong vortices with an air core exhibited an increasing fluctuation trend between the intake and the downstream vertical bend. Weak Class C vortices dissipated within approximately 7D from the tunnel entrance, whereas the influence of Class B vortices persisted up to about 18D. No definite dissipation length could be established for strong Class A vortices within the tested tunnel length. Further experiments using substantially longer tunnels are recommended to determine the attenuation distance of high-strength vortices conclusively.

***Author Contributions***

All authors contributed to the study conception and design. Material preparation, data collection and analysis were performed by all authors.

***Data Availability Statement***

The data will be available upon reasonable request.

***Acknowledgements***

The model tests carried out at the Water Research Institute of the Ministry of Energy. In this way, the director and colleagues of the Hydraulic Structures Department of the Water Research Institute, especially Dr. Amir Reza Zarrati and Dr. Hamed Sarkardeh, are sincerely appreciated.

***Ethical Considerations***

The authors avoided data fabrication, falsification, plagiarism, and misconduct.

***Funding***

That no funds, grants, or other support were received during the preparation of this manuscript.

***Conflict of Interest***

The authors declare that they have no conflict of interest.

## References

Agbayani, N., Karami, H., Mousavi, S.F., & Sarkardeh, H. (2019). Experimental study of the effect of the trashrack on the vortex at the intake of the hydroelectric power plants in various flow rates and submergence depths. *Journal of Dam and Hydroelectric Power plant*, 6(21),49-62. https://www.researchgate.net/publication/334770912_Experimental_study_of_the_effect_of_the_trashrack_on_the_vortex_at_the_intake_of_the_hydroelectric_power_plants

Amiri, S. M., Zarrati, A. R., Roshan, R., & Sarkardeh, H. (2011). Surface vortex prevention at power intakes by horizontal plates. *Journal of Water Management (ICE)*, 164(4),193-200. https://doi.org /10.1680/wama.1000009

Azarpira, M., Sarkardeh, H., Tavakkol, S., Roshan, R., & Bakhshi, H. (2014). Vortices in dam reservoir: A case study of Karun III dam. *Journal of Sādhanā*, 39(5), 1201-1209. https://doi.org/10.1007/s12046-014-0252-7

Bajracharya, T. R., Shakya, S. R., Timilsina, A. B., & Dhaka, J. (2020). Effects of geometrical parameters in gravitational water vortex turbines with conical basin. *Journal of Renewable Energy*. 1-16. https://doi.org/10.1155/2020/5373784

ÇELEBIOĞLU, K. (2019). Roughness coefficient of a highly calcined penstock. *Teknik Dergi, Paper 545*, 9309-9325. https://doi.org/10.18400/tekderg.447265

Constantinescu, G. S., Patel, V. C., 1998, A numerical model for simulation of pump intake flow and vortices. *Journal of Hydraulic Engineering*, 124(5), 123-134. https://doi.org/10.1061/(ASCE)0733-9429(1998)124:2(123)

Daggett, L. L.,& Keulegan, G. H. (1974). Similitude in free-surface vortex formation. J Hydraul Eng, 100, 1565–1580. https://doi.org/10.1061/ JYCEAJ.0004105

Guilliver, J.S., & Rindels, A. J. (1987). Weak vortices at vertical intakes. *Journal of Hydraulic Engineering*, 113(9), 1101-1116. https://doi.org/10.1061/(ASCE)0733-9429(1987)113:9(1101)

Jain, A. K., Raju, K. G. R., & Garde, R. J. (1978). Vortex formation at vertical pipe intake. *J Hydraul Eng* , 100(10), 1427–1445. https://doi.org/ 10.1061/JYCEAJ.0005087

Keller, J., Möller, G., Boes, R.M. (2014). PIV measurements of air-core intake vortices. *Journal of Flow Measurement and Instrumentation*, 40(40), 74–81. https://doi.org/10.1016/j.flowmeasinst.2014.08.004

Leon, A. S. (2016). Determining optimal discharge and optimal penstock diameter in water turbines, international symposium on hydraulic structures. *Utah State University*, Portland, Oregon, USA, 27-30. https://doi.org/10.15142/T390628160853

Manogaran, T., Zainol, M. R. R. M. A., Wahab, M. K. A., Aziz, M. S. A., Abd Aziz, N., Zahari, N. M., & Radzi, M. R. M. (2023). Free-surface vortices mitigation using anti-vortex plates in dam intakes through CFD. *CFD Letters*, 15(6), 26-41. https://doi.org/10.37934/cfdl.15.6.2641

Möller, G. Detert, M., & Boes, R. M. (2015). Vortex-induced air entrainment rates at intakes, *Journal of Hydraulic Engineering*, 141(11), 1-8. https://doi.org/10.1061/(ASCE)HY.1943-7900.0001036

Möller, G., Detert, M., & Boes, R. M. (2012). Air entrainment due to vortices: State-of the-art. 2nd International Association of Hydraulic Engineering Europe Congress, *IAHR Press*, Munich, Germany. http://hdl.handle.net/20.500.11850/63100

Moukam, T., François, N., Thomas, D., & Bienvenu, K. (2022). Numerical evaluation of turbulent friction on walls in the penstock of the Three-Gorges Dam by the Swamee-Jain method. *International Journal of Civil and Environmental Engineering*, 16(6). https://doi.org/10.2166/nh.2024.054

Odgaard, A. J. (1986.) Free surface air core vortex. *J Hydraul Eng* , 112(7), 610–619. https:// doi. org/ 10. 1061/(ASCE) 0733- 9429(1986)112:7(610)

Padmanabhan, M., & Larsen, J. (2001). Chapter 10.2: Intake modeling. Pump handbook, *McGraw-Hill*, New York. https://turbosan.com/pdf/pumphandbook.pdf

Partovi Azar, S. , Farsadizadeh, D. , Hosseinzadeh Dalir, A. , Salmasi, F., & Sadraddini, A. (2010). Estimation of Critical Submergence at Intake System of Aydoghmush Dam Using FLUENT Model. *Water and Soil Science*, *20*(3), 1-14. https://water-soil.tabrizu.ac.ir/article_1328.html?lang=en

Rahm, L. (1953). Flow problems with respect to intakes and tunnels of Swedish hydro-electric power plants. Bulletin, No. 36, *Institution of hydraulic at the Royal Institute of Technology*, Stockholm, Sweden. https://public.ucrlib.aspace.cdlib.org/repositories/5/archival_objects/582280

Roshan, R. (2023). Laboratory investigation on the effect of anti-vortex plates and reservoir geometry on the hydrodynamics of vortex flow in power plant Intakes. PhD thesis in hydraulic structures, *Razi University*, Kermanshah, Iran.

Roshan, R., & Ghobadian, R. (2022). The Effect of anti-vortex plates on vortex dissipation, discharge coefficient and inlet loss coefficient in hydropower intakes. *Journal of Hydraulics*, 17(3), 15-29. https://doi.org/10.30482/jhyd.2022.302255.1547

Roshan, R., & Ghobadian, R. (2023). The effect of reservoir geometry on the critical submergence depth in hydroelectric power plants intake. *Applied Water Science*, 13, 155, 2-9, https://doi.org/10.1007/s13201-023-01960-z

Sarkardeh, H., Jabbari, E., Zarrati, A.R., & Tavakkol, S. (2013). Velocity field in a reservoir in the presence of an air-core vortex. *Journal of Water Management (ICE)*, 164(4), 193–200. https://doi.org/ 10.1680/wama.13.00046

Sarkardeh, H., Zarrati, A. R., Jabbari, E., & Roshan, R. (2012). Discussion of prediction of intake vortex risk by nearest neighbors modeling. *Journal of Hydraulic Engineering*, 137(6), 701-705. https://doi.org/10.1061/(ASCE)HY.1943-7900.0000344

Sarkardeh, H., Zarrati, A. R., & Roshan, R. (2010). Effect of intake head wall and trash rack on vortices. *Journal of Hydraulic Research*, 48(1), 108-112. https://doi.org/10.1080/00221680903565952

Singhal, M. K., & Kumar, A. (2015). Optimum design of penstock for hydro projects. *International Journal of Energy and Power Engineering* , 4(4), 216-226. https://doi.org/10.11648/j.ijepe.20150404.14

Suerich-Gulick, F., Gaskin, S. J., Villeneuve, M., & Parkinson, É. (2014). Characteristics of free surface vortices at low-head hydropower intakes. *Journal of Hydraulic Engineering*, 140(2), 291-299. https:// doi.org /10.1061/(ASCE)HY.1943-7900.0000826

Sukhapure, K., Burns, A., Mahmud, T., & Spooner, J. (2018). CFD modelling and validation of loss Coefficients for penstock bifurcation in hydropower schemes. *3rd Thermal and Fluids Engineering Conference (TFEC)*, 395-406.http://dx.doi.org/10.1615/TFEC2018.cmd.021574

Zheng, G., Gu, Z., Xu, W., Lu, B., Li, Q., Tan, Y., & Li, L. (2023). Gravitational surface vortex formation and suppression control: A review from hydrodynamic characteristics. *Processes*, 11(42), 3-20. https://doi.org/10.3390/pr11010042